

Parametric Study of Different Shaped Planar Antennas with DGS for Handheld Wireless Communication.

A thesis is submitted in partial fulfillment of the requirements for the degree of Bachelor of Science in Electrical, Electronic, and Communication Engineering (EECE), Pabna University of Science and Technology, Pabna-6600, Bangladesh.

By

**Roll No. : 150542
Reg. No. : 1054179
Session : 2014-2015**

Pabna University of Science and Technology, Pabna-6600, Bangladesh.

April, 2022

DECLARATION

I, Sajeeb Chandra Das, hereby declare that the work presented here is originally done by me and has not been published or submitted elsewhere for the requirement of a degree. Any literature date or work done by others and cited within this thesis has been due acknowledged and listed in the reference section.

Date: April, 2022
.....

Sajeeb Chandra Das

Roll No. : 150542

Reg. No. : 1054179

Dept. of Electrical, Electronic, and Communication Engineering,
Pabna University of Science and Technology,
Pabna-6600, Bangladesh.

CERTIFICATE

This is to certify that the thesis entitled, “Parametric Study of Different Shaped Planar Antennas with DGS for Handheld Wireless Communication.”, submitted by Sajeeb Chandra Das, Roll No. 150542 in partial fulfillment of the requirement for session 2014-2015 at Pabna University of Science and Technology, is based on the investigation and record of the research work carried out by him under my supervision and guidance.

The candidate has fulfilled all the prescribed requirements. The thesis which is based on candidate's own work has not been submitted elsewhere for a degree or diploma.

In my opinion, the thesis is of standard required for the award of a Bachelor of Science degree in engineering.

Thesis Supervisor

.....
Liton Chandra Paul

Assistant Professor

Dept. of Electrical, Electronic, and Communication Engineering,
Pabna University of Science and Technology,
Pabna-6600, Bangladesh

ACKNOWLEDGEMENT

First of all, I am grateful to the Almighty for the good health and well-being that were necessary to complete this book. I would like to thank my parents for giving so much support. I am also thankful to all of the teachers for enlighten my knowledge.

I have no words to express my gratitude for my teacher and supervisor, Liton Chandra Paul, Assistant Professor, Department of Electrical, Electronic, and Communication Engineering, Pabna University of Science and Technology.

I would like to convey my gratitude to our honorable Professor Md. Saiful Islam, Chairman, Department of Electrical, Electronic, and Communication Engineering, Pabna University of Science and Technology for providing me necessary facilities and permission to carry out this work.

DEDICATION

By the grace of the almighty, I dedicate this research work to my beloved parents for their unconditional love and support from the very beginning of my life. Then I would like to dedicate this research to my three honorable teachers Md. Masudur Rahman, Mahbuba Akhter Jahan, and Liton Chandra Paul sir from three stages of my academic life for their enormous support, guidance, and inspiration to be a researcher moreover an actual human being. Specially, I would like to convey my immense gratitude to my honorable supervisor Liton Chandra Paul sir for believing and inspiring me to be the person I am.

ABSTRACT

Different shaped planar antennas are designed and proposed with parametric study for handheld wireless applications. The CST Microwave Studio Suite is used to design and simulate all the antennas. All the antennas are etched on Rogers RT5880 (lossy) substrate with compact size. The small size of the antennas has a few drawbacks of narrower bandwidth and low gain, which are improved by introducing defected ground structure (DGS) on the ground plane. The different shapes of the antennas help to get proper current distribution with omnidirectional radiation patterns. The first two antennas demonstrated in chapter 3 and chapter 4 operate in mm-wave bands. The wideband antenna at chapter 3 operates over a wider bandwidth of 4.846 GHz with peak gain and directivity of 6.1 dB and 7.8 dBi respectively for mm-wave 5G application. The DGS antenna represented at chapter 4 cover a larger bandwidth of 5.85 GHz (25.52 GHz - 31.37 GHz) for mm-wave 5G at 28 GHz range. This band is licensed in USA, EU, Japan, China, Korea and India. At chapter 5, the spiral shaped dual band antenna resonates at 3.61 GHz (3.53-3.7 GHz) and 5.56 GHz (4.7-7.24 GHz) for Sub-6 GHz 5G and WiFi-5/6 applications. The rose-shaped antenna demonstrated in chapter 6 resonates at 3.19 GHz with a very good reflection coefficient of -57.27 dB and a large bandwidth of 3.04 GHz (2.7-5.74 GHz). It is suitable for Sub-6 GHz handheld applications due to its compact size and other parametric performances. Finally, the plus-shaped antenna introduced in chapter 7 operates in Sub-6 GHz band over a wider bandwidth of 2.56 GHz with gain and directivity. The antenna shows very high efficiency of 98% for Sub-6 GHz 5G and WiMAX applications in handheld devices. All the antennas are well optimized with a VSWR value very close to unity which indicates very good impedance matching of those antennas. The detailed abstract of those individual antennas is introduced in respective chapters. The wider bandwidth, high gain, and directivity with very good reflection coefficients of those antennas make them suitable candidates for handheld wireless applications.

CONTENTS

Declaration	II
Certificate	III
Acknowledgement	IV
Dedication	V
Abstract	VI
List of Figures	XI
List of Tables	XIV

CHAPTER-1 INTRODUCTION	1
1.1 Introduction	1
1.2 Literature Review	2
1.3 Problem Statement	3
1.4 Motivation	4
1.5 Design Methodology	4
1.6 Expected Outcome	5
1.7 Benefits of This Research on Bangladesh	5
1.8 Thesis Organization	6
References	7
CHAPTER-2 ANTENNA BASIC CONCEPT AND PARAMETERS	9
2.1 Antenna	9
2.2 Antenna Feeding Techniques	9
2.2.1 Microstrip Line Feed	9

2.2.2 Coaxial Probe Feed	9
2.2.3 Proximity Coupled Feed	12
2.2.4 Aperture Coupled Feed	12
2.3 Microstrip Patch Antennas	13
2.3.1 Advantages of Microstrip Patch Antennas	14
2.3.2 Disadvantages of Microstrip Patch Antennas	15
2.3.3 Applications of Microstrip Patch Antennas	16
2.4 Planar Antennas	16
2.5 Fundamental Radiation Parameters of Antenna	17
2.5.1 Directivity	17
2.5.2 Gain	18
2.5.3 Antenna Efficiency	19
2.5.4 Radiation Pattern	20
2.5.5 Reflection Coefficient	21
2.5.6 VSWR	21
2.5.7 Return Loss	22
2.5.8 Bandwidth	23
2.5.9 Impedance Matching	23
2.5.10 Polarization	24
2.5.11 Front to Back Ratio	26
2.5.12 Axial Ratio	26
2.5.13 Surface Current	27
2.6 Substrate of Microstrip Patch Antenna	27
2.6.1 Rogers RT5880	28

2.7 Simulation Tool (CST Microwave Studio Suite)	29
References	29
CHAPTER-3 A WIDEBAND MICROSTRIP PATCH ANTENNA WITH SLOTTED GROUND PLANE FOR 5G APPLICATION	31
3.1 Abstract	31
3.2 Introduction	31
3.3 Design of Wideband 5G Antenna	33
3.4 Analysis of Simulation Results	35
3.5 Conclusion	42
References	42
CHAPTER-4 A LOW PROFILE MICROSTRIP PATCH ANTENNA WITH DGS FOR 5G APPLICATION	44
4.1 Abstract	44
4.2 Introduction	44
4.3 Design of 5G Antenna With DGS	46
4.4 Results and Analysis of Proposed Antenna	49
4.5 Conclusion	56
Reference	56
CHAPTER-5 A DUAL BAND MINIATURIZED SPIRAL-SHAPED PATCH ANTENNA FOR 5G AND WiFi-5/6 APPLICATIONS	59
5.1 Abstract	59
5.2 Introduction	59
5.3 Spiral-Shaped Patch Antenna	61

5.4 Conclusion	69
References	69
CHAPTER-6 A WIDEBAND ROSE-SHAPED PATCH ANTENNA WITH A GROUND SLOT FOR SUB-6 GHz APPLICATION	
6.1 Abstract	71
6.2 Introduction	71
6.3 Design of Rose-shaped Patch Antenna	74
6.4 Results and Analysis of Rose-shaped Antenna	75
6.5 Conclusion	82
References	82
CHAPTER-7 A SLOTTED PLUS SHAPED PATCH ANTENNA WITH DGS FOR SUB-6 GHz/WiMAX APPLICATIONS	
7.1 Abstract	84
7.2 Introduction	84
7.3 Design and Structure of the PSPA	87
7.4 Simulation, Results and Discussion	89
7.5 Conclusion	96
References	96
CHAPTER-8 CONCLUSION	98
8.1 Conclusion	98
8.2 Recommendation for Future Work	99
Appendix	101

LIST OF FIGURES

Fig. 2.2.1: Different feeding techniques for Microstrip Antennas.	11
Fig. 2.2.2: Effect of feeding techniques on parameters.	13
Fig. 2.3.1: Microstrip Patch Antenna.	14
Fig. 2.4.1: Different types of planar antennas.	17
Fig. 2.5.1: Directivity and Gain.	18
Fig. 2.5.2: Radiation pattern of a generic directional antenna.	20
Fig. 2.5.3: Impedance matching of antenna.	24
Fig. 2.5.4: Commonly used Polarization schemes.	25
Fig. 2.5.5: Front to Back Ratio of antenna.	26
Fig. 2.5.6: Axial Ratio of antenna.	27
Fig. 3.3.1: Proposed slotted ground 5G antenna. (a) Front view, (b) Back view, (c) 3D view.	34
Fig. 3.4.1: S11 curve of the proposed 5G antenna.	35
Fig. 3.4.2: VSWR of the proposed 5G antenna.	36
Fig. 3.4.3: 3D Gain at 27.47 GHz of the proposed antenna.	36
Fig. 3.4.4: 3D Directivity at 27.47 GHz of the proposed antenna.	37
Fig. 3.4.5: Gain and directivity Vs frequency of the proposed 5G antenna.	37
Fig. 3.4.6: E field pattern of the proposed 5G antenna.	38
Fig. 3.4.7: H-Field pattern of the proposed 5G antenna.	39
Fig. 3.4.8: Radiation Efficiency.	40
Fig. 3.4.9: Z – Parameters (a) Real part and (b) Imaginary part.	40

Fig. 4.2.1: 5G connectivity with other networks.	46
Fig. 4.3.1: Proposed 5G antenna with DGS. (a) Front view, (b) Back view, (c) 3D view.	48
Fig. 4.4.1: S11 curve of the proposed 5G antenna.	49
Fig. 4.4.2: VSWR of the proposed 5G antenna.	50
Fig. 4.4.3: 3D Gain at 27.26 GHz of the proposed antenna.	50
Fig. 4.4.4: 3D Directivity at 27.26 GHz of the proposed antenna.	51
Fig. 4.4.5: E field pattern of the proposed 5G antenna.	52
Fig. 4.4.6: H-Field pattern of the proposed 5G antenna.	53
Fig. 4.4.7: Gain and directivity Vs frequency of the proposed 5G antenna.	53
Fig. 4.4.8: Radiation Efficiency.	54
Fig. 4.4.9: Z – Parameters (a) Real part and (b) Imaginary part.	55
Fig. 5.3.1: Proposed Spiral-shaped patch antenna. (a) Front view, (b) Back view.	61
Fig. 5.3.2: Reflection coefficient of the spiral-shaped antenna.	62
Fig. 5.3.3: Gain and directivity.	65
Fig. 5.3.4: E-Field and H-Field of the antenna.	66
Fig. 5.3.5: VSWR of Spiral-shaped antenna.	67
Fig. 5.3.6: Radiation Efficiency	67
Fig. 5.3.7: Surface current at (a) 3.61 GHz, (b) 5.05 GHz, (c) 5.56 GHz and (d) 6.85 GHz.	68
Fig. 6.2.1: Immersive use of Sub-6 GHz Bands.	72
Fig. 6.3.1: Proposed rose-shaped antenna	74

Fig. 6.4.1: S11 Curve of the rose-shaped antenna.	76
Fig. 6.4.2: VSWR of the rose-shaped antenna.	76
Fig. 6.4.3: Gain and directivity curve of the rose-shaped antenna.	78
Fig. 6.4.4: Fields (E and H) of the Rose-shaped antenna.	79
Fig. 6.4.5: Radiation Efficiency.	80
Fig. 6.4.6: Surface current: (a) at 3.19 GHz and (b) at 5.5 GHz	80
Fig. 7.3.1: Proposed PSPA with DGS.	88
Fig. 7.4.1: Reflection coefficient of the designed PSPA.	90
Fig. 7.4.2: Gain and directivity curve of the designed PSPA.	91
Fig. 7.4.3: E-field and H-field curve of the PSPA.	92
Fig. 7.4.4: VSWR of the PSPA.	92
Fig. 7.4.5: Radiation Efficiency.	93
Fig. 7.4.6: Current distribution of the PSPA at 3.12 GHz.	93
Fig. 7.4.7: Z – Parameters (a) Real part and (b) Imaginary part.	94

LIST OF TABLES

TABLE 3.3.1:	Design summary of proposed wideband patch antenna for 5G	34
TABLE 3.4.1:	Performance metrics of the proposed 5G antenna.	41
TABLE 3.4.2:	Comparison table.	41
TABLE 4.3.1:	Design summary of proposed microstrip patch antenna with DGS for 5G.	48
TABLE 4.4.1:	Performance metrics of the proposed 5G antenna with DGS.	54
TABLE 4.4.2:	Comparison with relevant work.	55
TABLE 5.3.1:	Comparison table.	68
TABLE 6.3.1:	Design summary of proposed RSPA.	75
TABLE 6.4.1:	Performance metrics of the Rose-shaped patch antenna.	81
TABLE 6.4.2:	Comparison with relevant work.	81
TABLE 7.2.1:	Sub-6 GHz 5G frequency bands for different countries and regions.	85
TABLE 7.3.1:	Parameters' list of the designed PSPA.	89
TABLE 7.4.1:	Results of the designed PSPA.	94
TABLE 7.4.2:	Comparison table.	95
TABLE 8.1.1:	Summarization of the research.	99

Chapter - 1

INTRODUCTION

1.1 Introduction

The world is surfing in a wireless era in this 21st century. Wireless communication has brought the technological revolution in every aspect of life. To fulfill the huge demand of higher data rate, wider coverage, ultra-low latency and massive connectivity researchers are developing different types of antennas day by day. Planar microstrip patch antennas are the most popular types of antennas for its important features to use in different handheld applications. Microstrip patch antennas has some desirable features like simplicity, robust, compatibility of integration, cost effective, energy efficient, light weight and ease of fabrication. The low-profile characteristics of these planar antennas also has some drawbacks of narrow bandwidth, low efficiency which are reduced by introducing slots, partial ground plane, defected ground structure (DGS).

Microstrip patch antennas with different shaped radiator and DGS can be operate in both mm-wave and Sub-6 GHz bands. This research is towards the applications of mm-wave 5G, Sub-6 GHz 5G, WIFI, WiMAX and other applications of handheld wireless communications. These mm-wave and Sub-6 GHz 5G has opened the door of numerous innovation and connectivity to implement IoT, cloud computing, D2D connectivity, smart traffic system, smart-home, virtual reality, augmented reality, AI services, automated industrial infrastructure, robotics, HD live streaming, virtual reality, augmented reality, innovation in space and astronomy, health services and remote education as the world moving towards virtuality [1-3]. The mm-wave 5G is power efficient with very faster data rate. There is no spectral crunch in mm-wave. On the other hand, Sub-6 GHz 5G is more ready to go technology with wider coverage and low cost. In this research different effective parameters of planar antennas are optimized to operate in respective bands. The optimization of these antennas is done by using different shapes of radiating patches. The slotted ground plane and defected ground structures have improved the bandwidth, gain and other decisive parameters of these antennas. The CST Microwave Studio Suite is used to design and simulate these planar antennas. The Rogers RT5880 material with dielectric constant of 2.2, loss

tangent of 0.0009 and thickness of 0.79 mm is used as substrate and copper (annealed) material with thickness of 0.035 mm is used for radiating patches and ground plane.

1.2 Literature Review

To keep up with the race of wireless world and innovation, numerous antennas are developed by RF researchers all over the world. Over the years, the research on microstrip patch antennas has introduced a revolution in numerous wireless applications. Some significant works for Sub-6 GHz and mm-wave applications are introduced in [4-15]. In terms of mm-wave a 28/38 GHz slotted microstrip antenna is introduced in [4] with an acceptable antenna gain (7.88 dB) but lower in bandwidth (1.4306 GHz). The Rogers RT 5880 material is used to simulate this antenna in the CST microwave studio suite. The overall dimension of this antenna is $55 \times 110 \text{ mm}^2$. In [5] a dual band mm-wave antenna with the size of $4 \times 9.45 \text{ mm}^2$ is presented for 5G mobile applications. Although the size of the antenna is comparatively lower, the gain of the antenna is only 2.3 dB at 28 GHz resonance frequency. A square-shaped slot antenna is proposed in [6] for 5G applications. Although the dimension of the antenna is moderate and built in Rogers RT 5880 substrate with thickness 0.127 mm, the gain of this antenna is comparatively lower and it is 4 dB at 28 GHz. In [7], a dual-band microstrip antenna with a large frequency ratio for 5G applications is introduced. In the work, the antenna is designed on a TLY-5-0200 dielectric substrate (dielectric constant of 2.2) with a thickness of 0.508 mm, and the size of the antenna is $30 \times 44 \text{ mm}^2$.

The researcher has done numerous works also in Sub-6 GHz bands. In [8], a multi-slotted rectangular stepped patch antenna is designed with a dimension of $20 \times 30 \text{ mm}^2$. The antenna covers 3.15-5.55 GHz for Sub-6 GHz applications. It has a decent average gain of 2.35dBi and efficiency is about 74.7%. The antenna is well optimized to provide omnidirectional radiation. A simple circular patch antenna is introduced in [9], with a compact size of $20 \times 28 \text{ mm}^2$. It operates over a wide bandwidth of 2.77 GHz (3.05 GHz to 5.82 GHz) for the Sub-6 GHz band. The rectangular slot in the ground has a key impact on impedance matching of the antenna. As it uses standard FR4 substrate, the high dielectric loss of it results in very low average gain and efficiency. In [10] a compact F-shaped slotted antenna is proposed for WLAN/WiMAX

applications. The antenna is designed on FR4 substrate with a compact dimension of $19 \times 25 \text{ mm}^2$. The rectangular patch with two F-shaped slots and a circular patch at ground plane facilitate the triple band operation with proper impedance matching. In [11], a partially slotted ground rectangular printed antenna is designed for the Sub-6 GHz band. The antenna has a dimension of $28 \times 40 \text{ mm}^2$ with bandwidth of 700 MHz (3.3 GHz - 4 GHz). The bandwidth is improved by using a polygon-shaped slot on the partial ground plane. The antenna has a decent gain of 2.5 dB despite its simplicity. For Wi-Fi applications, an oval-shaped CPW-Fed monopole antenna is introduced in [12] with a volume of $20 \times 8.7 \times 0.4 \text{ mm}^3$ and a range of 5.15-7.29 GHz with suitable gain and efficiency for WiFi-5/6. In [13], a compact dual-band antenna with rectangular slot and inverted U-shaped stub is presented for sub-6 GHz 5G wireless applications. It provides high peak gain of 7.17 dBi in spite of its smaller dimension ($36 \times 31 \text{ mm}^2$) but the bandwidth is very narrow. A double layer dual band filtering antenna for Sub-6 GHz band is discussed in [14]. Though it has higher gain in both bands, its bigger dimension and 3D structure makes it less applicable in compact devices. A line stripe ultra-wideband antenna with dielectric resonators is demonstrated in [15] for 5G applications. The rectangular resonators enhance the efficiency of the antenna despite of its miniaturized structure. The sawtooth orientation at ground plane ensures proper impedance matching for higher order radiation modes.

This research is aimed on design and parametric study of both mm-wave and Sub-6 GHz band operated planar antennas. The first two antennas in chapter 3 and 4 operate in mm-wave 28 GHz 5G band which is licensed in USA, EU, Japan, China, Korea and India. The antennas introduced in chapter 5-7 can operate in USA (3.7 - 4.2), Europe (3.4 - 3.8), China (3.3 - 3.6) and (4.8 – 5), Japan (3.6 – 4.1) and (4.5 – 4.9), Korea (3.4 - 3.7) and (3.7 – 4), India (3.3 – 3.6), Australia (3.4 - 3.7) for Sub-6 GHz lower 5G applications. The detailed literature reviews of particular antennas are discussed in the respective chapters (from chapter 3 to chapter 7).

1.3 Problem Statement

The low profile planar microstrip patch antennas are most demanding for their optimum performance with compact design. We need best performance under hood simple planar design. Generally, the radiation performance of an antenna reduces with the decrement of the antenna

size. These low-profile patch antennas suffer from serious drawbacks such as narrow bandwidth, low gain and high VSWR values. Researcher are finding solutions to design compact planar antennas with wider bandwidth, high gain, improved directivity, higher efficiency and optimum VSWR which is close to unity. To get this performance, researchers have to take into accounts many aspects of antennas during design process. It's quite challenging to optimize these antennas with additional methodology of DGS on ground plane or different shapes of radiating patch. By using DGS, it's hard to maintain the proper current distribution of the antenna. On the other hand, different shapes of antennas have huge effect on polarization. The researcher should be focused on different tradeoffs of parameters and designs to get required performances.

1.4 Motivation

Due to increasing demand, planar microstrip patch antennas are the hot cake among the electromagnetic researchers. They are low profile, light weight and efficient radiator. As the world is moving towards the wireless era, RF researchers are highly motivated to develop high performance planar antennas. Mobile technology has evolved from first generation (1G) technology to latest fifth generation (5G) technology with higher data rate. The 5G network system has brought tremendous revolution in every sector of life such as smart transportation, tele-medicine, E-learning, smart home, virtual reality, HD broadcasting, cloud computing, IoT and AI services [1-3]. On the other hand, WiFi 5/6 and WiMAX has improved the data sharing speed and massive connectivity in indoor conditions. This research is primarily based on the parametric study of different shaped planar antenna which are mostly used in mm-wave 5G and Sub-6 GHz 5G or other applications to keep up with the race of wireless era.

1.5 Design Methodology

Planar microstrip patch antennas are incorporated with substrate, ground plane, radiating patch and a feed line to feed the power to be radiated. The design and simulation of different shaped planar antennas are done by using Computer Simulation Technology (CST) Microwave Studio software. Different shapes of the radiators are optimized in accordance with the defected ground

structure (DGS) to get desired bandwidth, gain and directivity. The slotted ground planes in the optimized design of these antennas aided to increase the bandwidth with proper current distribution. The width of the feed line is well optimized by numerous simulations to get proper impedance matching of the design which helps to get very good VSWR values (close to unity) and less power reflection. The impedance of these designs kept very close to 50 Ohms as the impedance of standard SMA connectors. All the designs and performance parameters are cross checked by both Time Domain (TD) and Frequency Domain (FD) solvers to buttress as well as ensure the stability of these designs.

1.6 Expected outcomes

This research was directed to the parametric study of different shaped radiators along with slotted ground planes. The main focus was to get required parametric performances such as high gain, directivity, good return loss, wider bandwidth, high radiation efficiency with proper impedance matching in compact design. These antennas were designed and simulated to be used in handheld wireless communications in both mm-wave and Sub-6 GHz bands. The primary application of this research was always targeted to 5G technology. The size of these antennas was kept minimal for ease of integration in practical implementation.

1.7 Benefits of This Research on Bangladesh

The technological advancement is one of the key factors in a country's development. Bangladesh is taking the step to move forward in the race of science and technology. One of the fastest-growing industries in Bangladesh is the electronics industry. Wireless communication and RF handheld devices are the most important part of this technological revolution. Antenna plays a vital role in wireless communication systems and RF handheld devices [16]. Researchers are developing numerous types of antennas to fulfill the increasing demand.

The development of antennas has great potential from both economic and business perspectives. By developing different antennas and facilitating the research on antennas, there can be huge job

opportunities for RF engineers and different job-seeking people in the country. The innovation of the latest RF devices will be boosted by manufacturing antennas locally. The cost of importing different types of antennas from the global market will be reduced by a huge margin, which will grow up the high-tech industry of Bangladesh. Many popular Bangladeshi electronics brands including Walton Electronics, Singer Bangladesh, Jamuna Electronics, and Vision Electronics (PRAN-RFL Group) are developing different RF devices and exporting them to the global market. The local companies such as Butterfly Group, Rangs Group, Fair Group, and Transcom Group manufacture and assembles wireless Electronic devices, smartphones, TV, and other devices in collaboration with foreign brands such as Samsung, Whirlpool, LG, Sony, and Sharp. This research will aid the RF industry of Bangladesh to mark the place of Bangladesh in global tech-society and allow it to survive and thrive in competitive markets.

1.8 Thesis Organization

The parametric study of different shaped antennas is the primary consideration of this research. This work analyzed the performances of different shaped radiators of antennas along with defected ground structure. Here five different antennas are designed and simulated for applications of mm-wave and Sub-6GHz handheld wireless communications. In chapter 2, basic concept of microstrip patch antennas with different feeding techniques were described briefly, followed by an introduction of fundamental radiation parameters of conventional antenna. A wideband microstrip patch antenna with slotted ground plane is introduced in chapter 3 for 5G application in mm-wave. Chapter 4 describes a low profile microstrip patch antenna for mm-wave 5G. The antenna can be operated over a wider bandwidth of 5.85 GHz with the inclusion of defected ground structure or DGS. A spiral-shaped patch antenna with a compact size of $20 \times 20 \times 0.79$ mm³ is demonstrated in chapter 5 for Sub-6 GHz 5G and WIFI-5/6 applications where the spiral-shaped radiator and the partial ground plane facilitated to get omnidirectional radiation with high gain and directivity. Chapter 6 analyzed a rose-shaped patch antenna with a semi-circular slotted ground plane to get optimized parametric performances for Sub-6 GHz applications. In chapter 7, a slotted plus-shaped patch antenna is studied with defected ground structure for Sub-6 GHz/WiMAX applications where the DGS improves the current distribution

and proper impedance matching of the antenna. Finally, chapter 8 traces the conclusion of the research with future work plan.

REFERENCES

- [1] H. Yu, H. Lee and H. Jeon," What is 5G? Emerging 5G Mobile Services and Network Requirements", Sustainability, 2017 - mdpi.com.
- [2] B. Y. Zikria, S. W. Kim, M. K. Afzal, H. Wang, and M. H. Rehmani,"5G Mobile Services and Scenarios: Challenges and Solutions" Sustainability, vol 10, no. 3626, pp 1-9, 2018.
- [3] M. Agiwal, A. Roy and N. Saxena, "Next Generation 5G Wireless Networks: A Comprehensive Survey," in IEEE Communications Surveys & Tutorials, vol. 18, no. 3, pp. 1617-1655, third quarter 2016, doi: 10.1109/COMST.2016.2532458.
- [4] H.M. Marzouk, M.I. Ahmed, and A.A. Shaalan, "A Novel Dual-band 28/38 GHz slotted microstrip MIMO antenna for 5G mobile applications," Proceedings of the International Symposium on Antennas and Propagation and USNC-URSI Radio Science Meeting, 2019, pp. 607-608.
- [5] C. Han, G. Huang, T. Yuan, and C. Sim, "A Dual-Band Millimeter-Wave Antenna for 5G Mobile Applications," Proceedings of the IEEE International Symposium on Antennas and Propagation and USNC-URSI Radio Science Meeting, 2019.
- [6] J. L. Li, M. H. Luo, and H. Liu, "Design of a slot antenna for future 5G wireless communication systems," Proceedings of the Progress In Electromagnetics Research Symposium 2017, pp. 739-741.
- [7] F. Xiao, X. Lin, and Y. Su, "Dual-band structure-shared antenna with large frequency ratio for 5G communication applications," IEEE Antennas and Wireless Propagation Letters, vol. 19, no. 12, pp. 2339-2343, Dec. 2020.
- [8] R. Azim et al., "A multislotted antenna for LTE/5G Sub-6 GHz wireless communication applications," Int'l Journal of Microwave and Wireless Technologies, vol. 13, no. 5, pp.486–496, 2021.
- [9] R. Azim, R. Akter, A.K.M.M.H. Siddique, L. C. Paul, M.T. Islam, "Circular patch planar ultra-wideband antenna for 5G sub-6 GHz wireless communication applications," Journal of Optoelectronics and Advanced Materials, Vol. 23, no. 3-4, pp. 127-133, 2021.
- [10] A. K. Gautam, L. Kumar, B. K. Kanaujia and K. Rambabu, "Design of Compact F-Shaped Slot Triple-Band Antenna for WLAN/WiMAX Applications," in IEEE Transactions on Antennas and Propagation, vol. 64, no. 3, pp. 1101-1105, March 2016, doi: 10.1109/TAP.2015.2513099.
- [11] A. Kapoor, R. Mishra and P. Kumar, "Compact wideband-printed antenna for sub-6 GHz fifth generation applications", Int. Journal on Smart Sensing and Intelligent Systems, vol 13, no 1, pp. 1-10, 2020.

Chapter 1

- [12] J. Kulkarni and C. Y. D. Sim, "Wideband CPW-Fed Oval-Shaped Monopole Antenna for WiFi5 and Wi-Fi6 Applications," *Progress In Electromagnetics Research C*, vol. 107, pp. 173- 182, 2021.
- [13] I. Ishteyaq, I. S. Masoodi and K. Muzaffar, "A compact double-band planar printed slot antenna for sub-6 GHz 5G wireless applications," *Int. Journal of Microwave and Wireless Technologies*, vol 13, no 5, pp. 469 - 477, 2020.
- [14] Y. Li, Z. Zhao, Z. Tang, Y. Yin, "A low-profile, dual-band filtering antenna with high selectivity for 5G sub-6 GHz applications," *Microw Opt Technol Lett.*, vol. 61, pp. 2282– 2287, 2019.
- [15] M. Z. Mahmud, M. Samsuzzaman, L. C. Paul, M. R. Islam, Ayman A. Althuwayb, M. T. Islam, A dielectric resonator based line stripe miniaturized ultra-wideband antenna for fifth-generation applications, *International Journal of Communication Systems*, 10.1002/dac.5013, 34, 18, (2021).
- [16] Luk, Kwai-Man. "The importance of the new developments in antennas for wireless communications." *Proceedings of the IEEE* 99.12 (2011): 2082-2084.

Chapter - 2

ANTENNA BASIC CONCEPT AND PARAMETERS

2.1 Antenna

An antenna is a metallic device that captures and transmits electromagnetic waves (EM signal). It is a transitional equipment between free space and guiding structures (i.e., transmission line, coaxial line, waveguide etc.) [1]. In another words, an antenna is an electromagnetic transducer which can be used in transmitting mode to convert guided waves to radiated free space waves or to convert free-space waves to guided waves [2]. For the first case the antenna is called transmitting antenna and in the latter case the antenna is called receiving antenna though modern days antennas can be used for both purposes using different modes. Researcher are developed different types of antennas over the years such as:

- Wire Antennas
- Aperture Antennas
- Microstrip Antennas
- Array Antennas
- Reflector antennas
- Lens Antennas

Here in this work our main focus will be the Microstrip patch antennas more precisely planar antennas which are most popular among the researcher for their salient features.

2.2 Antenna Feeding Techniques

Different type of antennas can be fed by different methods. There are several feeding techniques of microstrip patch antennas to feed or transmit electromagnetic energy as shown in Fig. 2.2.1. The impact of feeding is very important to get optimum performances of antenna to improve the

antenna input impedance matching, return loss, bandwidth and other parameters [3]. The basic feeding techniques of microstrip patch antennas can be classified into two categories: (a) Contacting and (b) Non-contacting feeding. In the first case, the RF power is fed directly to the radiating patch using a connecting element such as a microstrip line or coaxial probe and in the latter non-contacting method, electromagnetic field coupling is done to transfer power. The four most popular feeding techniques used in terms of microstrip patch antennas are the microstrip line, coaxial probe (both contacting methods), aperture coupling and proximity coupling (both non-contacting methods) [4]. The effect of different feeding techniques in terms of parameters is shown in Fig. 2.2.2.

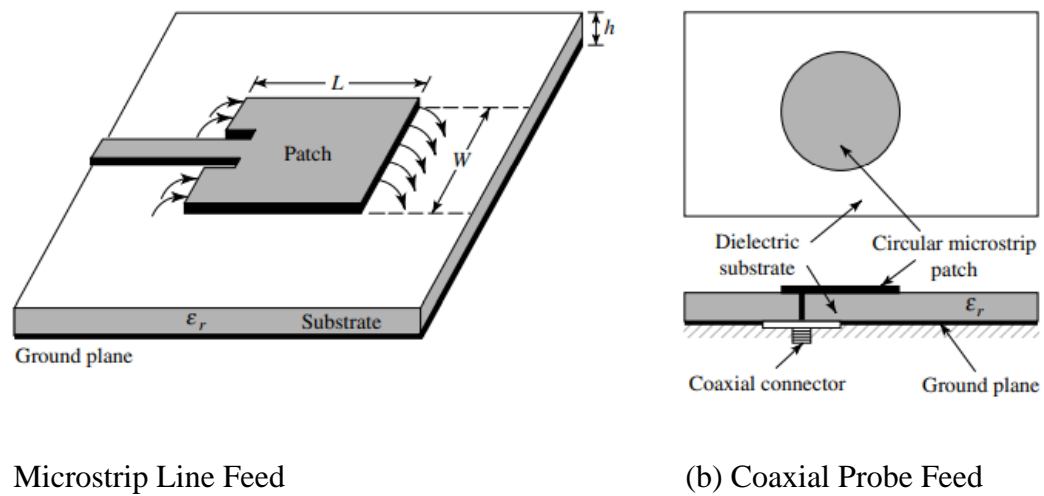
2.2.1 Microstrip Line Feed

In microstrip line feed technique, a conducting strip is connected directly to the edge of the radiating patch. The conducting strip is smaller in width as compared to the patch. This kind of feed arrangement has the advantage that the feed can be etched on the same substrate to provide a planer structure. However, increase the thickness of the dielectric substrate being used surface waves and spurious feed radiation also increases, which hampers the bandwidth 2-5% of the antenna. This feed radiation also leads to undesired cross polarized radiation. This method is advantageous due to its simple planar structure. The purpose of the inset cut in the patch is to match the impedance of the feed line to the patch input impedance without the need for any additional matching element. This can be achieved by properly adjusting the inset cut position and dimensions. Hence this is an easy feeding scheme because it provides ease of fabrication and simplicity in modelling as well as impedance matching [5].

2.2.2 Coaxial Probe Feed

The coaxial feed or probe feed is a very common technique used for feeding Microstrip patch antennas. The inner conductor of the coaxial connector extends through the dielectric and is soldered to the radiating patch, while the outer conductor is connected to the ground plane. The main advantage of this type of feeding scheme is that the feed can be placed at any desired

location inside the patch in order to match with its input impedance [1]. However, its major drawback is that it provides narrow bandwidth and is difficult to model since a hole has to be drilled in the substrate and the connector protrudes outside the ground plane, thus not making it completely planar for thick substrates. Also, for thicker substrates, the increased probe length makes the input impedance more inductive, leading to matching problems. It is seen above that for a thick dielectric substrate, which provides broad bandwidth, the microstrip line feed and the coaxial feed suffer from numerous disadvantages. So, to reduce these types of disadvantages, we will study non-contacting schemes [4].



(a) Microstrip Line Feed

(b) Coaxial Probe Feed

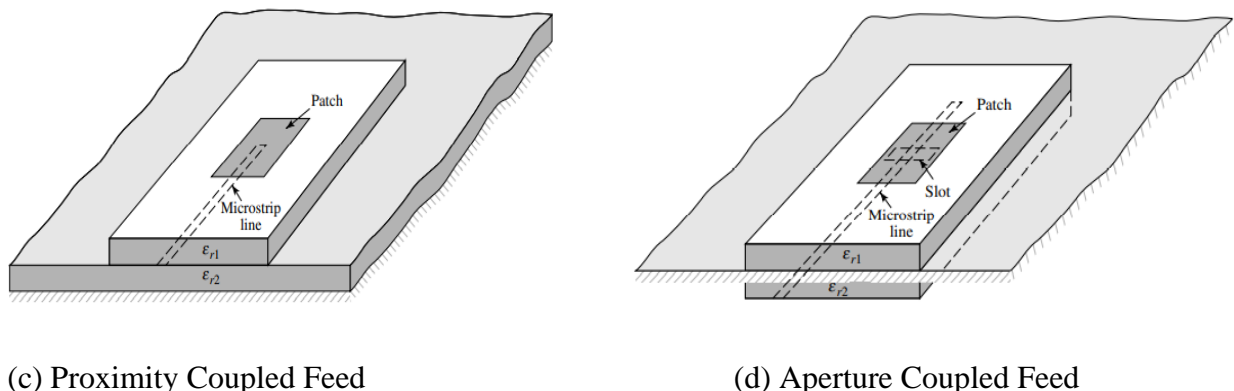


Fig. 2.2.1: Different feeding techniques for Microstrip Antennas.

2.2.3 Proximity Coupled Feed

This type of feed technique is also called as the electromagnetic coupling scheme. Two dielectric substrates are used such that the feed line is between the two substrates and the radiating patch is on top of the upper substrate. The main advantage of this feed technique is that it eliminates spurious feed radiation and provides very high bandwidth (as high as 13%) due to overall increase in the thickness of the microstrip patch antenna. This scheme also provides choices between two different dielectric media, one for the patch and one for the feed line to optimize the individual performances [4]. This method is advantageous to reduce harmonic radiation of microstrip patch antenna implemented in a multilayer substrate. Though it allows for planar feeding, less line radiation compared to microstrip feed, it requires multilayer fabrication, alignment is important for input match.

2.2.4 Aperture Coupled Feed

In this type of feed technique, the radiating patch and the microstrip feed line are separated by the ground plane as shown in figure 4 (A). Coupling between the patch and feed line is made through a slot or an aperture in the ground plane [1]. Variations in the coupling will depend upon the size i.e., length and width of the aperture. To optimize the result for wider bandwidths and better return losses. The coupling aperture is usually centred under the patch leading to lower cross-polarization due to symmetry of the configuration. Since the ground plane separates the patch and the feed line so spurious radiation is minimized. Aperture coupled feeding is attractive because of advantages such as no physical contact between the feed and radiator, wider bandwidths, and better isolation between antennas and the feed network. Furthermore, aperture-coupled feeding allows independent optimization of antennas and feed networks by using substrates of different thickness or permittivity.

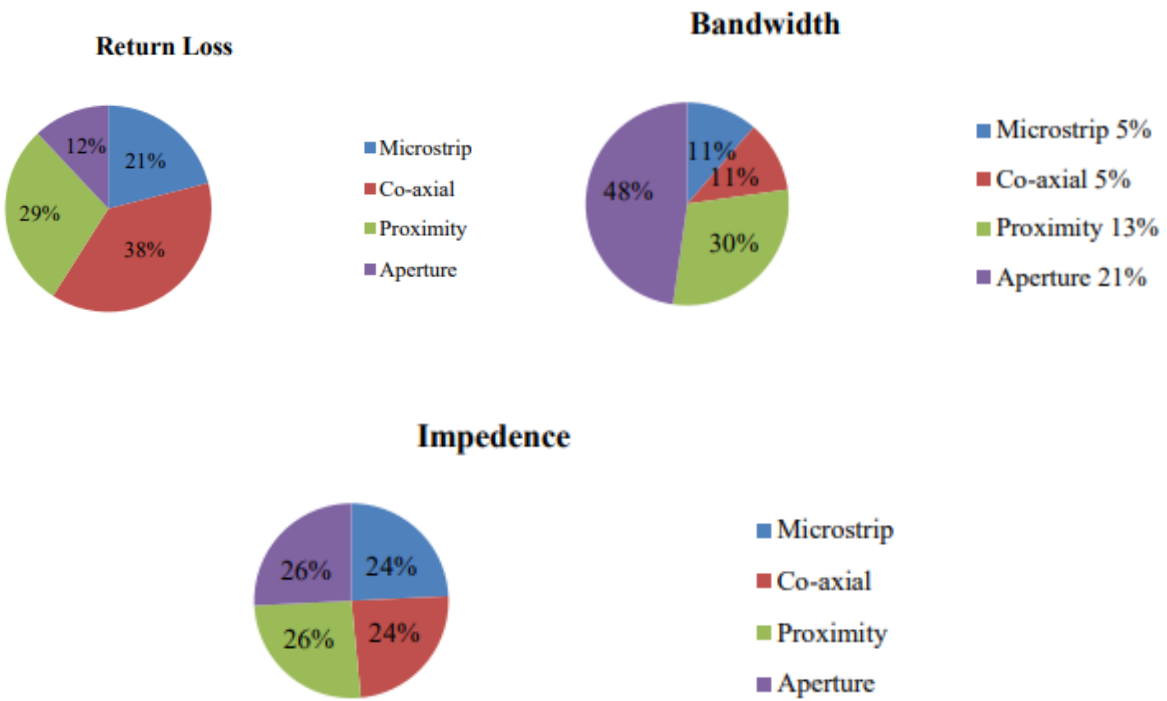


Fig. 2.2.2: Effect of feeding techniques on parameters.

2.3 Microstrip Patch Antennas

Microstrip patch antenna is one of the popular technologies in antennas and electromagnetic applications. It is widely used now days in the wireless communication system due to its low profile, simplicity and compatibility with printed circuit technology. Microstrip geometries were originally introduced in the 1950s [6]. A microstrip patch antenna consists of a conducting patch of any planar or non-planar geometry on one side of a dielectric substrate with a ground plane on the other side [7]. Microstrip or printed patch antennas are used in almost all wireless systems with recent advancements in printed circuit technology. The purpose of microstrip or patch antenna is to radiate and receive electromagnetic energy in microwave range and it plays an important role in wireless communication applications. The performance and operation of a microstrip antenna is dependent on the geometry of the printed patch and the material characteristics of the substrate onto which the antenna is printed.

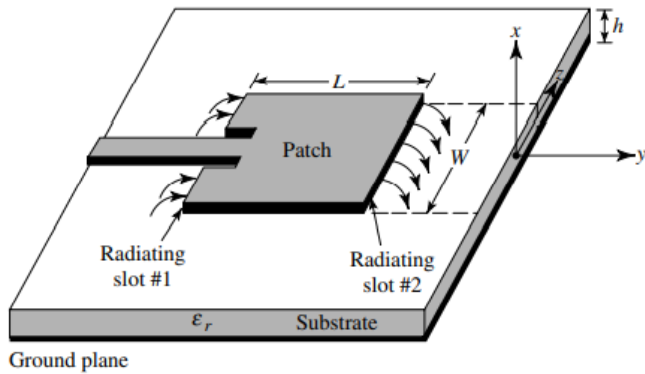


Fig. 2.3.1: Microstrip Patch Antenna.

Due to its planar configuration and ease of integration with microstrip technology, the microstrip patch antenna has been heavily studied and is often used as elements for an array. A large number of microstrip patch antennas have been studied to date [8]. An exhaustive list of the geometries along with their salient features is available. The rectangular and circular patches are the basic and most commonly used microstrip antennas. These patches are used for the simplest and the most demanding applications. Rectangular geometries are separable in nature and their analysis is also simple. The circular patch antenna has the advantage of their radiation pattern being symmetric.

2.3.1 Advantages of Microstrip Patch Antennas

Microstrip patch antennas (MPA) have several advantages compared to conventional antennas [6]. They can cover a wide range from 100MHz to 100GHz. Some of the principal advantages of MPAs are:

- i. They are light in weight.
- ii. They occupy low volume.
- iii. They are of low-profile planer configuration.
- iv. They can be made conformal to planar and non-planar surfaces.
- v. Their ease of mass production leads to a low fabrication cost.
- vi. They are easy to implement on the device.

- vii. They are easier to integrate with other MICs on the same substrate.
- viii. They allow both linear polarization and circular polarization with simple feed.
- ix. They can be made compact for use in personal mobile communication.
- x. They allow for dual- and triple-frequency operations.
- xi. They act as an efficient radiator.
- xii. They have low scattering cross section.
- xiii. They are mechanically robust when mounted on rigid surfaces.
- xiv. They are Resistant to shock and vibration.
- xv. They are well compatible for embedded antennas in handheld wireless devices.
- xvi. The feed line can be easily fabricated at the same time on the substrate.

2.3.2 Disadvantages of Microstrip Patch Antennas

However, Microstrip patch antennas also have some limitations as compared to conventional ones. These are:

- i. They have narrow bandwidth.
- ii. The efficiency is low.
- iii. They have low gain.
- iv. They have low power handling capacity.
- v. They have low isolation between radiating elements and feed.
- vi. Complex feed structure required for high performance arrays.
- vii. Large ohmic loss in the feed structure of arrays.
- viii. Extraneous radiation from feed and junctions.
- ix. Excitation of surface waves.
- x. Polarization purity is difficult to achieve.

However, there are methods, such as increasing the height of the substrate, that can be used to extend the efficiency (to as large as 90 percent if surface waves are not included) and bandwidth (up to about 35 percent).

2.3.3 Applications of Microstrip Patch Antennas

In high-performance aircraft, spacecraft, satellite, and missile applications, where size, weight, cost, performance, ease of installation, and aerodynamic profile are constraints, low-profile antennas may be required. Presently there are many other government and commercial applications, such as mobile radio and wireless communications, that have similar specifications. To meet these requirements, microstrip antennas are used in different applications such as:

- i. Satellite Communication and Direct Broadcast Service (DBS).
- ii. Mobile Communication Systems.
- iii. Doppler and other Radars.
- iv. Missile and Telemetry.
- v. Remote Sensing and Environmental Instrumentation.
- vi. Satellite Navigation Receivers.
- vii. Command and control systems.
- viii. Radio Altimeter.
- ix. Biomedical Radiators and Intruder Alarms.
- x. Personal Wireless Communication Systems and Service.

2.4 Planar Antennas

In general, all antennas comprising planar or curved surface radiators or their variations and at least one feed are termed 'planar antennas'. Printed microstrip patch antennas, slot antennas, suspended plate antennas, planar inverted-L and inverted-F antennas (PILAs and PIFAs), sheet monopoles and dipoles, roll monopoles, and so on, are typical planar antennas used extensively in wireless communication systems. Usually, they exhibit merits such as simple structure, low cost, low profile, small size, high polarization purity or broad bandwidth [9]. Planar antennas can be different types such as Planar Monopoles, Polygonal Monopoles, Elliptical Monopoles etc. [10].

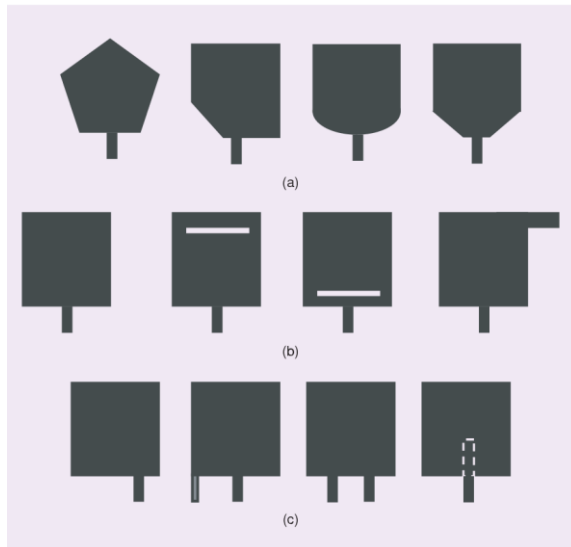


Fig. 2.4.1: Different types of planar antennas.

2.5 Fundamental Radiation Parameters of Antenna

Antenna radiation parameters describe the performance of the antenna that how good the antenna is for its respective applications. Antenna parameters are the measurement tools to characterize its performances. Some of the parameters are interrelated and not all of them need be specified for complete description of the antenna performance.

2.5.1 Directivity

Directivity is a fundamental antenna parameter. It is a measure of how 'directional' an antenna's radiation pattern is. An antenna that radiates equally in all directions would have effectively zero directionality, and the directivity of this type of antenna would be 1 (or 0 dB) [11]. The directivity of an antenna is defined as “the ratio of the radiation intensity U in a given direction from the antenna to the radiation intensity averaged over all directions. The average radiation intensity is equal to the total power P_{rad} radiated by the antenna divided by 4π . If the direction is not specified, the direction of maximum radiation intensity is implied.” Stated more simply, the directivity of a non-isotropic source is equal to the ratio of its radiation intensity U in a given

direction over the radiation intensity U_0 of an isotropic source. In mathematical form, it can be written as

$$D = \frac{U}{U_0} = \frac{4\pi U}{P_{rad}} \quad (2.5.1)$$

Directivity is a dimensionless ratio and may be expressed numerically or in decibels (dB). Directivity is identical to the peak value of the directive gain; these values are specified without respect to antenna efficiency thus differing from the power gain (or simply "gain") whose value is reduced by an antenna's efficiency. The directivity of an isotropic source is unity since its power is radiated equally well in all directions. For all other sources, the maximum directivity will always be greater than unity, and it is a relative "figure of merit" which gives an indication of the directional properties of the antenna as compared with those of an isotropic source [1].

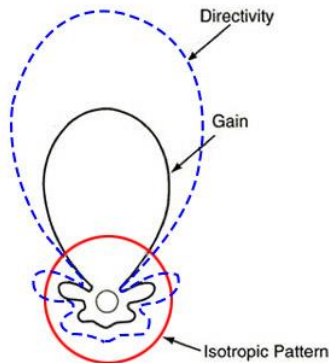


Fig. 2.5.1: Directivity and Gain.

2.5.2 Gain

The term Gain describes how much power is transmitted in the direction of peak radiation to that of an isotropic source. Antenna gain is more commonly quoted than directivity in an antenna's specification sheet because it takes into account the actual losses that occur. Although the gain of the antenna is closely related to the directivity, it is a measure that takes into account the efficiency of the antenna as well as its directional capabilities. Gain is one of the realized

quantities in antenna theory. In general, gain is less than directivity. It introduces ohmic and other losses [12].

Gain the ratio of the intensity, in a given direction, to the radiation intensity that would be obtained if the power accepted by the antenna were radiated isotropically. The radiation intensity corresponding to the isotropically radiated power is equal to the power accepted (input) by the antenna divided by 4π . In equation form this can be expressed as

$$\text{Gain} = 4\pi \frac{\text{radiation intensity}}{\text{total input (accepted)power}} \quad (2.5.2)$$

Gain is usually measured in dB. An antenna with a low gain emits radiation in all directions equally, whereas a high-gain antenna will preferentially radiate in particular directions. Antenna Gain (G) can be related to directivity (D) and antenna efficiency (ϵ_r) by:

$$G = \epsilon_r D \quad (2.5.3)$$

2.5.3 Antenna Efficiency

The efficiency of an antenna is a ratio of the power delivered to the antenna relative to the power radiated from the antenna. A high efficiency antenna has most of the power present at the antenna's input radiated away. A low efficiency antenna has most of the power absorbed as losses within the antenna, or reflected away due to impedance mismatch. Simply, an Antenna is meant to radiate power given at its input, with minimum losses. The efficiency of an antenna explains how much an antenna is able to deliver its output effectively with minimum losses in the transmission line. The mathematical expression for antenna efficiency is given below-

$$\eta_e = \frac{P_{rad}}{P_{input}} \quad (2.5.4)$$

Where η_e is the antenna efficiency, P_{rad} is the power radiated, P_{input} is the input power for the antenna. Being a ratio, antenna efficiency is a number between 0 and 1. However, antenna efficiency is commonly quoted in terms of a percentage; for example, an efficiency of 0.5 is the same as 50%. Antenna efficiency is also frequently quoted in decibels (dB); an efficiency of 0.1

is 10% or (-10 dB), and an efficiency of 0.5 or 50% is -3 dB. An antenna does not have an efficiency of 100% (or 0 dB). Antenna efficiency losses are typically due to:

- Conduction losses (due to finite conductivity of the metal that forms the antenna).
- Dielectric losses (due to conductivity of a dielectric material near an antenna).
- Impedance mismatch loss.

2.5.4 Radiation Pattern

An antenna radiation pattern or antenna pattern is defined as “a mathematical function or a graphical representation of the radiation properties of the antenna as a function of space coordinates. In most cases, the radiation pattern is determined in the far field region and is represented as a function of the directional coordinates. A radiation pattern defines the variation of the power radiated by an antenna as a function of the direction away from the antenna. This power variation as a function of the arrival angle is observed in the antenna's far field. Various parts of a radiation pattern are referred to as lobes, which may be sub classified into major or main, minor, side, and back lobes [1]. A radiation lobe is a “portion of the radiation pattern bounded by regions of relatively weak radiation intensity.”

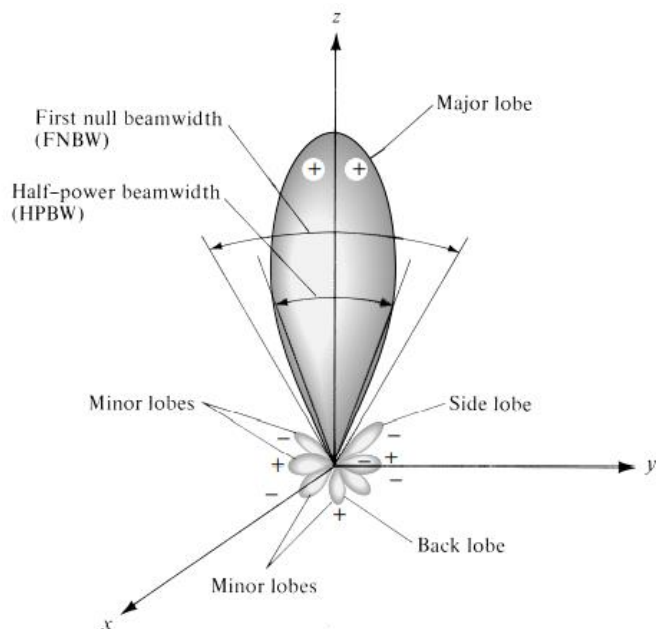


Fig. 2.5.2: Radiation pattern of a generic directional antenna.

A pattern is "isotropic" if the radiation pattern is the same in all directions. Antennas with isotropic radiation patterns don't exist in practice, but are sometimes discussed as a means of comparison with real antennas. Some antennas may also be described as "omnidirectional", which for an actual antenna means that the radiation pattern is isotropic in a single plane. Examples of omnidirectional antennas include the dipole antenna and the slot antenna and we will analyze various shaped planar omnidirectional antennas in the next chapters.

2.5.5 Reflection Coefficient

The reflection coefficient is a parameter that describes how much of an electromagnetic wave is reflected by an impedance discontinuity in the transmission medium. The reflection coefficient is a very useful quality when determining VSWR or investigating the match between. In the context of antennas and feeders, the reflection coefficient is defined as the figure that quantifies how much of an electromagnetic wave is reflected by an impedance discontinuity in the transmission medium. The reflection coefficient is equal to the ratio of the amplitude of the reflected wave to the incident wave. The reflection coefficient is usually denoted by the symbol gamma. Note that the magnitude of the reflection coefficient does not depend on the length of the line, only the load impedance and the impedance of the transmission line. Also, note that if $Z_L=Z_0$, then the line is "matched". In this case, there is no mismatch loss and all power is transferred to the load. At this point, you should begin to understand the importance of impedance matching: grossly mismatched impedances will lead to most of the power reflected away from the load.

2.5.6 VSWR

VSWR stands for Voltage Standing Wave Ratio, and is also referred to as Standing Wave Ratio (SWR). The VSWR is basically a measure of the impedance mismatch between the feeding system and the antenna. The higher the VSWR the greater is the mismatch. The minimum possible value of VSWR is unity and this corresponds to a perfect match. If the impedance of the antenna, the transmission line and the circuitry do not match with each other, then the power will

not be radiated effectively. Instead, some of the power is reflected back. VSWR is a function of the reflection coefficient, which describes the power reflected from the antenna.

$$\text{VSWR} = \frac{1+|\Gamma|}{1-|\Gamma|} \quad (2.5.5)$$

$$\Gamma = \frac{v_r}{v_i} = \frac{z_{in}-z_s}{z_{in}+z_s} \quad (2.5.6)$$

Where, Z_{in} = Input impedance of the antenna, Z_s = Source impedance, Γ = reflection coefficient, V_r = Amplitude of the reflected wave, V_i = Amplitude of the incident wave.

The VSWR is always a real and positive number for antennas. The smaller the VSWR is, the better the antenna is matched to the transmission line and the more power is delivered to the antenna. The minimum VSWR is 1.0. In this case, no power is reflected from the antenna, which is ideal. A practical antenna structure should have an input impedance of either 50 ohm or 75 Ohm since most radio equipment is built with this impedance. In general, if the VSWR is under 2 the antenna match is considered very good and little would be gained by impedance matching.

2.5.7 Return Loss

Return loss is the reflection of the power of a signal, when it is entered in a transmission line. RL is a parameter similar to the VSWR to indicate how well the matching is between the feeding system, the transmission lines, and the antenna. The RL is

$$RL = -20 \log |\Gamma| (\text{dB}) \quad (2.5.7)$$

To obtain perfect matching between the feeding system and the antenna, $\Gamma = 0$ is required and therefore, from the equation above, $RL = \text{infinity}$. In such a case no power is reflected back. Similarly, at $\Gamma = 1$, $RL = 0 \text{ dB}$, implies that all incident power is reflected. Usually return losses ranging from 10 dB to 12 dB are acceptable. For practical applications a VSWR of 2 is acceptable and this corresponds to a return loss of 9.54 dB [3].

2.5.8 Bandwidth

IEEE defines bandwidth as “The range of frequencies within which the performance of the antenna, with respect to some characteristic, conforms to a specified standard.” The bandwidth can be considered to be the range of frequencies, on either side of a center frequency (usually the resonance frequency for a dipole), where the antenna characteristics (such as input impedance, pattern, beamwidth, polarization, side lobe level, gain, beam direction, radiation efficiency) are within an acceptable value of those at the center frequency. Often, the desired bandwidth is one of the determining parameters used to decide upon an antenna. For instance, many antenna types have very narrow bandwidths and cannot be used for wideband operation. The bandwidth of an antenna is the range of frequencies over which the antenna can operate properly [12]. If the highest frequency of the band is FH, lowest frequency of the band is FL and the center frequency of the band is FC, then bandwidth can be defined as,

$$BW = 100 \times (FH - FL) / FC \quad (2.5.8)$$

The bandwidth can also be specified as the frequency range over which the VSWR is less than 2 (which corresponds to a return loss of 9.5 dB or 11 % reflected power). Sometimes for stringent applications, the VSWR requirement is specified to be less than 1.5 (which corresponds to a return loss of 14 dB or 4 % reflected power) [3].

$$BW = \frac{VSWR-1}{Q\sqrt{VSWR}} \quad (2.5.9)$$

2.5.9 Impedance Matching

Impedance Matching is the process of removing mismatch loss. That is, we want to minimize the reflection coefficient, to reduce the power reflected from the load (the antenna), and maximize the power delivered to the antenna. This is one of the fundamental tasks in getting an antenna to radiate, and hence is one of the more important topics in antenna theory. To achieve perfect matching, we want the antenna or load impedance to match the transmission line. That is, we want $Z_L=Z_0$ (or $Z_{in}=Z_0$). In Smith Chart terms, we want to move the impedance Z_L towards the center of the Smith Chart, where the reflection coefficient Γ is zero. According to the standard

definition, “The approximate value of impedance of a transmitter, when equals the approximate value of the impedance of a receiver, or vice versa, it is termed as Impedance matching.” Impedance matching is necessary between the antenna and the circuitry. The impedance of the antenna, the transmission line, and the circuitry should match so that maximum power transfer takes place between the antenna and the receiver or the transmitter.

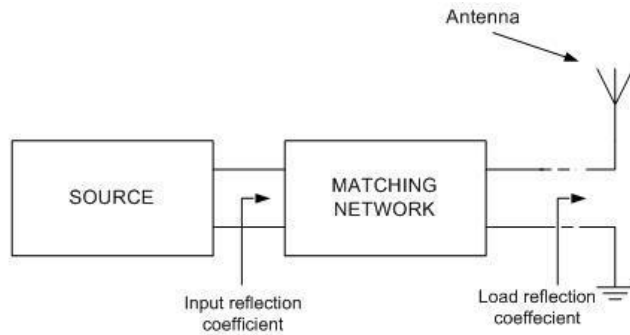


Fig. 2.5.3: Impedance matching of antenna.

2.5.10 Polarization

Polarization is one of the fundamental characteristics of any antenna. Polarization of an antenna in a given direction is defined as “the polarization of the wave transmitted (radiated) by the antenna. Note: When the direction is not stated, the polarization is taken to be the polarization in the direction of maximum gain.” In practice, polarization of the radiated energy varies with the direction from the center of the antenna, so that different parts of the pattern may have different polarizations. Polarization of a radiated wave is defined as “that property of an electromagnetic wave describing the time-varying direction and relative magnitude of the electric-field vector; specifically, the figure traced as a function of time by the extremity of the vector at a fixed location in space, and the sense in which it is traced, as observed along the direction of propagation.” Polarization may be classified as linear, circular, or elliptical as shown in Fig. 2.5.4 [1].

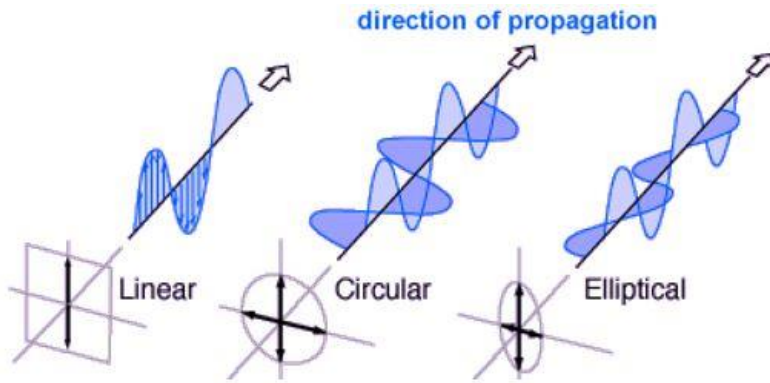


Fig. 2.5.4: Commonly used Polarization schemes.

- **Linear Polarization:** A time-harmonic wave is linearly polarized at a given point in space if the electric-field (or magnetic-field) vector at that point is always oriented along the same straight line at every instant of time. It is a type of polarization in which all the waves possess similar alignment in space either vertical or horizontal .
- **Circular Polarization:** A time-harmonic wave is circularly polarized at a given point in space if the electric (or magnetic) field vector at that point traces a circle as a function of time. Antennas that are designed to radiate horizontally, vertically along with all planes in between are called circularly polarized antenna.
- **Elliptical Polarization:** A time-harmonic wave is elliptically polarized if the tip of the field vector (electric or magnetic) traces an elliptical locus in space. Elliptically polarized waves are again generated from the two linearly polarized waves like the circularly polarized waves.

This simple concept is important for antenna to antenna communication that a horizontally polarized antenna will not communicate with a vertically polarized antenna. Due to the reciprocity theorem, antennas transmit and receive in exactly the same manner. Hence, a vertically polarized antenna transmits and receives vertically polarized fields. Consequently, if a horizontally polarized antenna is trying to communicate with a vertically polarized antenna, there will be no reception.

2.5.11 Front to Back Ratio

The Front to Back Ratio (F/B Ratio) of an antenna is the ratio of power radiated in the front/main radiation lobe and the power radiated in the opposite direction (180 degrees from the main beam).

$$\text{Front to Back Ratio} = \frac{\text{Forward Power (F)}}{\text{Backward Power (B)}} \quad (2.5.10)$$

This ratio tells us the extent of backward radiation and is normally expressed in dB. This parameter is important in circumstances where interference or coverage in the reverse direction needs to be minimized. It is a parameter used in describing directional radiation patterns for antennas. If an antenna has a unique maximum direction, the front-to-back ratio is the ratio of the gain in the maximum direction to that in the opposite direction. This parameter is usually given in dB.

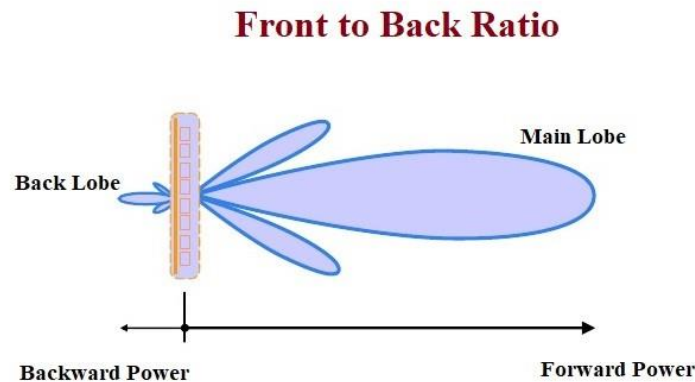


Fig. 2.5.5: Front to Back Ratio of antenna.

2.5.12 Axial Ratio

The Axial Ratio (AR) of an antenna is defined as the ratio between the major and minor axis of a circularly polarized antenna pattern. If an antenna has perfect circular polarization then this ratio would be 1 (0 dB). However, if the antenna has an elliptical polarization then this ratio would be greater than 1 (>0 dB).

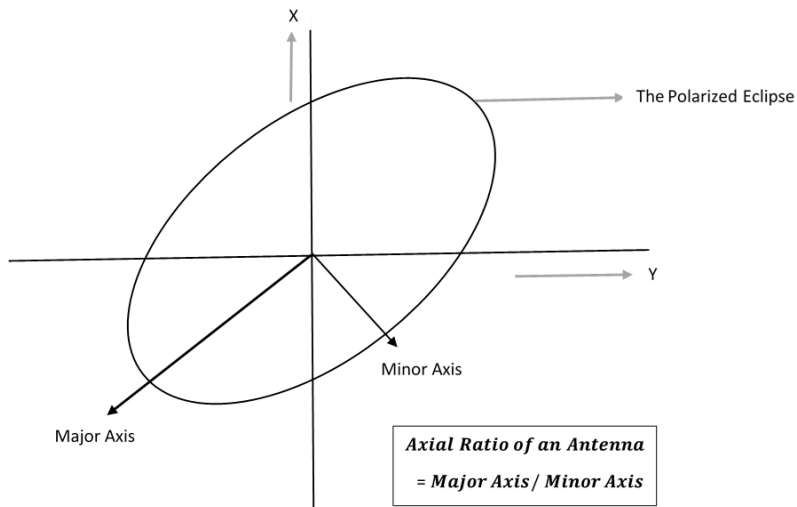


Fig. 2.5.6: Axial Ratio of antenna.

This ratio tells us the deviation of an antenna from the ideal case of circular polarization over a specified angular range. For example: ‘Axial Ratio: <1.25 dB for $\pm 20^\circ$ from main beam’- this indicated that the antenna deviation from the main beam is less than 1.25 dB in the that given 20° . Typically, axial ratios are quoted for circularly polarised antennas [13].

2.5.13 Surface Current

A surface current is an approximation. In metallic antennas, the surface current is an actual electric current that is induced by an applied electromagnetic field. The electric field pushes charges around. Pretty much any simulation package that handles metals will be able to visualize the surface current for you. The method of moments, for example, works by calculating the surface current on conductors. The current distribution of planar patch antennas are represented in surface current.

2.6 Substrate of Microstrip Patch Antenna

Substrate is a base or container on which microstrip patch (metallic sheet) antenna is fabricated and it plays important role in microstrip antenna functioning. In case of microstrip patch antenna,

the substrate is need to create a separation between two metal surfaces and thus facilitate electric field Generation. From maxwell equation, this E-Field leads to generation of magnetic field and finally an electromagnetic wave is generated and we call it as radiation in case of antennas. The substrate in microstrip antennas is also needed for the mechanical support of the antenna. To provide this support, the substrate should consist of a dielectric material, which may affect the electrical performance of the antenna, circuits and transmission line. A substrate must, therefore, simultaneously satisfy the electrical and mechanical requirements, which is sometimes difficult to meet. Right substrate selection is a must on the basis of cost, efficiency and size. Patch antenna is fabricated by etching the antenna element pattern in metal trace bonded to an insulating dielectric substrate with a continuous metal layer bonded to the opposite side of the substrate which forms a ground plane. However, Substrate (dielectrics) are used for improved electrical and mechanical stability. Here in this we used Rogers RT5880 as substrate of different shaped planar patch antennas.

2.6.1 Rogers RT5880

Rogers RT5880 has a low dielectric constant and low dielectric loss or loss tangent, making them well suited for high frequency/broadband applications [14]. In this work we have analyzed parametric study of different shaped planar antennas based on Rogers RT5880 substrate. Rogers RT5880 is a popular substrate among antenna researchers for its salient features and performances. It has a good dielectric constant of 2.2, loss tangent of 0.0009 and thermal conductivity of 0.2 W/k/m. There are several benefits of using Rogers RT5880 as substrate such as:

1. Lowest electrical loss.
2. Low moisture absorption that is why ideal for high moisture environments.
3. Isotropic.
4. Uniform electrical properties over frequency.
5. Excellent chemical resistance.
6. Lead free process compatible.
7. Easily cut, shared and machined to shape.

2.7 Simulation Tool (CST Microwave Studio Suite)

The computer simulation technology (CST) microwave studio suite software is used to design and simulate all the planar antennas in this work. CST MICROWAVE STUDIO® (CST MWS) is a specialist tool for the 3D EM simulation of high frequency components. CST MWS enables the fast and accurate analysis of high frequency (HF) devices such as antennas, filters, couplers, planar and multi-layer structures and SI and EMC effects. CST MWS quickly gives you an insight into the EM behavior of high frequency designs and offers further solver modules for specific applications. It can be embedded in various industry standard workflows through the CST user interface.

CST software makes available Time Domain and Frequency Domain solvers, CST MWS offers further solver modules for specific applications. It has a vast built-in material library and several built-in phantoms. Filters for the import of specific CAD files and the extraction of SPICE parameters enhance design possibilities and save time. Electromagnetic field solvers for applications across the EM spectrum are contained within a single user interface in CST Studio Suite. The solvers can be coupled to perform hybrid simulations, giving engineers the flexibility to analyze whole systems made up of multiple components in an efficient and straightforward way. CST Studio Suite is used in leading technology and engineering companies around the world. It offers considerable product to market advantages, facilitating shorter development cycles and reduced costs. Simulation enables the use of virtual prototyping. Device performance can be optimized, potential compliance issues identified and mitigated early in the design process, the number of physical prototypes required can be reduced, and the risk of test failures and recalls minimized.

REFERENCES

- [1] Constantine A. Balanis. Antenna Theory Analysis and Design (2005) by John Wiley & Sons.
- [2] Fang, D. G. (2017). Antenna theory and microstrip antennas. CRC Press.
- [3] Varshney, H. Kumar, et al. "A survey on different feeding techniques of rectangular microstrip patch antenna." International Journal of Current Engineering and Technology 4.3 (2014): 1418-1423.

- [4] Kumar, Amit, J. Kaur, and R. Singh. "Performance analysis of different feeding techniques." International journal of emerging technology and advanced engineering 3.3 (2013): 884-890.
- [5] Singh, Gurdeep, and J. Singh. "Comparative analysis of microstrip patch antenna with different feeding techniques." International Conference on Recent Advances and Future Trends in Information Technology (iRAFIT2012) Proceedings published in International Journal of Computer Applications®(IJCA). 2012.
- [6] Mishra, Ranjan. "An overview of microstrip antenna." HCTL Open International Journal of Technology Innovations and Research (IJTIR) 21.2 (2016): 1-17.
- [7] Garg, Ramesh, et al. Microstrip antenna design handbook. Artech house, 2001.
- [8] Singh, Indrasen, and V. S. Tripathi. "Micro strip patch antenna and its applications: a survey." Int. J. Comp. Tech. Appl 2.5 (2011): 1595-1599.
- [9] Chen, Z. Ning, and M. Y. W. Chia. Broadband planar antennas: design and applications. John Wiley & Sons, 2006.
- [10] Chen, Zhi Ning, et al. "Planar antennas." IEEE microwave magazine 7.6 (2006): 63-73.
- [11] <https://www.antenna-theory.com/basics/directivity.php>
- [12] Raithatha, Udit, and S. S. Kashyap. "Microstrip Patch Antenna Parameters, Feeding Techniques & Shapes of the Patch-A Survey." International Journal of Scientific & Engineering Research 6.4 (2015).
- [13] <https://www.everythingrf.com/community/what-is-axial-ratio-of-an-antenna>
- [14] <https://rogerscorp.com/advanced-electronics-solutions/rt-duroid-laminates/rt-duroid-5880-laminates>

Chapter - 3

A WIDEBAND MICROSTRIP PATCH ANTENNA WITH SLOTTED GROUND PLANE FOR 5G APPLICATION

3.1 Abstract

A wide band microstrip patch antenna has been designed and presented for fifth generation (5G) wireless application. The proposed antenna is etched on Rogers RT 5880 (lossy) dielectric substrate material (dielectric constant of 2.2, loss tangent of 0.0009) having compact size of $20 \times 20 \times 0.79$ mm³. It shows gain of 5.22 dB, directivity of 7.48 dBi and VSWR of 1.036 at resonant frequency 27.47 GHz. Slots on the metallic ground plane are made to enhance the intended performance parameters including larger bandwidth and better impedance matching of the antenna. The antenna presents very good return loss (-35.03 dB at resonant frequency 27.47 GHz) over a wideband of mm-wave operating frequency ranging from 26.154 GHz to 31 GHz. Due to the scope of obtaining large bandwidth in mm-wave, it is possible to gain a huge amount of data rate at lower latency in 5G technology and the proposed antenna provides a large bandwidth of 4.846 GHz for mm-wave 5G application.

3.2 Introduction

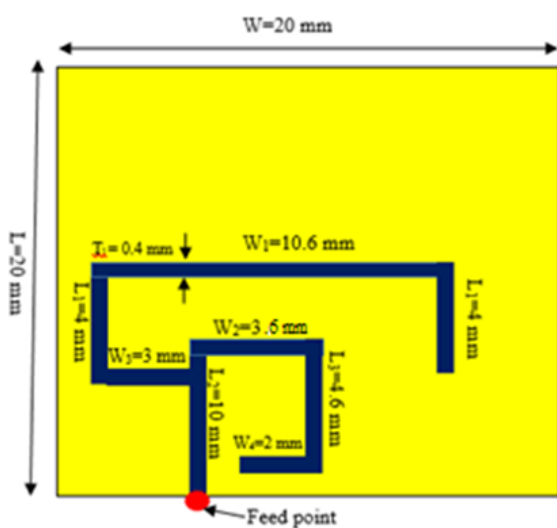
At present, the higher throughput with lower latency in wireless communications is necessary for billion-billion mobile devices and Internet of Things (IoT) that leads the transition of 4G technologies to 5G technologies [1-4]. The key performance indicators (KPI) in 4G such as traffic volume density, data rate, spectral efficiency, energy efficiency are very combatively much poorer than 5G technologies. The 5G technologies enhance the performance of 4G especially speed of the mobile network due to its huge bandwidth option. To support the high data rate, the millimetre wave (mm-wave) band is a promising option due to its high bandwidth [5-7]. Since the lower frequency (LF) bands are occupied and spectral crunch occurs at LF bands,

technologies are switched to mm-wave bands [8]. To mitigate spectral crunch and unlicensed option of mm-wave, it attracts the researcher to deploy various 5G antennas to support huge data traffic for 5G technologies. According to the Shannon's noisy channel capacity formula, $C = B\log_2(1 + SNR)$, the data rate for wireless communications solely depends on bandwidth and signal to noise ratio (SNR) [9]. Therefore, due to the scope of obtaining large bandwidth in mm-wave, it is possible to gain a huge amount of data rate at lower latency in 5G technology. To achieve high gain with large bandwidth, microstrip patch antenna is a suitable candidate [10]. In any wireless communications, microstrip antenna is an attractive choice due to its ease to fabrication, lower volume and low cost facilities. Many researchers are exploiting mm-wave microstrip antennas for 5G communications. In [11], a microstrip patch antenna is proposed at 28 GHz with dimension $55 \times 115 \text{ mm}^2$ for 5G mobile applications. A 28/38 GHz slotted microstrip antenna is introduced in [12] with an acceptable antenna gain (7.88 dB) but lower in bandwidth (1.4306 GHz). The Rogers RT 5880 material is used to simulate this antenna in the CST microwave studio suite. The overall dimension of this antenna is $55 \times 110 \text{ mm}^2$. An aperture coupled microstrip antenna at centre frequency of 28 GHz is proposed in [13] with overall dimension $18 \times 14 \text{ mm}^2$ with peak simulation gain of 6.5 dB. A square-shaped slot antenna is proposed in [14] for 5G applications. Although the dimension of the antenna is moderate and built in Rogers RT 5880 substrate with thickness 0.127 mm, the gain of this antenna is comparatively lower and it is 4 dB at 28 GHz. Two hexagonal grid antennas having 10 cells and 12 cells are designed and analysed in [15] for 28 GHz 5G communication.

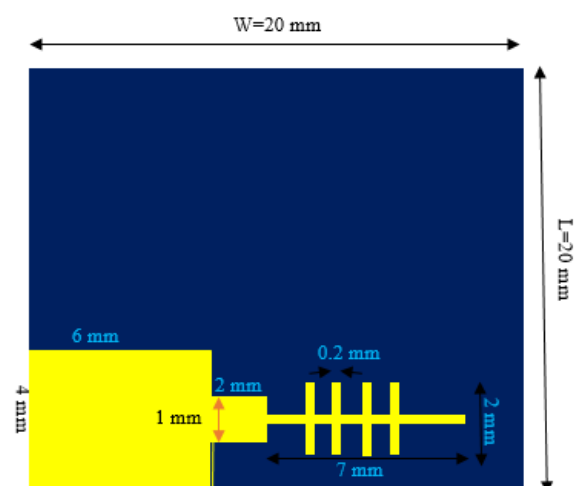
The main contribution of this chapter is to design a slotted ground plane microstrip patch antenna at centre frequency of 27.47 GHz with large bandwidth of 4.846 GHz (26.154 GHz - 31 GHz) to support high data rates for future 5G applications with optimum antenna size. The rest of the chapter is organized as follows: the design of the proposed antenna is introduced in section 3.3. Necessary simulated results and performance analysis of the antenna are presented in section 3.4. At last, in section 3.5, some concluding remarks and future scope of this research work are presented.

3.3 Design of Wideband 5G Antenna

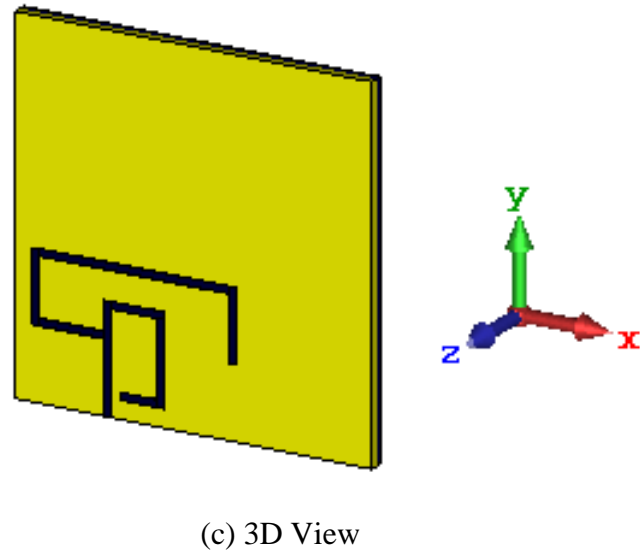
The computer simulation technology (CST) microwave studio suite software is used to design and simulate the proposed antenna. The Rogers RT 5880 (lossy) material with dielectric constant of 2.2, loss tangent of 0.0009 and thickness of 0.79 mm is used as the substrate of the designed antenna. Copper (annealed) material is used to design the main radiating element as well as the ground plane of the antenna. Both the radiating element and the ground plane have thickness of 0.035 mm. The width of the radiating element of the patch is 0.4 mm and the largest horizontal line length is 10.6 mm. The horizontal and vertical lines generate inductive and capacitive impedance that effectively matches with the port impedance. The overall volume of dimension of the antenna is $20 \times 20 \times 0.79$ mm³. The schematic front view of the designed antenna with all the dimensions is shown in Fig. 3.3.1 (a).



(a) Front View



(b) Back View



(c) 3D View

Fig. 3.3.1: Proposed slotted ground 5G antenna. (a) Front view, (b) Back view, (c) 3D view.

Back view and the 3D view of the proposed antenna are presented in Fig.3.3.1 (b) and Fig.3.3.1 (c) respectively. From the front view, it is seen that each radiating line has width 0.4 mm while in the back view the width of the slot in the ground plane is 0.2 mm. The length of each slot is 2 mm. The spacing between the slots is adjusted and obtains the resonance at 27.47 GHz which covers 28 GHz 5G band. The dimensional parameters of the designed 5G antenna are mentioned in the following table 3.3.1.

TABLE 3.3.1: DESIGN SUMMARY OF PROPOSED WIDEBAND PATCH ANTENNA FOR 5G.

Antenna Parameters	Length in mm
W	20
L	20
W ₁	10.6
W ₂	3

W_3	3.6
W_4	2
L_1	4
L_2	10
L_3	4.6
T_1	0.4

3.4 Analysis of Simulation Results

The return loss curve of the proposed wide band 5G antenna is shown in Fig. 3.4.1 which indicates that the resonant frequency is 27.47 GHz and bandwidth (-10 dB) is 4.846 GHz ranging from 26.154 GHz to 31 GHz. Fig. 3.4.2 shows the voltage standing wave ratio (VSWR) of the proposed antenna. It is evident that the VSWR value is 1.036 at the resonant frequency of 27.47 GHz which ensures the good impedance matching of the antenna.

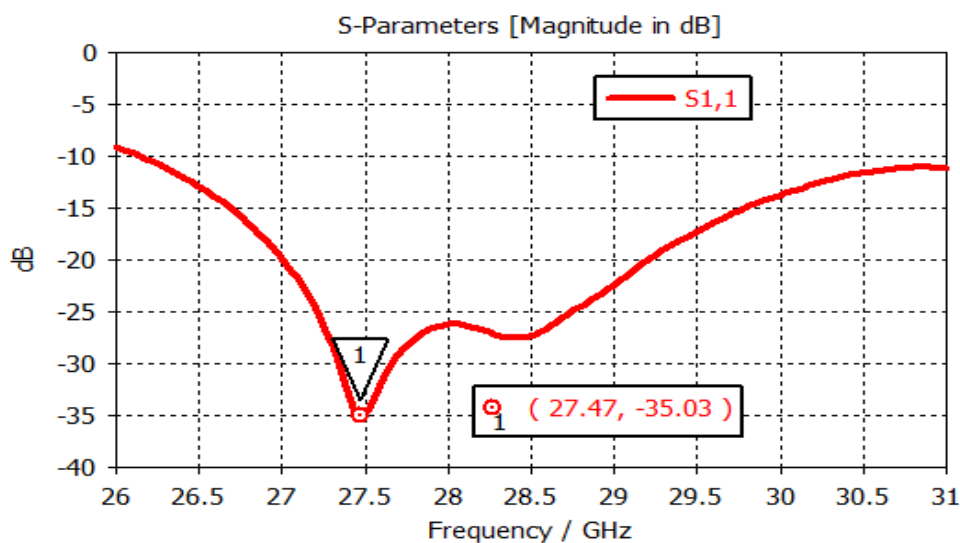


Fig. 3.4.1: S₁₁ curve of the proposed 5G antenna.

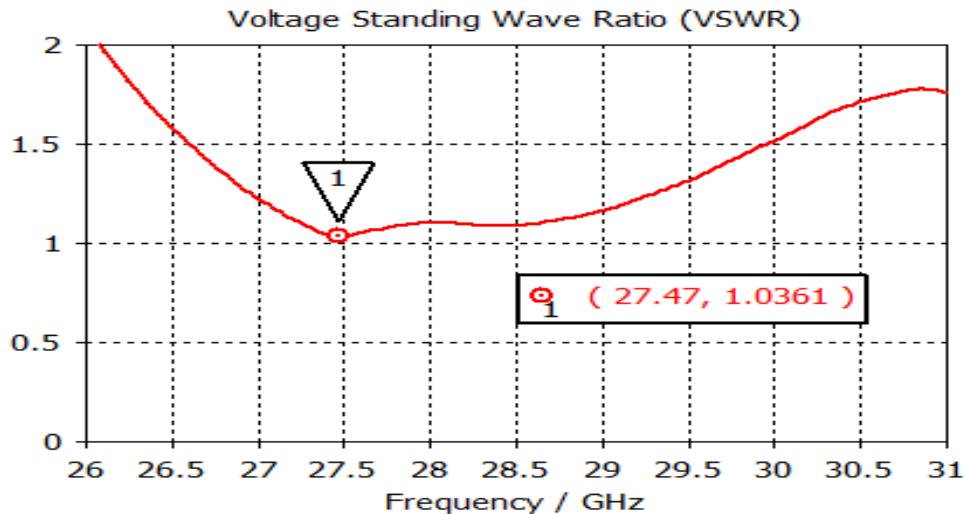


Fig. 3.4.2: VSWR of the proposed 5G antenna.

The 3D gain and directivity of the antenna are shown in Fig. 3.4.3. and Fig. 3.4.4 thereafter the gain and directivity Vs frequency is shown in Fig. 3.4.5. At the resonant frequency the gain and directivity are 5.22 dB and 7.48 dBi, respectively. The gain and directivity varies from 4.7 dB to 6.1 dB and 5.8 dBi to 7.8 dBi, respectively, within the large operating frequency band ranging from 26.154 GHz to 31 GHz which makes the proposed antenna usable for 5G applications.

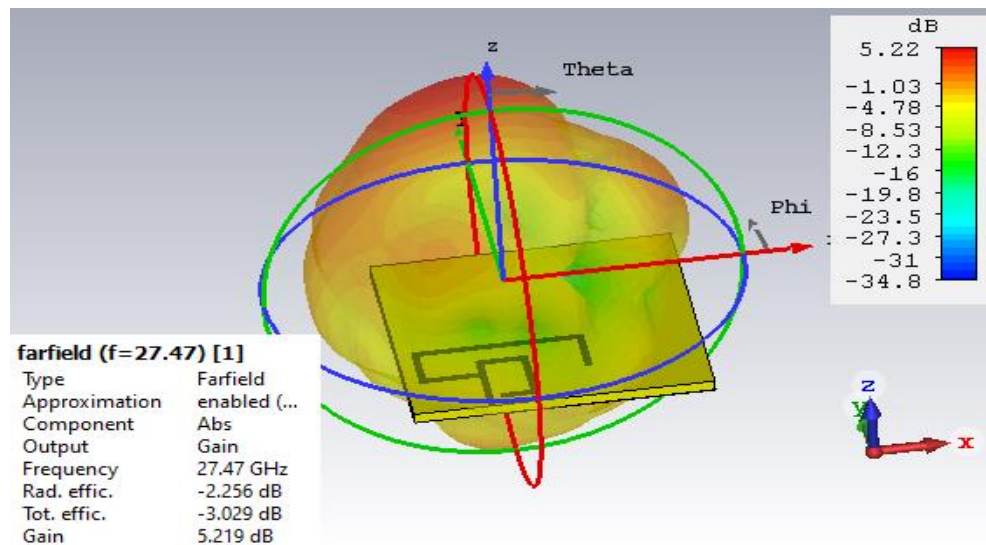
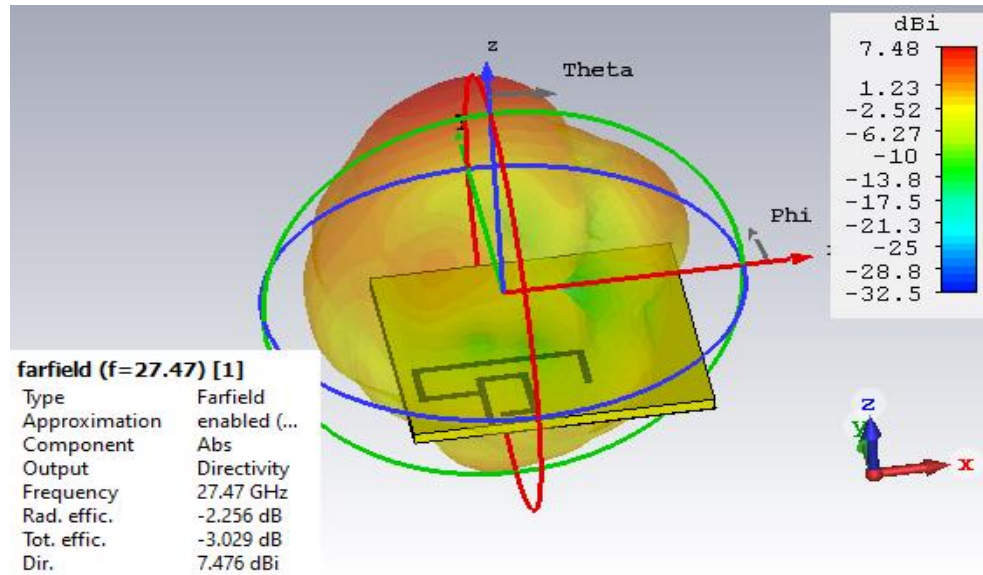
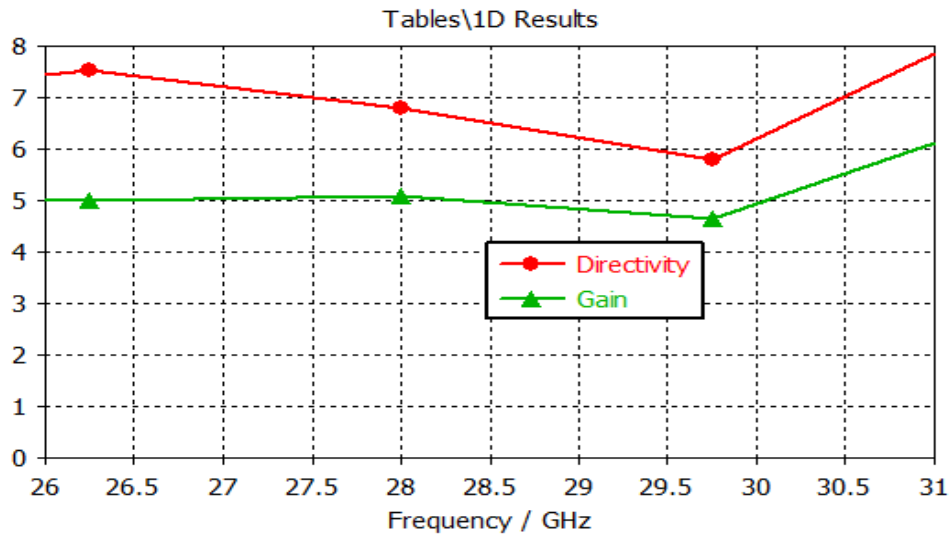
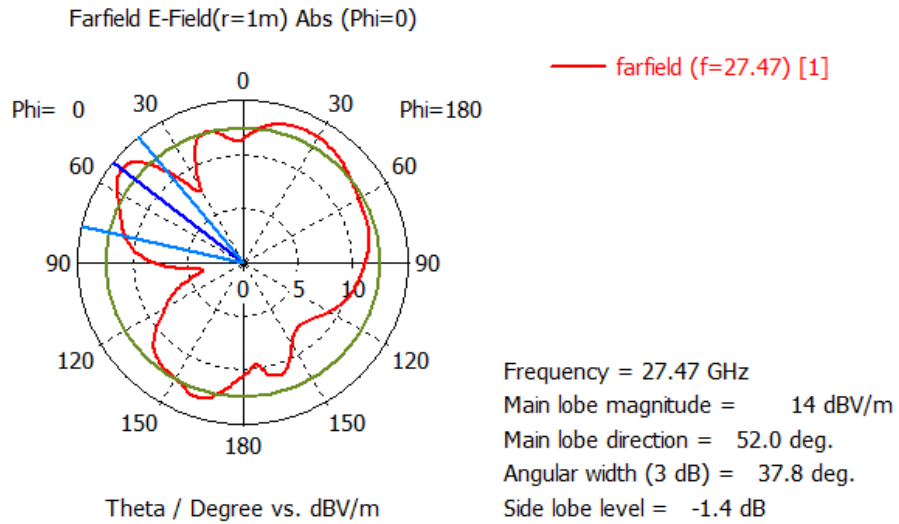


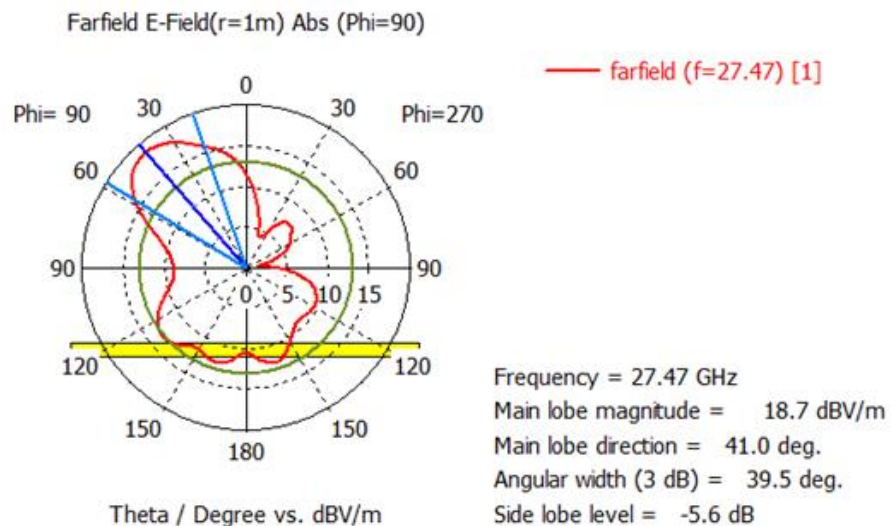
Fig. 3.4.3: 3D Gain at 27.47 GHz of the proposed antenna.

**Fig. 3.4.4:** 3D Directivity at 27.47 GHz of the proposed antenna.**Fig. 3.4.5:** Gain and directivity Vs frequency of the proposed 5G antenna.

The polar plots of radiation pattern of electric field (E field) at azimuth angle $\phi=0^0$ and $\phi=90^0$ are shown in Fig. 3.4.6 (a, b) at resonant frequency of 27.47 GHz.



(a) E-Field at $\phi = 0^\circ$



(b) E-Field at $\phi = 90^\circ$

Fig. 3.4.6: E field pattern of the proposed 5G antenna.

In Fig. 3.4.7 (a, b) the magnetic field (H field) at $\phi=0^\circ$ and $\phi=90^\circ$ are presented. From the E field pattern, it is clear that the lowest side lobe level (LSLL) is -5.6 dB and the maximum half power beam width (HPBW) is 39.5° at $\phi=90^\circ$. At $\phi=0^\circ$, the main lobe magnitude is 14 dBV/m for E field pattern and -37.5 dBA/m for H filed pattern Similarly, at $\phi=90^\circ$ the main lobe magnitude is

18.7 dBV/m for E field pattern and -32.8 dBA/m for H field pattern. For $\phi=0^0$, the main lobe is directed at 52^0 while for $\phi=90^0$ the main lobe is directed at 41^0 .

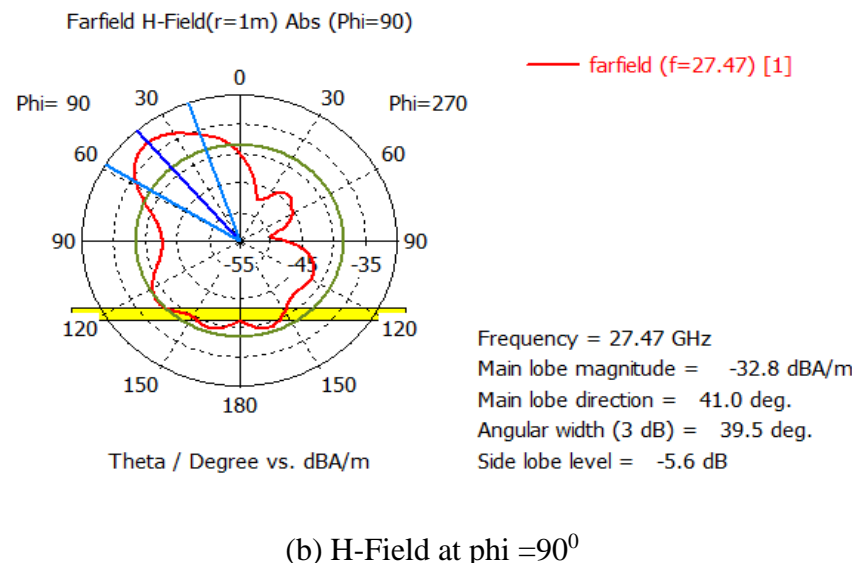
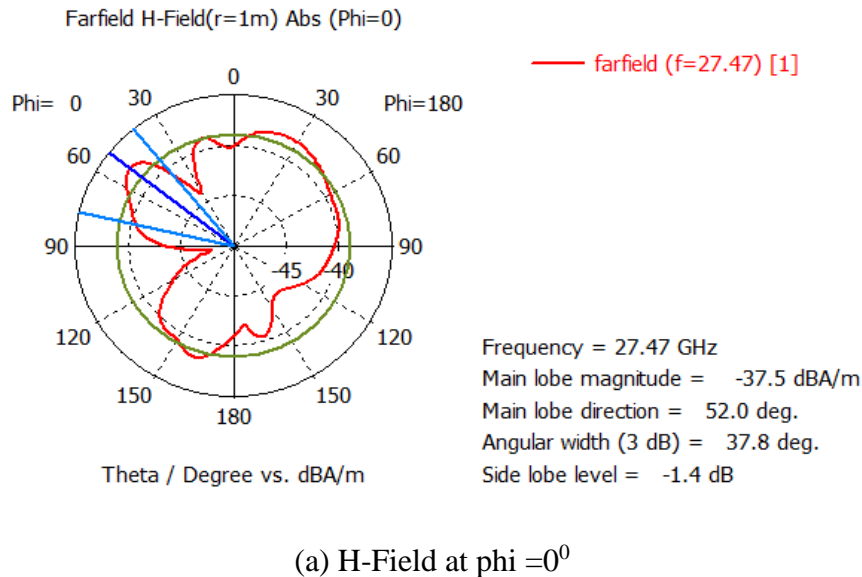


Fig. 3.4.7: H-Field pattern of the proposed 5G antenna.

The radiation efficiency of the proposed 5G antenna with a slotted ground plane is shown Fig. 3.4.8. The radiation efficiency is the ratio of gain to directivity (G/D). From Fig. 3.4.8, the average radiation efficiency is near about 70% (varies from 57% to 77%) which ensures a very good percentage of input power is radiated by the proposed 5G antenna.

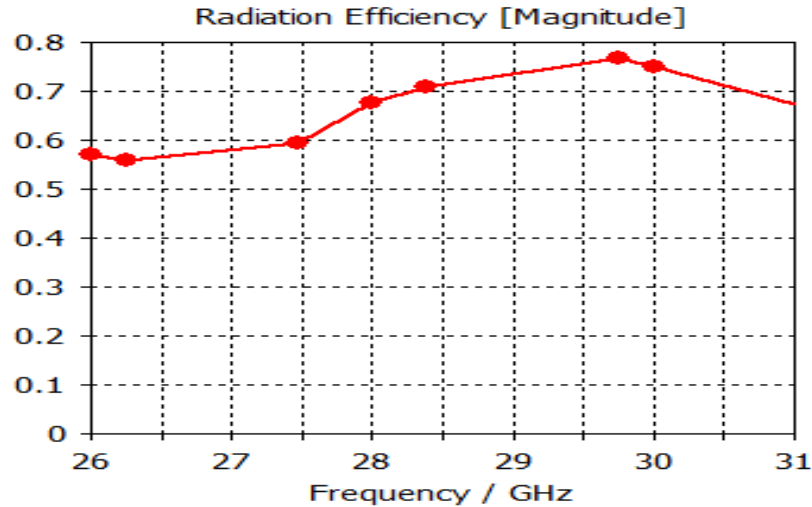


Fig. 3.4.8: Radiation Efficiency.

The Z- parameters of the proposed antenna are shown in Fig. 3.4.9. which indicates that the real part is close to 50Ω and imaginary part is close to 0 at 27.47 GHz.

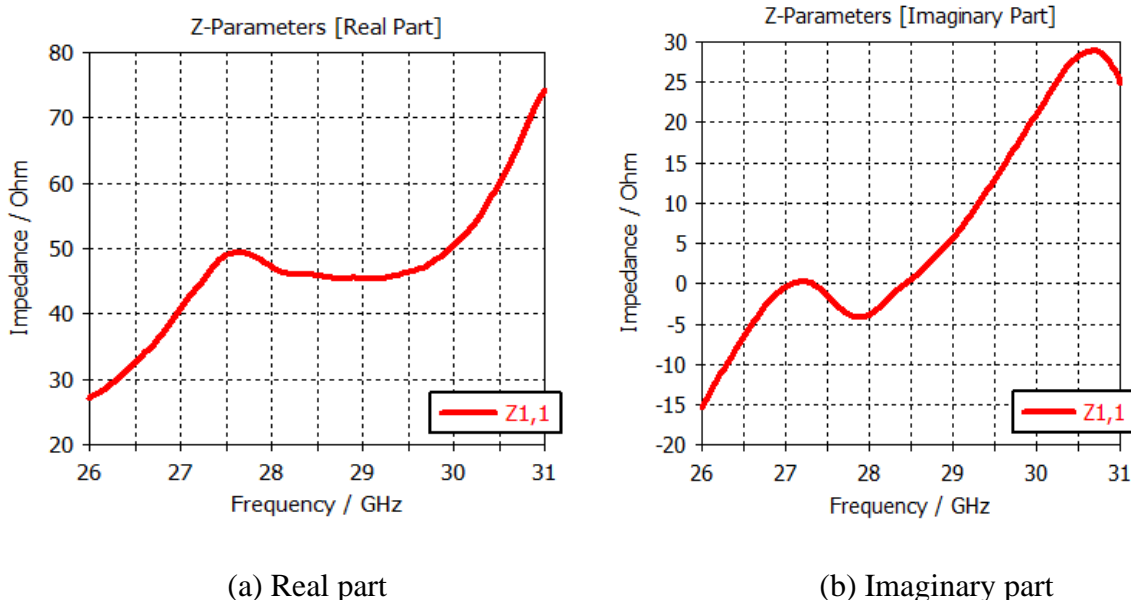


Fig. 3.4.9: Z – Parameters (a) Real part and (b) Imaginary part.

The overall antenna performance is summarized in table 3.4.1. The comparison table 3.4.2 shows the compatibility of the designed antenna.

TABLE 3.4.1: PERFORMANCE METRICS OF THE PROPOSED 5G ANTENNA.

Performance Parameter	Value
Resonant frequency (GHz)	27.47
Lower Cut off Frequency (GHz)	26.154
Higher Cut off Frequency (GHz)	31
-10 dB Bandwidth (GHz)	4.846
S parameter (dB)	-35.064
Gain (dB)	5.22
Directivity (dBi)	7.48
VSWR	1.036
Avg. Rad. Efficiency (%)	≈ 70

TABLE 3.4.2: COMPARISON TABLE.

Parameter	Reference No.				This work
	[11]	[12]	[14]	[15]	
Size (L×W) Mm ²	55 × 115	55 × 110	5×5	35×36	20×20
Substrate material	Rogers RT 5880	Rogers RT 5880	Rogers RT 5880	Teflon	Rogers RT 5880
Centre frequency (GHz)	≈ 27.9	≈ 27.5	38	28.49	27.47
Return loss (dB)	-27.908	≈ -37	≈ -43	-39.55	-35.03
Gain (dB)	7.182	7.88	4	8.841	5.22
BW (GHz)	2.305	1.0683	22	0.814	4.846

3.5 Conclusion

The presented microstrip patch antenna with slotted ground plane is suitable for 28 GHz next generation wireless mm-wave band. At the ground plane, four equal size slots are used to improve the antenna key performances and match the antenna impedance with the line impedance. The proposed antenna provides excellent performance metrics for 5G communications. The -10 dB bandwidth is 4.846 GHz that supports huge data capacity. The values of S-parameter and VSWR are -35.03 dB and 1.036, respectively. The antenna also possesses good average radiation efficiency ($\approx 70\%$) with acceptable gain over the entire large operating frequency band.

REFERENCES

- [1] H. Li, Y. Cheng, and Z. Ling, “Design of distributed and robust millimeter-wave antennas for 5G communication terminals,”*IEEE Access*, vol. 8, pp. 133420-133429, 2020.
- [2] W. Roh et al., “Millimeter-wave beamforming as an enabling technology for 5G cellular communications: theoretical feasibility and prototype results,”*IEEE Communications Magazine*, vol. 52, no. 2, pp. 106-113, 2014.
- [3] R. Azim, et al., “A multi-slotted antenna for LTE/5G sub-6 GHz wireless communication applications,”*International Journal of Microwave and Wireless Technologies*, vol. 13, no. 5, pp. 486 – 496, 2021.
- [4] R. Azim, R. Aktar, A. K. M. M. H. Siddique, L. C. Paul, and M. T. Islam, “Circular patch planar ultra-wideband antenna for 5G sub-6 GHz wireless communication applications,”*Journal of Optoelectronics and Advanced Materials*, vol. 23, no. 3-4, pp. 127 – 133, 2021.
- [5] M. Shafi et al., “5G: A Tutorial overview of standards, trials, challenges, deployment, and practice,”*IEEE Journal on Selected Areas in Communications*, vol. 35, no. 6, pp. 1201-1221, 2017.
- [6] Y.B. Zikria, S.W. Kim, M.K. Afzal, H. Wang, and M. H. Rehmani, “5G mobile services and scenarios: challenges and solutions,”*Sustainability*, vol. 10, no. 10, pp. 1-9, 2018.
- [7] T.S. Rappaport et al., “Millimeter wave mobile communications for 5G cellular: It will work!”,*IEEE Access*, vol. 1, pp. 335-349, 2013.
- [8] N. Sarker and M. R. Hossain Mondal, “Design and analysis of double E-shaped array antennas for an outdoor RFID system,”*Proceedings of International Conference on Electrical and Computer Engineering*, 2018, pp. 453-456.

- [9] M.A.A. Rgheff, “5G enabling technologies: Small cells, full-duplex communications, and full-dimension MIMO,” in *5G Physical Layer Technologies*, Wiley, 2019.
- [10] C. Deng, D. Liu, B. Yektakhah, and K. Sarabandi, “Series-fed beam-steerable millimeter-wave antenna design with wide spatial coverage for 5G mobile terminals,” *IEEE Transactions on Antennas and Propagation*, vol. 68, no. 5, pp. 3366-3376, 2020.
- [11] M.I. Ahmed, H.M. Marzouk, and A. Shaalan, “A two-element microstrip antenna 28/38 GHz for 5G mobile applications,” *Proceedings of the 6th International Conference on Advanced Control Circuits and Systems & 5th International Conference on New Paradigms in Electronics & Information Technology*, 2019, pp. 71-76.
- [12] H.M. Marzouk, M.I. Ahmed, and A.A. Shaalan, “A Novel Dual-band 28/38 GHz slotted microstrip MIMO antenna for 5G mobile applications,” *Proceedings of the International Symposium on Antennas and Propagation and USNC-URSI Radio Science Meeting*, 2019, pp. 607-608.
- [13] J. Kim and J. Oh, “Liquid-crystal-embedded aperture-coupled microstrip antenna for 5G applications,” *IEEE Antennas and Wireless Propagation Letters*, vol. 19, no. 11, pp. 1958-1962, 2020.
- [14] J. L. Li, M. H. Luo, and H. Liu, “Design of a slot antenna for future 5G wireless communication systems,” *Proceedings of the Progress In Electromagnetics Research Symposium 2017*, pp. 739-741.
- [15] L.C. Paul and M.M. Alam, “Millimeter-wave hexagonal grid microstrip array antenna for 5G communication,” *Proceedings of the 3rd International Conference on Electrical Information and Communication Technology 2017*, pp. 1-6.

Chapter - 4

A LOW PROFILE MICROSTRIP PATCH ANTENNA WITH DGS FOR 5G APPLICATION

4.1 Abstract

A low-profile microstrip patch antenna with defected ground structure (DGS) for 5G applications has been proposed in the chapter. The antenna has a large bandwidth of 5.85 GHz that supports huge data volume. The antenna is capable of operating from 25.52 GHz to 31.37 GHz with very good scattering properties. It possesses a return loss of -35.353 dB at the resonant frequency of 27.26 GHz. Rogers RT 5880 dielectric substrate having a relative permittivity of 2.2 and tangent loss of 0.0009 is used for the antenna. The volume of the antenna substrate is 20 mm×20 mm×0.79 mm. The gain and directivity of the patch antenna varies from 3 dB to 6 dB and 5.1 dBi to 7.9 dBi respectively within the operating frequency band ranging from 25.52 GHz to 31.37 GHz. The gain and directivity are 5.11 dB and 7.1 dB respectively at 27.26 GHz. The VSWR over the entire bandwidth of the antenna can be presented as $1 < \text{VSWR} < 2$. The maximum radiation efficiency of the proposed 5G antenna is approximately 66%. The modeling and simulation of the proposed design have been accomplished by CST.

4.2 Introduction

With the continuous development of technology, first-generation (1G) mobile technology is now switched to fifth-generation (5G) mobile technology [1-2]. Mobile technology is switched due to a lot of reasons such as massive connectivity, huge channel capacity and ease of incorporation with other cellular technologies [3-4]. For example, 5G can support the internet of things (IoT), radiofrequency technology (RFID), device to device (D2D) communication with higher network access capability [5-6]. Fig. 3.2.1. shows a sketch of connectivity of 5G with other wireless communication means. Although the evolution of 5G technology is based on 4G technology there

are huge technological differences. For instance, the orthogonal frequency division multiplexing (OFDM) is the key multiplexing technique for 4G, while in 5G non-orthogonal multiple access (NOMA) and NOMA-OFDM is used [7-9]. Since non-orthogonal subcarriers are used in the 5G technology, the errors arising in the 4G due to the loss of orthogonality among the subcarriers are greatly reduced. So 4G is very sensitive to frequency errors, hence tight specification for local oscillators is mandatory for fourth-generation cellular technology. The power domain NOMA (P-NOMA) and code domain NOMA (C-NOMA) both are very useful in 5G that ensures massive connectivity i.e. billion-billion IoT and RFID devices will be connected with the fifth generation cellular technology [7][10-11]. Another technological key difference between 4G and 5G is that the energy consumption of 5G is comparatively smaller than any other established cellular technology. For this reason, the running cost is lower in 5G than 4G. It is mentionable that the millimetre wave (mm-wave) spectrum for 5G is less costly than the allocated spectrum below 3GHz for 4G [12]. In terms of minimizing spectral crunch and per Hertz (Hz) cost optimization, researchers are greatly attracted to design antenna at the mm-wave band. Moreover, simple in structure and cost-efficient fabrication process, the microstrip patch antenna now is a good candidate for any sort of wireless communication.

A dual-band microstrip antenna with a large frequency ratio for 5G applications is introduced in [13]. In the work, the antenna is designed on a TLY-5-0200 dielectric substrate (dielectric constant of 2.2) with a thickness of 0.508 mm, and the size of the antenna is $30 \times 44 \text{ mm}^2$. In [14] a dual-band mm-wave antenna with the size of $4 \times 9.45 \text{ mm}^2$ is presented for 5G mobile applications. Although the size of the antenna is comparatively lower, the gain of the antenna is only 2.3 dB at 28 GHz resonance frequency. Aperture coupled microstrip antenna at the centre frequency of 28 GHz is proposed in [15] with an overall dimension of $18 \times 14 \text{ mm}^2$ with a peak simulation gain of 6.5 dBi. A square-shaped slot antenna is proposed in [16] for 5G applications. Although the dimension of the antenna is moderate and built-in Rogers RT5880 substrate with thickness 0.127mm, the gain of this antenna is comparatively lower and it is 4 dB at 28 GHz. Two hexagonal grid antennas having 10 cells and 12 cells are designed and analyzed in [17] for 28 GHz 5G communication.

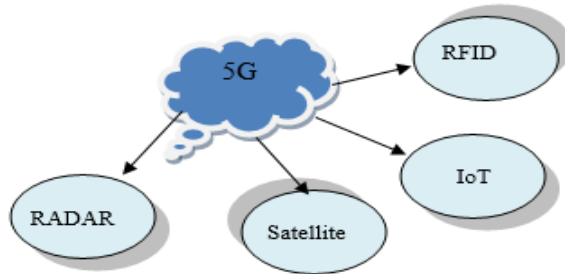


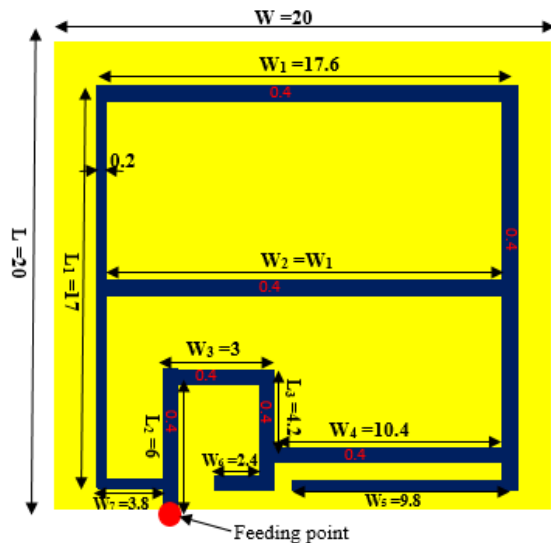
Fig. 4.2.1: 5G connectivity with other networks.

The prime focus of this chapter is to design a low profile wideband (25.52 GHz - 31.37 GHz) microstrip patch antenna with acceptable antenna performance at target resonance frequency 28 GHz for 5G communication. The square-shaped defected ground structures (DGS) are introduced in the ground plane to improve the directivity and gain of the proposed antenna. The remaining part of the chapter is organized as follows: the design of the proposed antenna using computer simulation technology (CST) is introduced in section 4.3. All the results and performance analyses of the proposed low-profile microstrip patch antenna with DGS are presented in section 4.4. Finally, a few notable remarks of this work are discussed briefly in section 4.5.

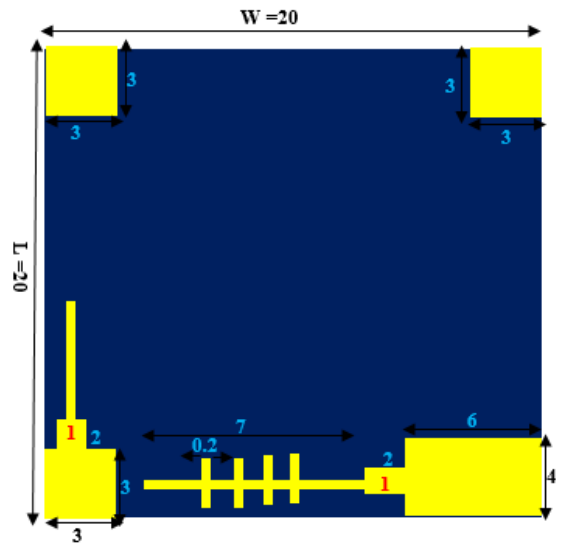
4.3 Design of 5G Antenna With DGS

The proposed low profile wideband 5G microstrip patch antenna with defected ground structure (DGS) has been designed on commercially available Rogers RT5880 substrate with permittivity of 2.2, loss tangent of 0.0009. The design has been simulated and optimized by using CST. The thickness of the dielectric substrate is 0.79 mm and the thickness of copper is 0.035 mm for the proposed design. The size of the proposed antenna is $20 \times 20 \text{ mm}^2$. The main radiating elements (copper metal) of the antenna with different arm lengths and widths are shown in Fig. 4.3.1. From Fig.4.3.1 (a) (Front view), it is seen that the two equal lengths horizontal parallel line ($W_1=W_2=17.6 \text{ mm}$) with a width of 0.4 mm and the two vertical parallel lines with length $L_1=17 \text{ mm}$ are designed to obtain good impedance matching characteristics of the antenna. The horizontal and vertical line generates inductive and capacitive impedances so that the antenna effective impedance is perfectly matched with the 50Ω waveguide port impedance. The W_3 , W_4 , W_5 , W_6 , W_7 , and L_2 , L_3 lines are adjusted to enhance the current distribution of the antenna as

well as to obtain broadband characteristics with excellent antenna performance. As shown in Fig. 4.3.1 (b), the ground plane of the proposed antenna is defected by adding four slots at four corners. Among the four slots three having dimension 3×3 mm² and the rest one having dimension 4×6 mm². In the ground plane, four vertical slots with a width of 0.2 mm and a length of 2 mm are proposed to complete the antenna design in the CST microwave studio suite. The deflection of the ground plane not only improves the impedance matching but also enhances the operating bandwidth. [18-20]. The 3D view of the proposed antenna is mentioned in Fig. 4.3.1 (c). The dimensional parameters of the proposed low-profile 5G antenna with DGS are presented in Table 4.3.1.



(a) Front View (all the dimensions are in mm)



(b) Back View (all the dimensions are in mm)

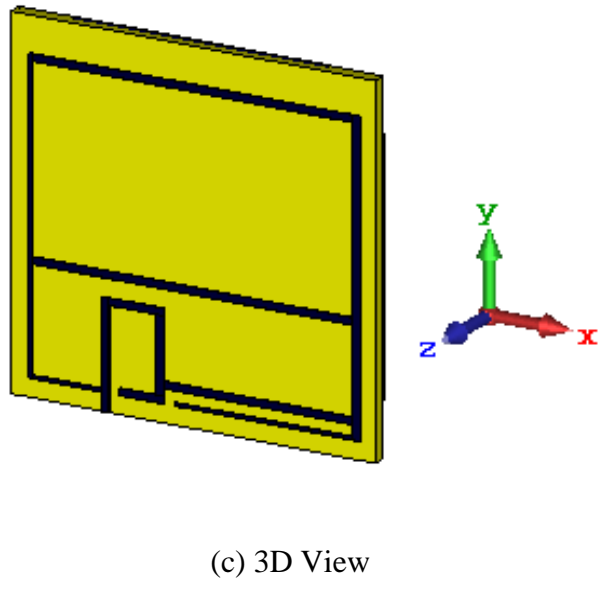


Fig. 4.3.1: Proposed 5G antenna with DGS. (a) Front view, (b) Back view, (c) 3D view.

TABLE 4.3.1: DESIGN SUMMARY OF PROPOSED MICROSTRIP PATCH ANTENNA WITH DGS FOR 5G.

Antenna Parameters	Length in mm
W	20
L	20
$W_1=W_2$	17.6
W_3	3
W_4	10.4
W_5	9.8
W_6	2.4
W_7	3.8
L_1	17
L_2	6
L_3	4.2

4.4 Results and Analysis of Proposed Antenna

The scattering parameter (S-parameter) of the proposed low profile 5G antenna with defected ground structure is depicted in Fig.4.4.1. From the figure, it is clear that the centre operating frequency of the antenna is 27.26 GHz with a very good return loss of -35.35 dB. The bandwidth (considered at -10 dB point) of the antenna is 5.85 GHz ranging from 25.52 GHz to 31.37 GHz which indicates excellent bandwidth coverage for upper 5G applications. The voltage standing wave ratio (VSWR) of the designed antenna is 1.034. Fig. 4.4.2 shows the variation of VSWR over the entire operating frequency band of the proposed antenna. The VSWR over the entire bandwidth is $1 < \text{VSWR} < 2$. In case of good impedance matching, the VSWR value should be very close to unity and from Fig.4.4.2, it can be conferred that the VSWR value is close to unity that ensures good impedance matching of the proposed design.

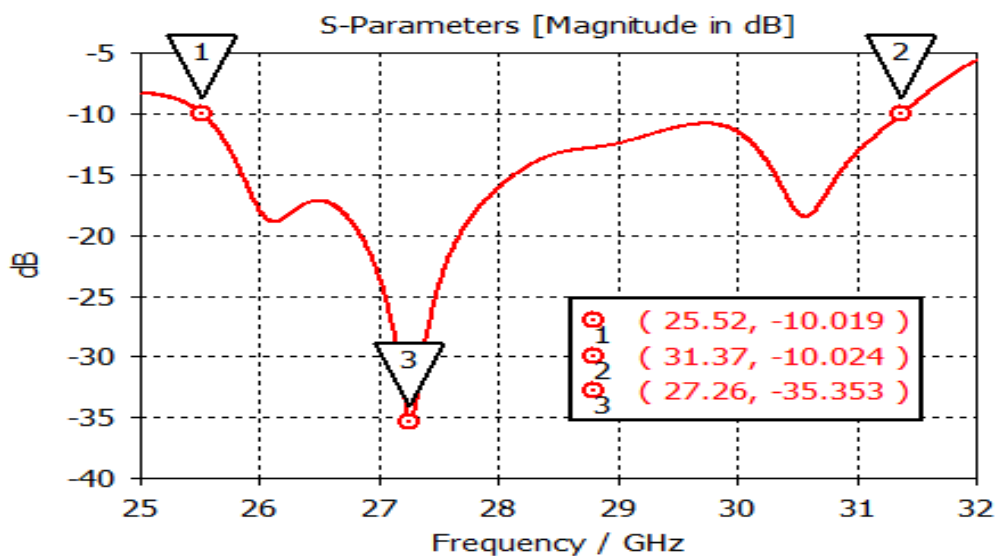


Fig. 4.4.1: S11 curve of the proposed 5G antenna.

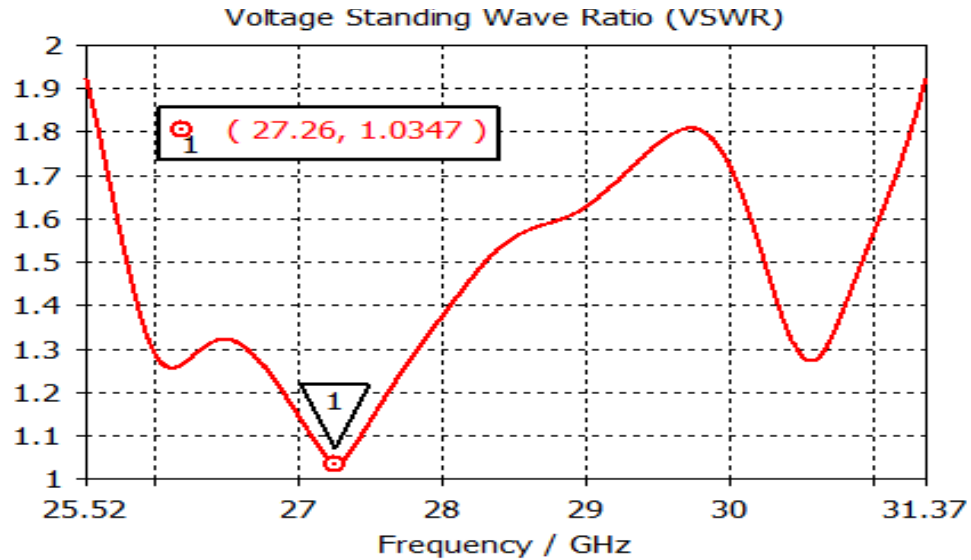


Fig. 4.4.2: VSWR of the proposed 5G antenna.

The 3D gain and directivity of the proposed antenna are shown in Fig. 4.4.3 and 4.4.4, respectively. The peak gain and directivity of the proposed antenna are 5.11 dB and 7.1 dB, respectively at a centre operating frequency of 27.26 GHz.

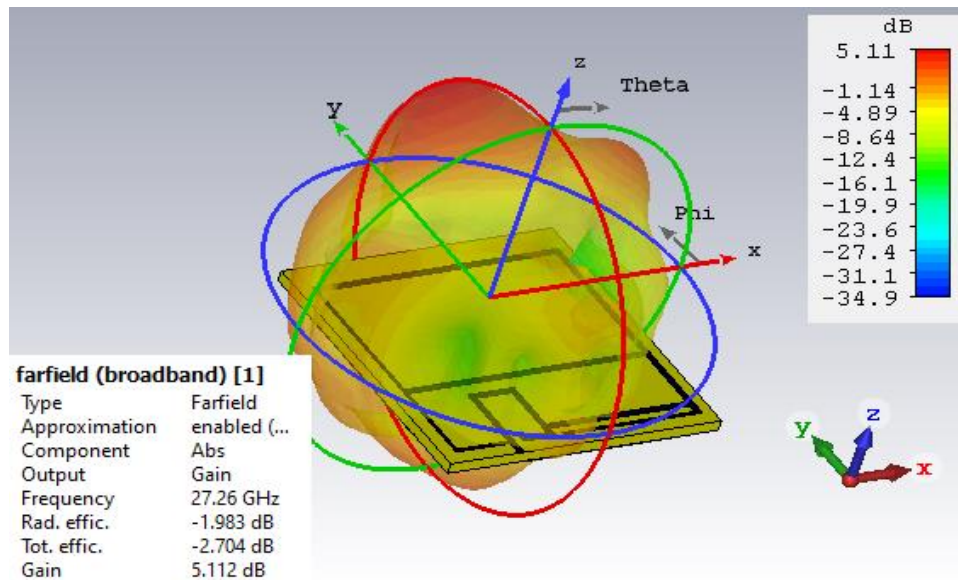


Fig. 4.4.3: 3D Gain at 27.26 GHz of the proposed antenna.

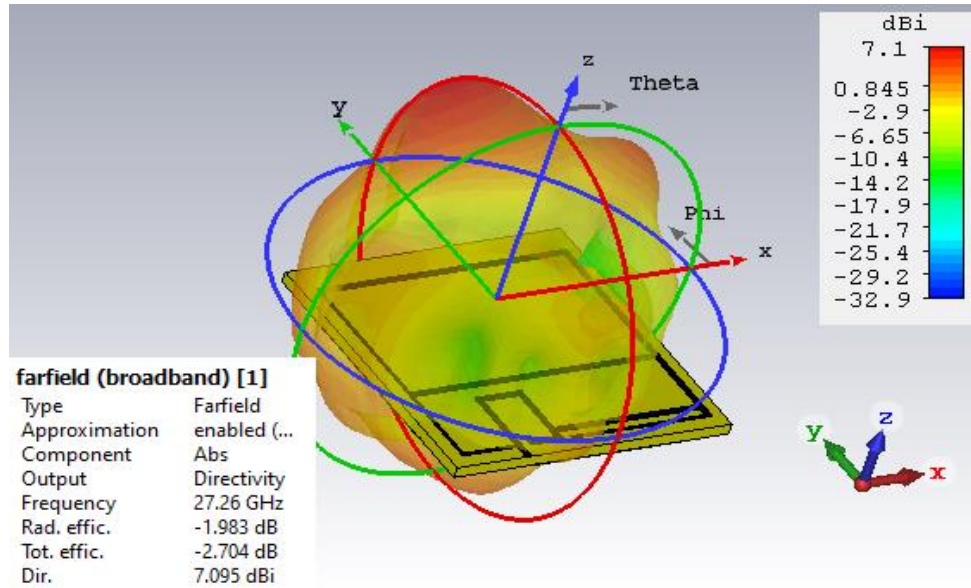
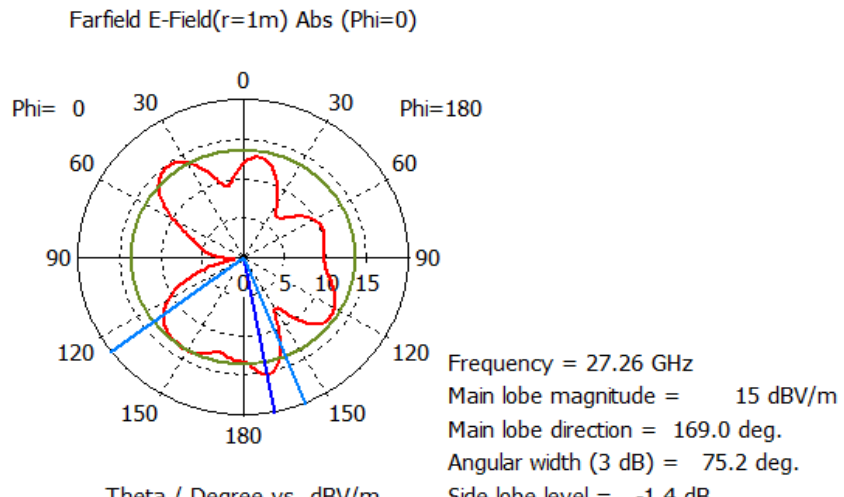
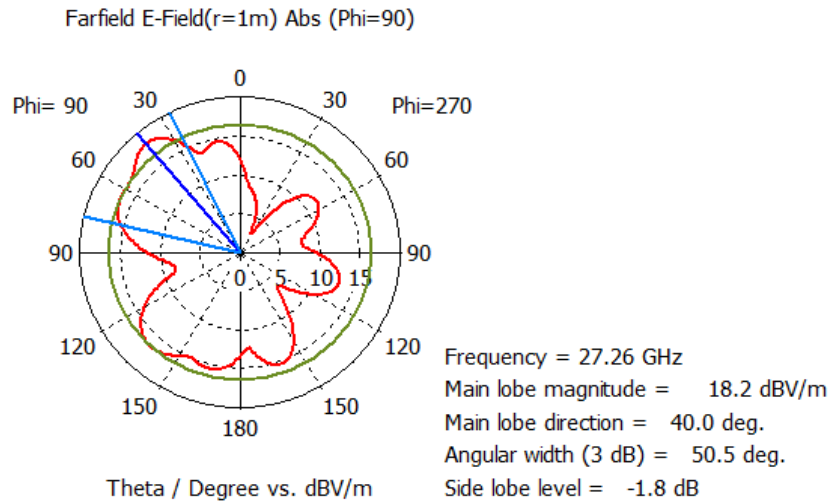


Fig. 4.4.4: 3D Directivity at 27.26 GHz of the proposed antenna.

The various polar plots of radiation patterns of the proposed antenna at 27.26 GHz are shown in Fig. 4.4.5. (a, b) and Fig. 4.4.6. (a, b). The electric field (E-field) pattern of the designed antenna is shown in Fig. 4.4.5. (a, b) while the magnetic field (H-field) pattern is shown in Fig. 4.4.6.(a, b).



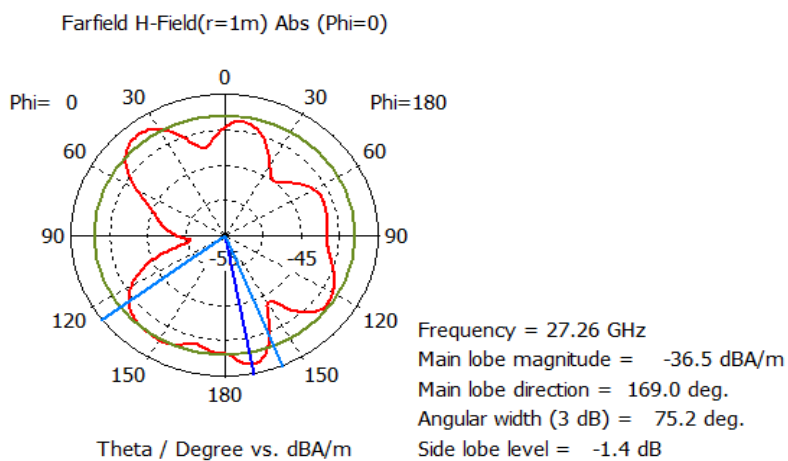
(a) E-Field at phi = 0^0



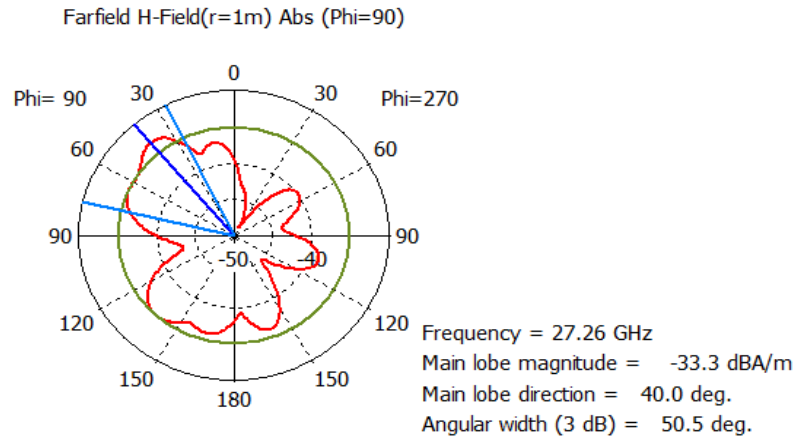
(b) E-Field at phi = 90°

Fig. 4.4.5: E field pattern of the proposed 5G antenna.

From the polar plot of the radiation pattern, the main lobe is directed at 169° for $\phi=0^\circ$ and 40° for $\phi=90^\circ$. The half-power beamwidth (HPBW) also known as 3 dB angular beam width is 75.2° for $\phi=0^\circ$ and 50.5° for $\phi=90^\circ$. For the E-field, the main lobe magnitude is 15 dBV/m at $\phi=0^\circ$ and 18.2 dBV/m at $\phi=90^\circ$. Similarly, for the H-field, the main lobe magnitude is -36.5 dBA/m at $\phi=0^\circ$ and -33.3dBA/m at $\phi=90^\circ$. It is worth sharing that the lowest side lobe level (LSLL) is -1.8 dB at $\phi=90^\circ$.



(a) H-Field at phi = 0°



(b) H-Field at phi = 90^0

Fig. 4.4.6: H-Field pattern of the proposed 5G antenna.

The gain and directivity Vs frequency curve of the proposed 5G antenna are shown in Fig. 4.4.7. From the figure, the gain and directivity of the microstrip patch antenna varies from 3dB to 6dB and 5.1dBi to 7.9 dBi respectively. The gain and directivity at the centre operating frequency of 27.26 GHz are 5.11 dB and 7.1 dB respectively.

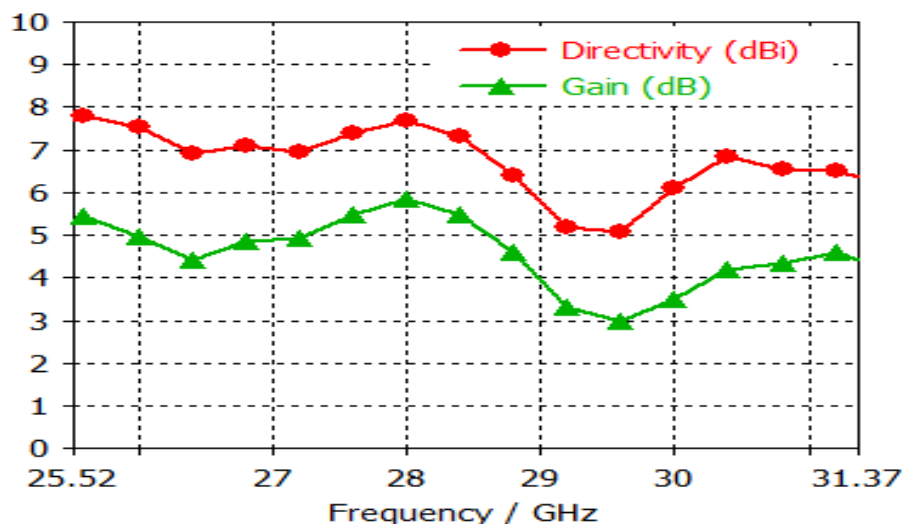


Fig. 4.4.7: Gain and directivity Vs frequency of the proposed 5G antenna.

Fig.4.4.8. shows the radiation efficiency of the proposed 5G antenna. The radiation efficiency of the antenna can be defined as the ratio of gain to directivity (G/D) i.e. $\eta_{rad}=G(\text{dB}) - D(\text{dB})$. From

the radiation efficiency curve, the maximum η_{rad} is near about 66% which ensures a good amount of power is radiated by the antenna and antenna impedance is considerably matched with the waveguide port impedance. The overall antenna performances are listed in table 4.4.1.

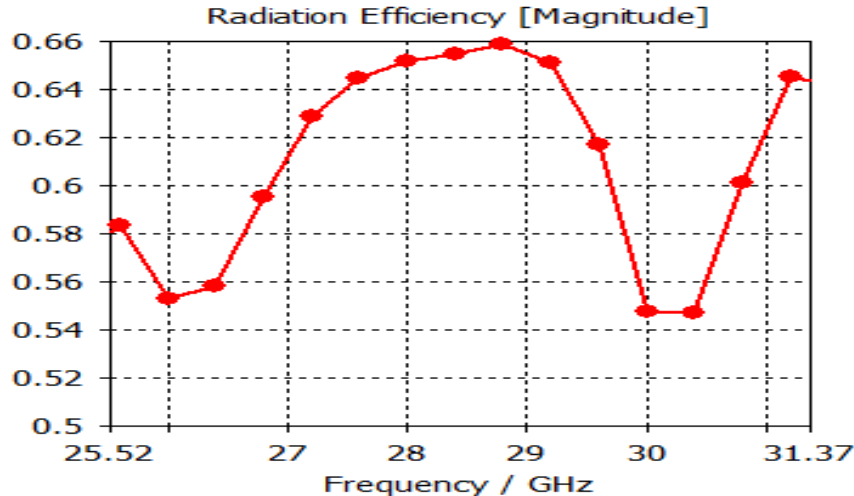


Fig. 4.4.8: Radiation Efficiency.

TABLE 4.4.1: PERFORMANCE METRICS OF THE PROPOSED 5G ANTENNA WITH DGS.

Name of the parameter	Value
Return loss (dB)	-35.353
Resonant frequency (GHz)	27.26
Gain (dB)	5.11
Directivity (dBi)	7.1
-10 dB Bandwidth (GHz)	5.85
Lower cut off frequency (GHz)	25.52
Higher cut off frequency (GHz)	31.37
VSWR	1.034
Maximum Radiation Efficiency (%)	≈66

The Z- parameters of the proposed antenna are shown in Fig. 4.4.9 which indicates that the real part is close to 50Ω and the imaginary part is close to 0 at 27.26 GHz. The comparison table 4.4.2 shows the compatibility of the designed antenna.

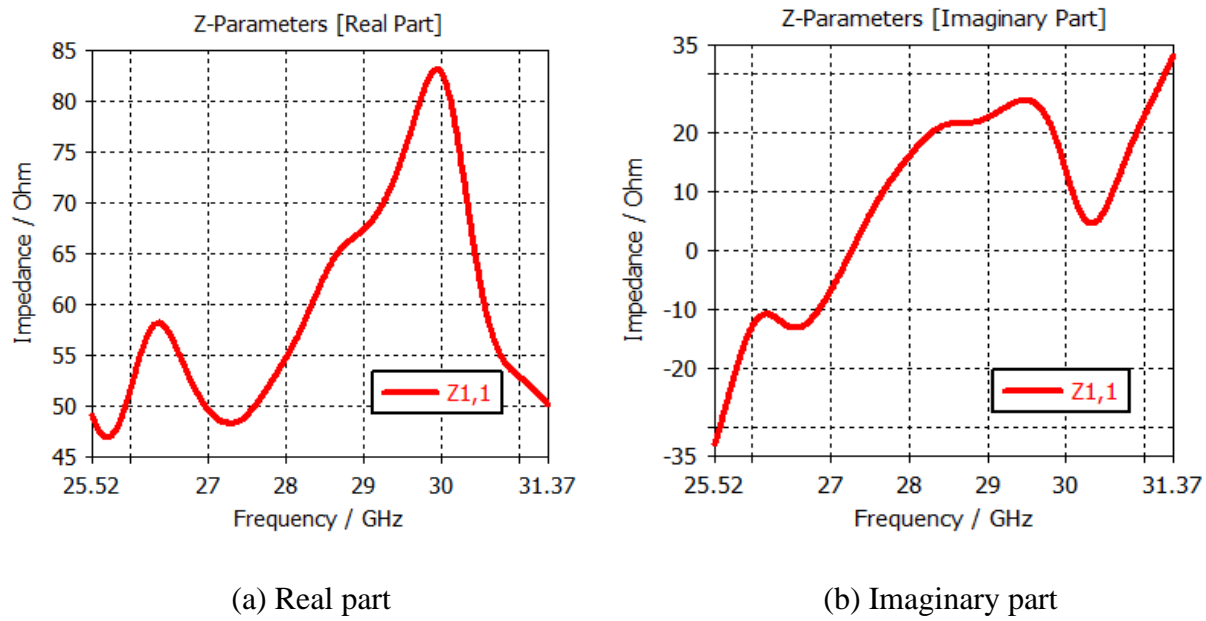


Fig. 4.4.9: Z – Parameters (a) Real part and (b) Imaginary part.

TABLE 4.4.2: COMPARISON WITH RELEVANT WORKS.

Parameter	Reference No.				This work
	[13]	[14]	[16]	[17]	
Size (L×W) mm ²	33×44	4×9.45	5× 5	35×36	20×20
Substrate material	TLY-5-0200	Material ($\epsilon_r=4.4$)	Rogers RT5880	Teflon	Rogers RT 5880
Frequency Range (GHz)	27.3– 28.8	25.2-34.3	20-42	28.1- 28.914	25.52- 31.37
Centre frequency	28	≈27.4	38	28.49	27.26

Return loss (dB)	≈ -30	-30	≈ -43	-39.55	-35.353
Gain (dB)	9.9	2.3	4	8.841	5.11
BW (GHz)	1.5	9.1	22	0.814	5.85

4.5 Conclusion

The use of defects at the ground plane enhances the current distribution and radiation characteristics of the proposed 5G antenna. The antenna has a large bandwidth of 5.85 GHz spanning from 25.52 GHz to 31.37 GHz. The value of return loss and VSWR throughout the operating frequency band shows the excellent impedance matching property. The gain, directivity, and radiation efficiency of the patch antenna are up to 6 dB, 7.9 dBi, and approximately 66% respectively within the large operating frequency spectrum. The VSWR over the entire bandwidth of the antenna can be expressed as $1 < \text{VSWR} < 2$ and VSWR is 1.034 at the resonant frequency of 27.26 GHz. The proposed low-profile microstrip patch antenna having a compact size of 316 mm³ with defected ground structure (DGS) can be considered as a suitable candidate for next-generation 5G communication.

REFERENCES

- [1] Y. B. Zikria, S.W. Kim, M. K. Afzal, H. Wang, and M. H.Rehmani, “5G Mobile services and scenarios: Challenges and solutions,”*Sustainability*, vol. 10, no 10, pp.1-9, 2018.
- [2] A. Ghosh, A. Maeder, M. Baker, and D. Chandramouli, “5G Evolution: A view on 5G cellular technology beyond 3GPP release 15,”*IEEE Access*, vol. 7, pp. 127639-127651, 2019.
- [3] S. Henry, A. Alsohaily, and E. S. Sousa, “5G is real: Evaluating the compliance of the 3GPP 5G new radio system with the ITU IMT-2020 requirements,”*IEEE Access*, vol. 8, pp. 42828-42840, 2020.

- [4] S. Chen and J. Zhao, "The requirements, challenges, and technologies for 5G of terrestrial mobile telecommunication," *IEEE Communications Magazine*, vol. 52, no. 5, pp. 36-43, 2014.
- [5] C. T. Pawan, S. H. Shivaraj, and M. R. Kounte, "RFID characteristics and its role in 5G communication," *Proceedings of the 4th International Conference on Trends in Electronics and Informatics 2020*, pp. 473-478.
- [6] N. Sarker, M. A. Islam, and M. R. H. Mondal, "Two novel multiband centimetre-wave patch antennas for a novel OFDM based RFID system," *Journal of Communications*, vol. 13, no. 6, 2018.
- [7] L. Dai, B. Wang, Y. Yuan, S. Han, I. C. lin, and Z. Wang, "Non-orthogonal multiple access for 5G: solutions, challenges, opportunities, and future research trends," *IEEE Communications Magazine*, vol. 53, no. 9, pp. 74-81, 2015.
- [8] A.T. Abushabah and H. Arslan, "NOMA for multi-numerology OFDM systems," *Wireless Communications and Mobile Computing*, vol. 2018, pp. 1-10, 2018.
- [9] T. Tang, Y. Mao, and G. Hu, "A Fair power allocation approach to OFDM-based NOMA with consideration of clipping," *Electronics*, vol. 9, no. 10, p. 1743, 2020.
- [10] S. M. R. Islam, N. Avazov, O. A. Dobre, and K. Kwak, "Power-domain non-orthogonal multiple access (NOMA) in 5G systems: Potentials and challenges," *IEEE Communications Surveys & Tutorials*, vol. 19, no. 2, pp. 721-742, 2017.
- [11] N. Sarker and M. R. H. Mondal, "Design and analysis of double E-shaped array antennas for an outdoor RFID system," *Proceedings of the 10th International Conference on Electrical and Computer Engineering, 2018*, pp. 453-456.
- [12] M. A. A. Rgheff, "5G enabling technologies: Small cells, full-duplex communications, and full-dimension MIMO," in *5G Physical Layer Technologies*, Wiley, 2019.
- [13] F. Xiao, X. Lin, and Y. Su, "Dual-band structure-shared antenna with large frequency ratio for 5G communication applications," *IEEE Antennas and Wireless Propagation Letters*, vol. 19, no. 12, pp. 2339-2343, Dec. 2020.
- [14] C. Han, G. Huang, T. Yuan, and C. Sim, "A Dual-Band Millimeter-Wave Antenna for 5G Mobile Applications," *Proceedings of the IEEE International Symposium on Antennas and Propagation and USNC-URSI Radio Science Meeting, 2019*.
- [15] J. Kim and J. Oh, "Liquid-crystal-embedded aperture-coupled microstrip antenna for 5G applications," *IEEE Antennas and Wireless Propagation Letters*, vol. 19, no. 11, pp. 1958-1962, 2020.
- [16] J. L. Li, M. H. Luo, and H. Liu, "Design of a slot antenna for future 5G wireless communication systems," *Proceedings of the Progress In Electromagnetics Research Symposium 2017*, pp. 739-741.
- [17] L.C. Paul and M.M. Alam, "Millimeter-wave hexagonal grid microstrip array antenna for 5G communication," *Proceedings of the 3rd International Conference on Electrical Information and Communication Technology 2017*, pp. 1-6.

- [18] R. Azim, R. Aktar, A. K. M. M. H. Siddique, L. C. Paul, and M. T. Islam, “Circular patch planar ultra-wideband antenna for 5G sub-6 GHz wireless communication applications,” *Journal of Optoelectronics and Advanced Materials*, vol. 23, no. 3-4, pp. 127 – 133, 2021.
- [19] M. A. Dorostkar, R. Azim, and M. T. Islam, “A novel Γ -shape Fractal antenna for wideband communications”, *Procedia Technology*, vol. 11, pp.1285-1291, 2013.
- [20] R. Azim, M. T. Islam, and N. Misran, “Printed circular ring antenna for UWB applications,” *Proceedings of the International Conference on Electrical and Computer Engineering 2010*, pp. 361-363.

Chapter - 5

A DUAL BAND MINIATURIZED SPIRAL-SHAPED PATCH ANTENNA FOR 5G AND WiFi-5/6 APPLICATIONS

5.1 Abstract

A dual band spiral-shaped patch antenna (SPA) is designed and proposed for 5G and WiFi-5/6 applications. The Rogers RT 5880 (lossy) substrate with a compact size of $20 \times 20 \times 0.79$ mm³ has been used to design the spiral patch antenna. The dual band antenna resonates at 3.61 GHz (3.53-3.7 GHz) and 5.56 GHz (4.7-7.24 GHz) with very good reflection coefficients of -41.29 dB and -37.85 dB respectively which cover lower 5G (n48 CBRS (USA): 3.55 – 3.7GHz, Korea: 3.4-3.7 GHz), WiFi-5 (5.15– 5.85 GHz) and WiFi-6 (5.925 – 7.125 GHz) bands. It has gain of 1.503 dB, 2.767 dB and directivity of 3.057 dBi, 3.368 dBi and VSWR of 1.017, 1.025 at resonant frequencies 3.61 GHz and 5.56 GHz respectively. The peak gain and directivity of the SPA are 3.95 dB and 5 dBi. The spiral-shaped patch with optimized dimensions enhances the antenna performances and ensures good impedance matching to make it suitable for lower 5G and WiFi-5/6 applications.

5.2 Introduction

The world is surfing in an era of wireless communication. Wireless mobile technology has evolved from the foundation of mobile technology 1G to 2G (GSM) with more capacity of calling and texting and then to the 3G with a high data rate, 4G (LTE) with a faster data transferring technology [1-2] and finally recent revolutionary 5G technology with very low latency, huge channel capacity, ultra-high data rate and much more reliable communication network [3-5]. Researchers are focused on advanced 5G networks due to the modern-day's requirement of ultra-high speed, higher mobility, massive connections, high energy efficiency and cost effectiveness [6]. The 5G has expanded the door of internet of things (IoT), industrial

IoT (IIoT), AI and smart home appliances, autonomous driving, D2D communication, and many more technical opportunities [7].

Due to the increasing demand of higher data rate, smooth connectivity and multi-device usability, wireless communication is evolving tremendously. WiFi has changed the way of living in this technical era, which is IEEE 802.11 standard for WLAN [8]. By following the trend of increasing demand since last 24 years, WiFi has advanced from 1st recognized version IEEE 802.11 standard of 2.4 GHz to IEEE 802.11ac standard of 5 GHz which is also known as WiFi-5, WiFi-6 of IEEE 802.11ax standard of 2.4/5GHz and finally the latest generation WiFi 6E of IEEE802.11ax standard which has access of 6 GHz band [9]. Both WiFi-5 and WiFi-6 show the identical throughput value for the smallest number of users at the same 5GHz band but for a higher number of users WiFi-6 shows a bigger throughput value than WiFi-5 [10]. The coexistence of 5G and WiFi-5/6 can provide promising performance for a dramatic user-end experience. Both 5G and WiFi-5/6 can be complimentary for different functionalities like higher data rate, high mobility, ultra-low latency and higher capacity in different applications. The WiFi-6 is more suitable for indoor conditions and high-density areas. On the other hand, 5G is well suited for outdoor networks and connections with mobility [11]. Over the years, numerous antennas have been developed by RF researchers all over the world. Some significant antennas of Sub-6 GHz and WiFi bands are proposed in [12-16]. In [12], a multi-slotted rectangular stepped patch antenna is designed with a dimension of $20 \times 30 \text{ mm}^2$. The antenna covers 3.15-5.55 GHz for Sub-6 GHz applications. It has a decent average gain of 2.35dBi and efficiency is about 74.7%. The antenna is well optimized to provide omni-directional radiation. A low-profile circular patch planner antenna is introduced in [13] with a wide operating band (3.05 - 5.82 GHz) for Sub-6 GHz communication. The antenna has an overall dimension of $20 \times 28 \text{ mm}^2$ with a FR4 substrate of relative permittivity of 4.6. Though the antenna is simplest in structure and covers a wide band, it has a relatively very lower average gain and efficiency. For Wi-Fi applications, an oval-shaped CPW-Fed monopole antenna is introduced in [14] with a volume of $20 \times 8.7 \times 0.4 \text{ mm}^3$ and a range of 5.15-7.29 GHz with suitable gain and efficiency for WiFi-5/6. In [15], a rectangular monopole antenna with a compact dimension of $40 \times 20 \times 1.6 \text{ mm}^3$ is proposed for two resonant frequencies 3.5 GHz and 5.2 GHz. It possesses an optimum gain. In [16], a circular-

shaped long fed-line antenna ($20 \times 35 \times 0.8$ mm 3) with a partial ground structure is proposed for a range of 2.99 - 5.89 GHz. with stable gain but the efficiency is unspecified.

In this chapter, a dual band spiral-shaped patch antenna with a partial ground plane for 5G and WiFi-5/6 applications is demonstrated. The antenna is designed with a compact size of $20 \times 20 \times 0.79$ mm 3 on Rogers RT 5880 substrate. The antenna resonates at 3.61 GHz (3.53-3.7 GHz) and 5.56 GHz (4.7-7.24 GHz) with acceptable gain, directivity, and efficiency. The rest of the chapter is formatted as follows: In section 5.3, spiral-shaped patch antenna's description with analysis is presented and the conclusion is presented in section 5.4.

5.3 Spiral-Shaped Patch Antenna

The miniaturized SPA with a partial ground plane has been designed and simulated using the CST microwave studio. The Rogers RT 5880 (lossy) substrate (2.2, 0.0009) with a thickness of 0.79 mm has been used. To design the radiating spiral patch as well as the partial ground plane of the antenna, the Copper (annealed) material is used with thickness of 0.035 mm. The antenna is structured with a 2×2 mm 2 sized feeder and a spiral patch with width of 0.6 mm as shown in Fig. 5.3.1 (a). The length of the largest outer vertical line and smallest inner vertical ring are 18 mm and 2.2 mm. The partial ground plane is of 2×20 mm 2 as shown in Fig. 5.3.1 (b).

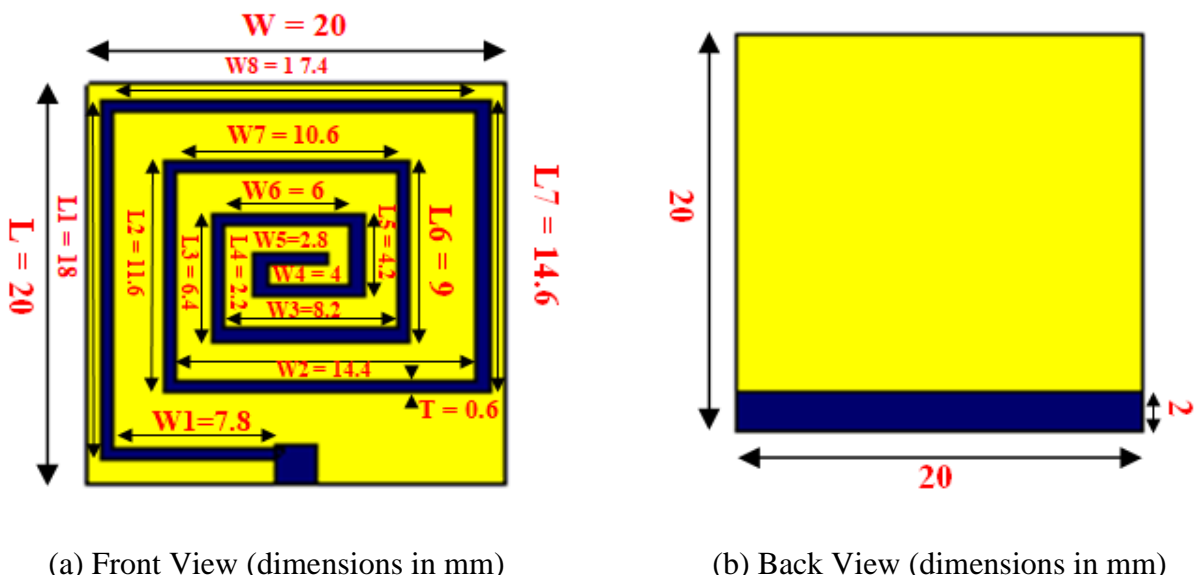


Fig. 5.3.1: Proposed Spiral-shaped patch antenna. (a) Front view, (b) Back view.

The scattering parameter of the SPA is shown in Fig. 5.3.2 where the dual band antenna resonates at 3.61 GHz and 5.56 GHz with very good reflection coefficients of 41.29 dB and 37.85 dB respectively. It covers dual bandwidth of 166 MHz (3.535-3.701) and 2.532 GHz (4.708-7.24) for lower 5G and WiFi-5/6 applications.

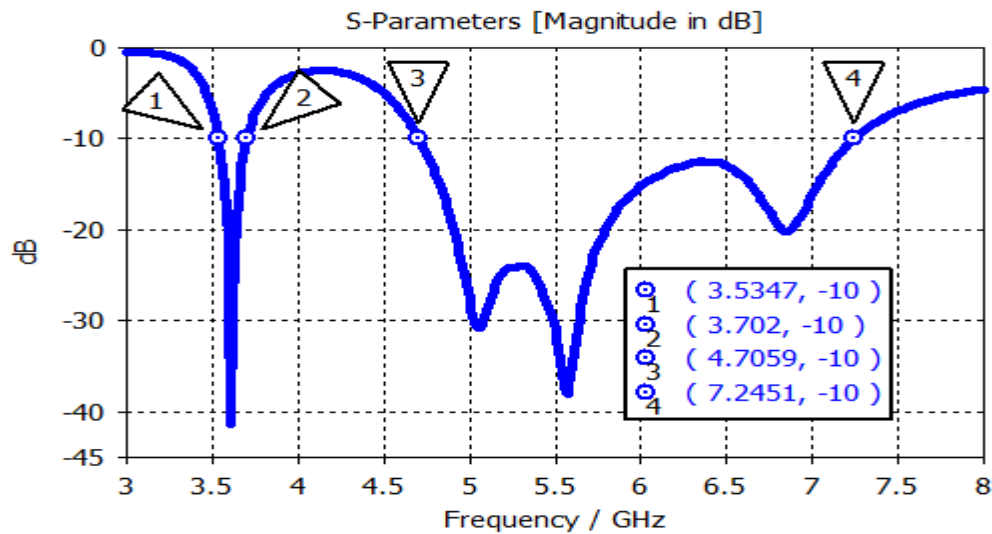
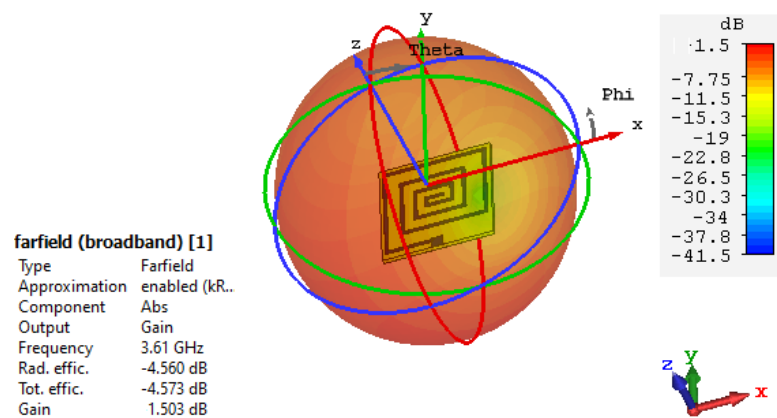
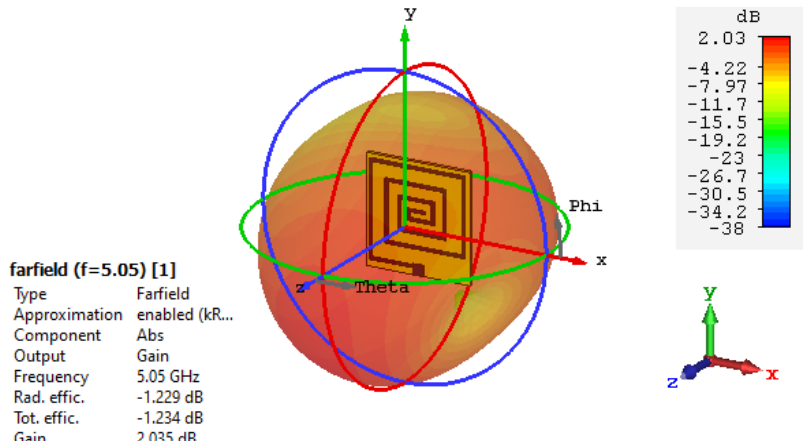


Fig. 5.3.2: Reflection coefficient of the spiral-shaped antenna.

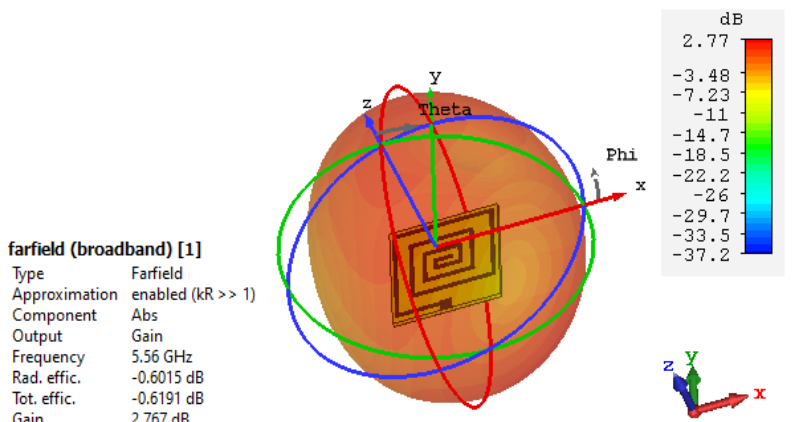
The gain and directivity profile at different frequencies of the spiral-shaped patch antenna are presented in Fig. 5.3.3. The gain of SPA at 3.61 GHz and 5.56 GHz are 1.5 dB and 2.67 dB. The gain varies from 1.5 dB to 3.95 dB. And the directivity at resonant frequencies are 3.057 dBi and 3.368 dBi and the directivity varies from 2.9 dBi to 5 dBi.



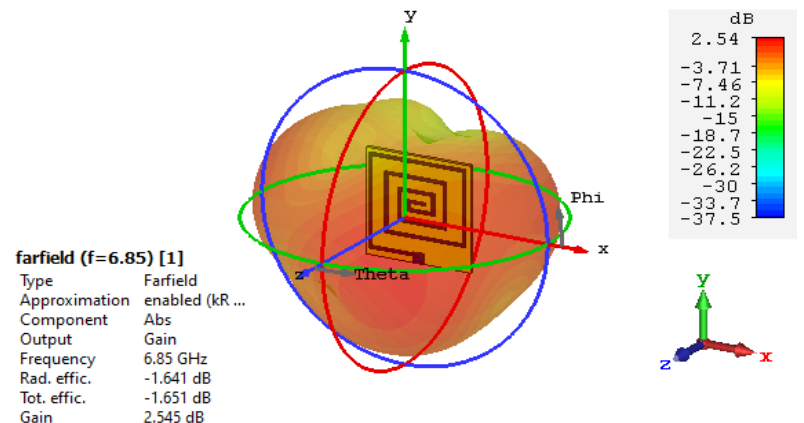
(a) Gain at 3.61 GHz



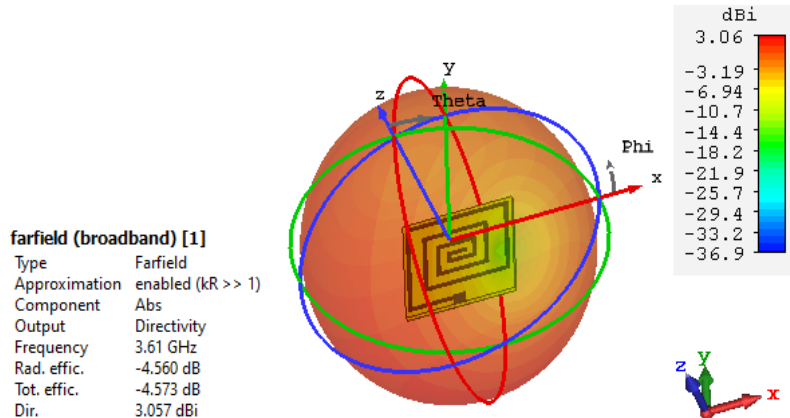
(b) Gain at 5.05 GHz



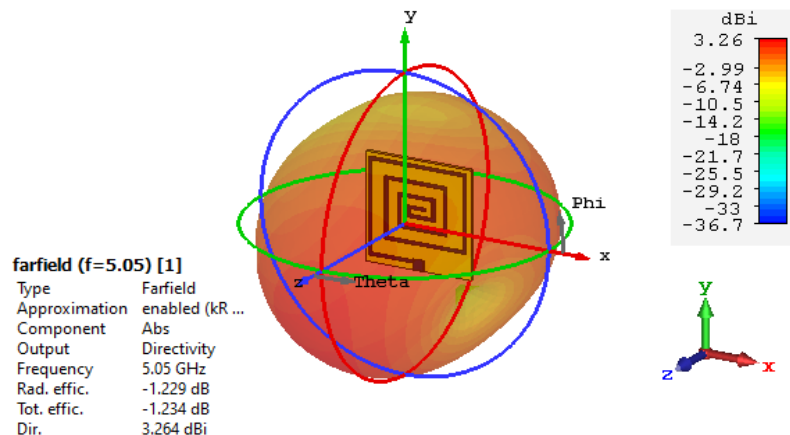
(c) Gain at 5.56 GHz



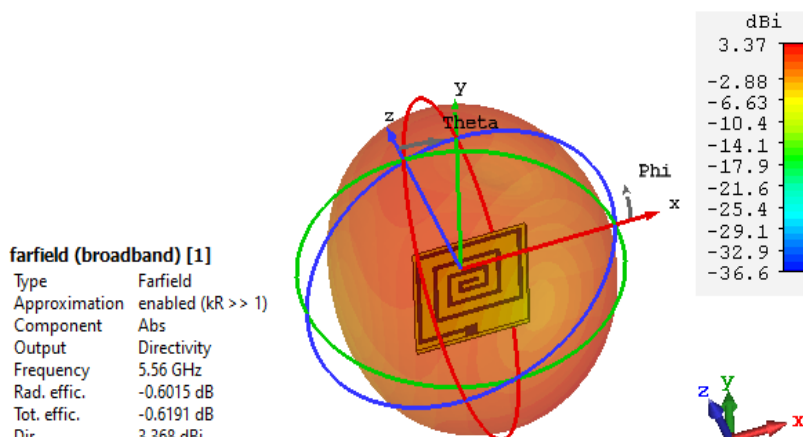
(d) Gain at 6.85 GHz



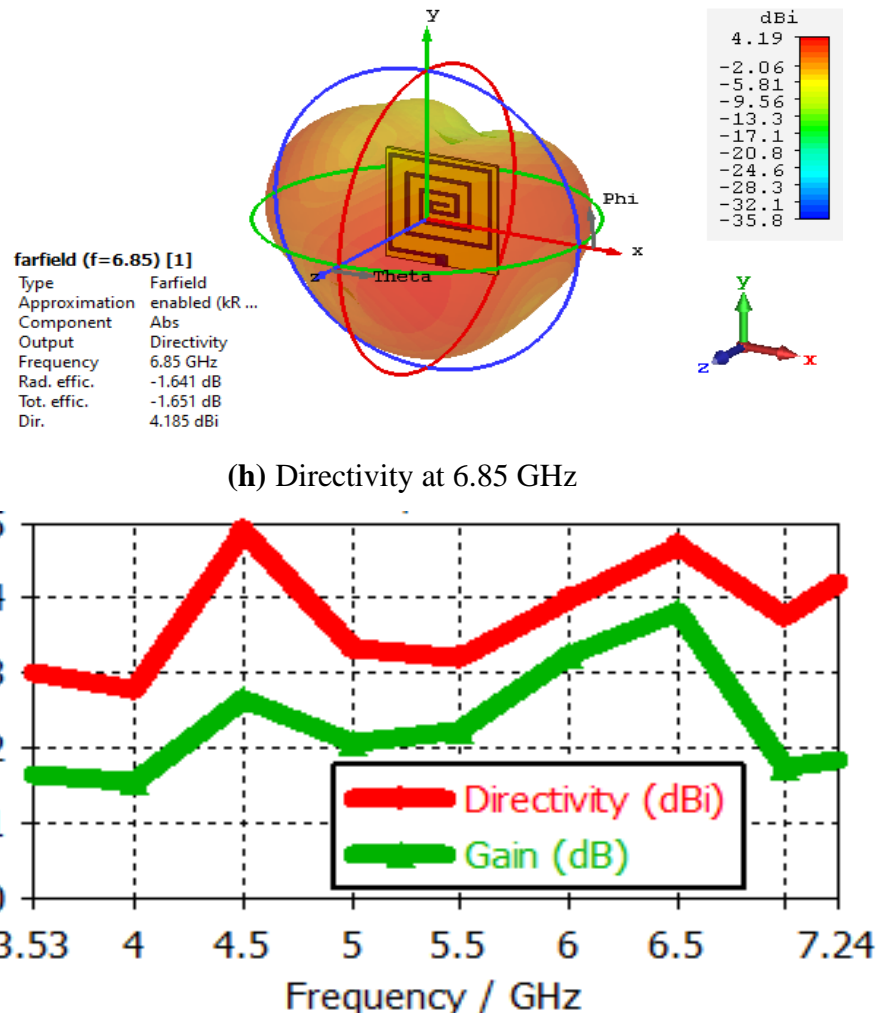
(e) Directivity at 3.61 GHz



(f) Directivity at 5.05 GHz



(g) Directivity at 5.56 GHz

**Fig. 5.3.3:** Gain and directivity.

The polar presentation of both electric and magnetic fields at 3.61 GHz, 5.05 GHz, 5.56 GHz and 6.85 GHz are depicted in Fig. 5.3.4. The main lobe of both fields is directed at 174^0 ($\phi=0^0$) and 166^0 ($\phi=90^0$) for 3.61 GHz, 4^0 ($\phi=0^0$) and 20^0 ($\phi=90^0$) for 5.05 GHz, 161^0 ($\phi=0^0$) and 1^0 ($\phi=90^0$) for 5.56 GHz, 105^0 ($\phi=0^0$) and 10^0 ($\phi=90^0$) for 6.85 GHz. Though, there are no side lobes at 5.05 GHz and 5.56 GHz, it only exists for 3.61 GHz and 6.85 GHz. The angular widths (3dB) are 302.4^0 ($\phi=0^0$) and 98^0 ($\phi=90^0$) at 3.61 GHz, 90.6^0 ($\phi=0^0$) and 243.8^0 ($\phi=90^0$) at 5.05 GHz, 242.1^0 ($\phi=0^0$) and 276.6^0 ($\phi=90^0$) at 5.56 GHz, 105.7^0 ($\phi=0^0$) and 75.6^0 ($\phi=90^0$) at 6.85 GHz.

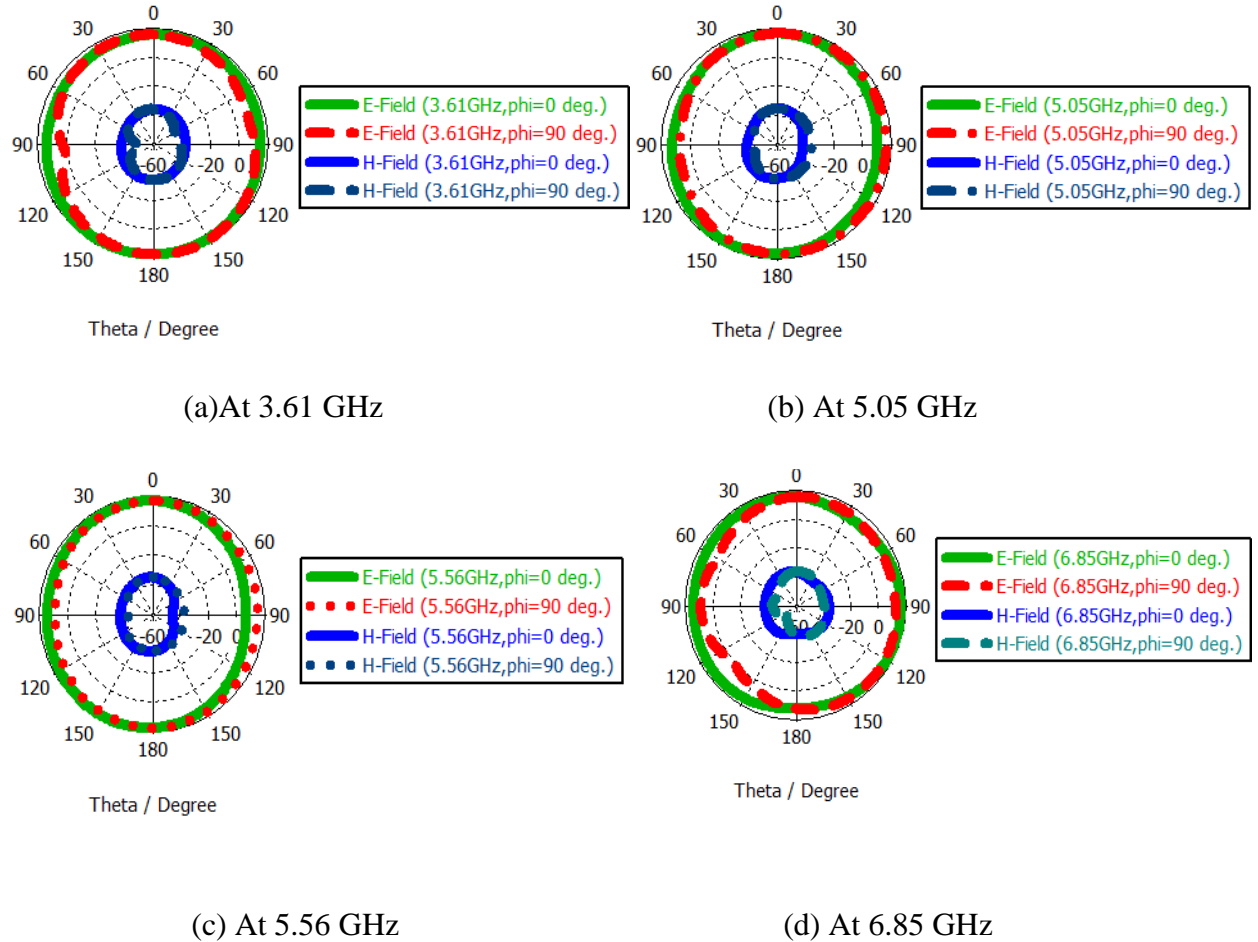
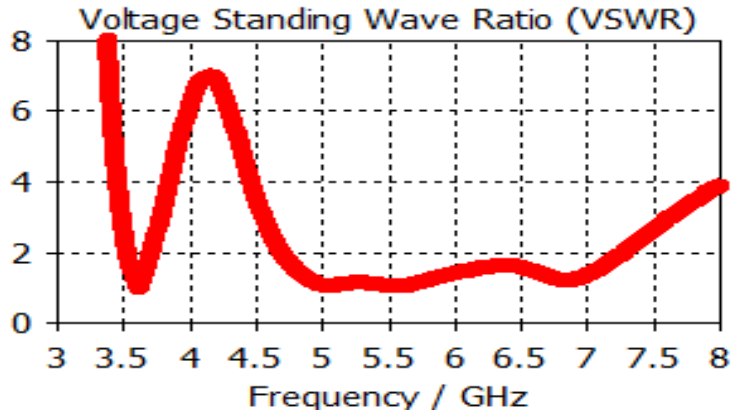
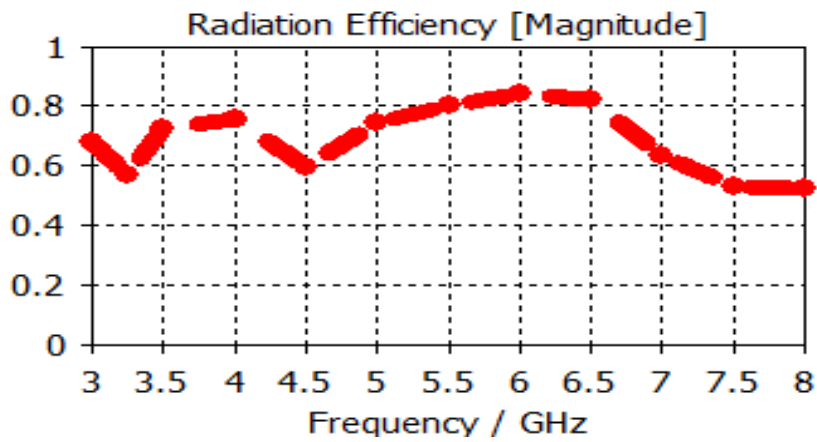
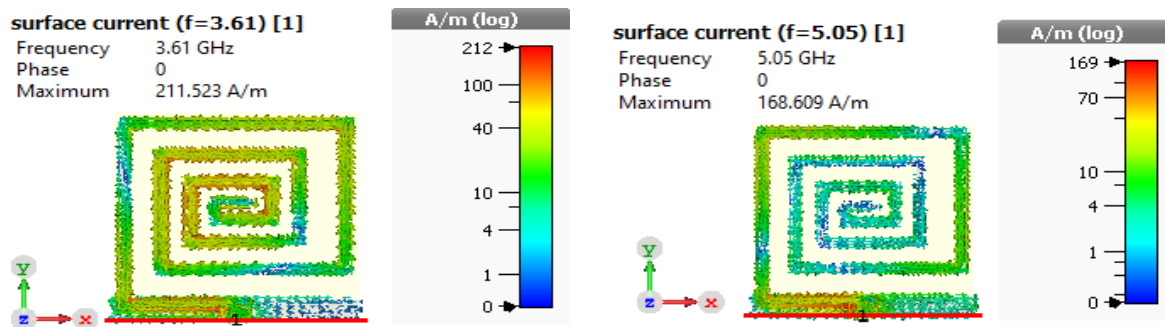


Fig. 5.3.4: E-Field and H-Field of the antenna.

The VSWR of the spiral-shaped antenna is depicted in Fig. 5.3.5. It has VSWR values of 1.017 and 1.025 at centre frequencies. The VSWR value over both operating bandwidths remains close to unity, which confirms very good impedance matching of the SPA. The efficiency represents the ratio of gain to directivity (G/D). The designed SPA shows maximum radiation efficiency of 83% (Fig. 5.3.6).

**Fig. 5.3.5:** VSWR of Spiral-shaped antenna.**Fig. 5.3.6:** Radiation Efficiency

The current distributions of the spiral-shaped patch antenna are shown in Fig. 5.3.7 at four different frequencies. We can see the design has a good distribution of current on the whole radiating element.



(a) At 3.61 GHz

(b) At 5.05 GHz

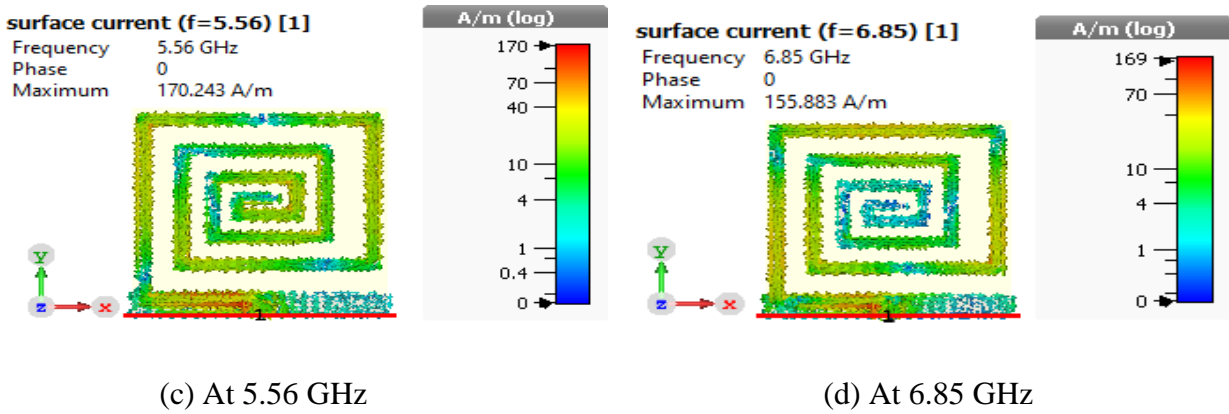


Fig. 5.3.7: Surface current at (a) 3.61 GHz, (b) 5.05 GHz, (c) 5.56 GHz and (d) 6.85 GHz.

At the end of this section, a comparison Table 5.3.1 has been inserted to present the compatibility and coherency of the proposed model. The proposed SPA model has the lowest area and good reflection coefficient profile in both lower 5G and WiFi-5/6 bands with wide bandwidth. It also has acceptable gain with omni-directional property.

TABLE 5.3.1: COMPARISON TABLE.

Parameter	Reference No.				This work
	[12]	[13]	[14]	[15]	
Size (L×W) mm ²	20 × 30	20 × 28	20×8.7	20×40	20×20
Centre frequency (GHz)	4.8	4.8	6.2	3.5 and 5.2	3.61 and 5.56
Reflection coefficient (dB)	-32.6	≈ -28	≈ -27	≈ -25 and ≈ -30	-41.29 and -37.85
Gain (dB)	2.35	2.45	2.25	2.6 and 2.3	1.5 and 2.67
BW (GHz)	2.4	2.77	2.14	0.4 and 1.4	0.166 and 2.53

5.4 Conclusion

The spiral-shaped patch and partial ground plane of the proposed miniaturized antenna improve the current distribution and radiation performances, which make it a suitable candidate for lower 5G and WiFi-5/6 communication. The antenna resonates at 3.61 GHz and 5.56 GHz with very good reflection coefficients of -41.29 dB and -37.85 dB respectively. The dual band spiral-shaped antenna (SPA) has a wide bandwidth and good VSWR which can be defined as $1 < \text{VSWR} < 2$. Though the SPA has a compact size of $20 \times 20 \text{ mm}^2$, it shows acceptable gain and directivity over the entire operating bandwidth with omni-directional property. Due to higher peak efficiency (83%) and required frequency coverage, the SPA can be claimed for the application of 5G and WiFi-5/6 communication.

REFERENCES

- [1] M.Benisha, R.Thandaiah Prabu, Thulasi Bai, "Evolution of Mobile Generation Technology," *Int'l Journal of Recent Technology and Engineering*, vol.7, no. 5S4, pp. 449-454, 2019
- [2] L. C. Paul, M. H. Ali, N. Sarker, M. Z. Mahmud, R. Azim and M. T. Islam, "A Wideband Rectangular Microstrip Patch Antenna with Partial Ground Plane for 5G Applications," *10th Int'l Conf. on Informatics, Electronics and Vision*, 2021, pp. 1-6.
- [3] A. Ghosh, A. Maeder, M. Baker and D. Chandramouli, "5G Evolution: A View on 5G Cellular Technology Beyond 3GPP Release 15," *IEEE Access*, vol. 7, pp. 127639-127651, 2019.
- [4] L. C. Paul et al., "A wideband microstrip patch antenna with slotted ground plane for 5G application," *Int'l Conf. on Science and Contemporary Technologies*, 2021, pp. 1-5.
- [5] L. C. Paul et al., "A low profile microstrip patch antenna with DGS for 5G application," *Int'l Conf. on Science and Contemporary Technologies*, 2021, pp. 1-6.
- [6] H. Yu, H. Lee and H. Jeon, "What is 5G? Emerging 5G Mobile Services and Network Requirements", *Sustainability, MDPI*, vol. 9, no. 10, 1848, pp. 1-22, 2017.
- [7] P.Varga et al., "5G Support for Industrial IoT Applications— Challenges, Solutions, and Research Gaps", *Sensors*, vol. 20, no. 3, 828, pp. 1-43, 2020.
- [8] K. Pahlavan and P. Krishnamurthy, "Evolution and Impact of Wi-Fi Technology and Applications: A Historical Perspective", *Int'l Journal of Wireless Information Networks*, vol. 28, pp. 3-19, 2021.

- [9] A.Vikulov and A.Paramonov, "Practical retrospective of 5-year evolution of the IEEE 802.11 client device capabilities", *12th Int'l Congress on Ultra Modern Telecommunications and Control Systems and Workshops*, 2020, pp. 296-300.
- [10] A.F. Rochim, B. Harijadi, Y. P. Purbanugraha, S. Fuad and K. A. Nugroho, "Performance comparison of wireless protocol IEEE 802.11ax vs 802.11ac", *Int'l Conf. on Smart Technology and Applications*, 2020, pp. 1-5.
- [11] A. Zreikat, "Performance Evaluation of 5G/WiFi-6 Coexistence", *Int'l Journal of Circuits*, vol. 14, pp. 903-913, 2020.
- [12] R. Azim et al., "A multislotted antenna for LTE/5G Sub-6 GHz wireless communication applications," *Int'l Journal of Microwave and Wireless Technologies*, vol. 13, no. 5, pp.486–496, 2021.
- [13] R.Azim, R. Aktar, A. K. M.M.H. Siddique, L. C. Paul and M.T. Islam, "Circular patch planar ultra-wideband antenna for 5G sub-6 GHz wireless communication applications," *Journal of Optoelectronics and Advanced Materials*, vol. 23, no. 3-4, pp. 127-133, 2021.
- [14] J. Kulkarni and C. Y. D. Sim, "Wideband CPW-Fed Oval-Shaped Monopole Antenna for Wi-Fi5 and Wi-Fi6 Applications," *Progress In Electromagnetics Research C*, vol. 107, pp. 173-182, 2021.
- [15] M. Rezvani; L Asadpor; R. Vahedpour, "A Compact Dual-Band Microstrip Monopole Antenna for WiMAX and WLAN Applications", *5th Conf. on Engineering Electromagnetics*, Iran, 19-20 April, 2017, pp. 1-4.
- [16] R. Azim, A. K. M. M. Haque Meaze, M. Shuhrawardy and L. C. Paul, "A Low Profile Wideband Planar Antenna for 5G Wireless Communication Applications," *National Conf. on Communications*, 2020, pp. 1-4.

Chapter - 6

A WIDEBAND ROSE-SHAPED PATCH ANTENNA WITH A GROUND SLOT FOR SUB-6 GHz APPLICATION

6.1 Abstract

A wideband rose-shaped patch antenna is designed and presented for Sub-6 GHz wireless applications. The antenna consists of a rose-shaped radiating patch and a semi-circular slotted ground plane. The Rogers RT5880 (lossy) material is used as a substrate with a compact size of $20 \times 35 \times 0.79$ mm³ to design the proposed antenna. The rose-shaped antenna resonates at 3.19 GHz with a very good reflection coefficient of -57.27 dB and a large bandwidth of 3.04 GHz (2.7-5.74 GHz). At resonant frequency 3.19 GHz, the antenna shows gain of 2.81 dB, directivity of 2.55 dBi and VSWR of 1.002 which ensures very good impedance matching of the proposed antenna. Due to its compact size, simple structure and well optimized radiation performances, the proposed antenna can be used at various Sub-6 GHz wireless applications.

6.2 Introduction

To meet the increasing demand of data hunger of numerous wireless devices and various technologies, Sub-6 GHz wireless technology has evolved to a new height. Sub-6 GHz bands are allocated for different applications such as Wi-Fi, WLAN, 4G (LTE) and specially for most demanding lower 5G applications. It can be predicted that by the end of 2021 the mobile phone users (5500 Million) will be greater than the bank account holders (5400 Million) or landlines (2900 Million) [1]. There is immersive use of Sub-6 GHz 5G bands in smart homes, virtual education, D2D connectivity, smart vehicles, 4K-8K media consuming, surveillance system, smart cities and many more. It has opened the door of IoT, augmented reality, cloud computing, virtual reality, space science to a new dimension [2-3]. For this diverse use, Sub-6 GHz wireless

bands fulfilled the requirements of higher data rate, massive connectivity, ultra-low latency, high traffic volume density, higher mobility and wider coverage [4].

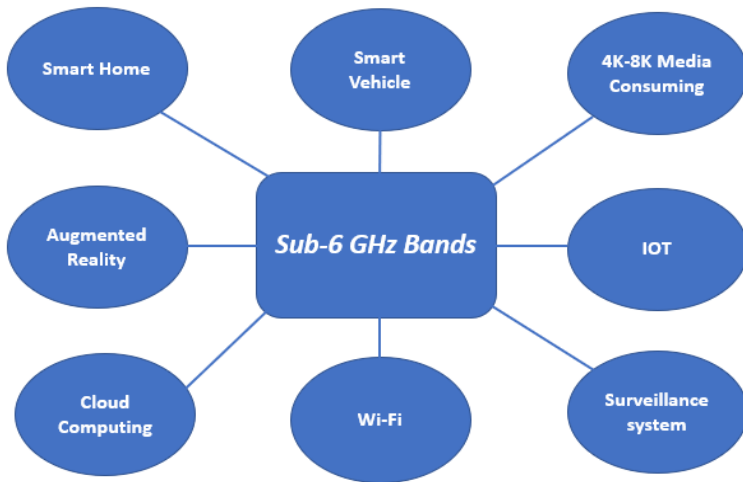


Fig. 6.2.1: Immersive use of Sub-6 GHz Bands.

Numerous service providers of different countries have deployed Sub-6 GHz bands of N77 (3.3-4.2 GHz), N78 (3.3-3.8 GHz) and N79 (4.4 - 5.0 GHz) 5G bands [5]. Due to global deployment of 5G, researchers are busy with the innovation of innumerable 5G antennas and microstrip antennas are the most preferable one for this requirement. Research interest on microstrip patch antennas is growing day by day due to some important features such as low profile, ease of integration, light weight, low cost and energy efficiency [6-8]. Good numbers of antennas are already developed to meet the huge popularity of Sub-6 GHz wireless applications. Some significant works of Sub-6 GHz antennas are proposed in [9-18]. In [9], a simple circular patch antenna is introduced, with a compact size of $20 \times 28 \text{ mm}^2$. It operates over a wide bandwidth of 2.77 GHz (3.05 GHz to 5.82 GHz) for the Sub-6 GHz band. The rectangular slot in the ground has a key impact on impedance matching of the antenna. As it uses standard FR4 substrate, the high dielectric loss of it results in very low average gain and efficiency. A flexible transparent patch antenna is presented in [10], with a substrate of PET and patch of AgHT-8. The antenna has an overall dimension of $58 \times 78 \times 0.9 \text{ mm}^3$ to compensate for the lower conductivity of AgHT-8 though it facilitates the flexibility of the antenna. It has an average gain of 3 dB and efficiency of 80% over the operating bandwidth. In [11], a partially slotted ground rectangular printed

antenna is designed for the Sub-6 GHz band. The antenna has a dimension of $28 \times 40 \text{ mm}^2$ with bandwidth of 700 MHz (3.3 GHz - 4 GHz). The bandwidth is improved by using a polygon-shaped slot on the partial ground plane. The antenna has a decent gain of 2.5 dB despite its simplicity. For a wider bandwidth, a multi-slotted antenna is proposed in [12]. It has a compact size of $24 \times 30 \text{ mm}^2$ to operate over a wide bandwidth of 2.46 GHz (3.15 GHz-5.61 GHz). The antenna performance varies with the dimension of the slots on the patch and ground plane's length. It has comparatively moderate average gain of 2.36 dBi and efficiency of 67.22% though it is etched on higher lossy FR4 substrate. In [13], a dual band antenna ($36 \times 31 \text{ mm}^2$) operating from 3.29 GHz to 3.63 GHz and 4.3 GHz to 5.2 GHz with a good peak gain of 7.17 dBi is presented. Where the 1st operating band is created by stub on the slot and 2nd operating band is created by feed patch and slot. It shows high gain and efficiency with acceptable SAR value but does not provide coverage of the entire Sub-6 GHz range. An ultra-wide band patch antenna is proposed in [14] with a wide bandwidth of 2.92 GHz (2.32 GHz-5.24 GHz). The antenna is designed on a Teflon substrate with a dimension of $47 \times 19 \text{ mm}^2$, where DGS has a great impact on making the bandwidth wider. Without any lumped element, a multi-slotted stepped patch antenna is introduced in [15] with a compact size of $20 \times 30 \text{ mm}^2$. It operates over wide bandwidth (3.15 GHz-5.55 GHz) with a decent average gain of 2.35 dBi and efficiency of 74.7 %. Slots on the radiator and ground plane are used to optimize the proposed antenna. In [16], a wideband microstrip antenna is proposed with two FR4 dielectric layers. It operates over 2.84 GHz to 5.17 GHz. It has limited hand-held applications due to its 3D structure and comparatively bigger dimensions of $63 \times 51.2 \times 4.5 \text{ mm}^3$ for the Sub-6 GHz band. Another double layer dual band filtering antenna for Sub-6 GHz band is discussed in [17]. Though it has higher gain in both bands, its bigger dimension and 3D structure makes it less applicable in compact devices. In [18], a FR-4 based planner antenna ($135 \times 80 \times 0.8 \text{ mm}^3$) having dual bands (0.7 - 0.96 GHz and 1.6 - 5.5 GHz) is presented.

In this work, a wideband rose-shaped patch antenna is discussed for the Sub-6 GHz band which is designed on a low volume Rogers RT5880 substrate. The proposed RSPA operates over a large bandwidth of 3.04 GHz (2.7 - 5.74 GHz) with a good gain, directivity and efficiency. The chapter is further formatted as follows: in section 6.3: design of rose-shaped patch antenna, in section 6.4: result and analysis of the antenna and finally in section 6.5: conclusion.

6.3 Design of Rose-shaped Patch Antenna

The rose-shaped patch antenna (RSPA) is designed by CST-MWS suite 2018. The rose-shaped patch etched on Rogers RT5880 (lossy) substrate (2.2, 0.0009). Copper (annealed) material with thickness of 0.035 mm is used to design the rose-shaped radiating patch and the slotted ground plane. The size of the RSPA is $20 \times 35 \times 0.79$ mm³.

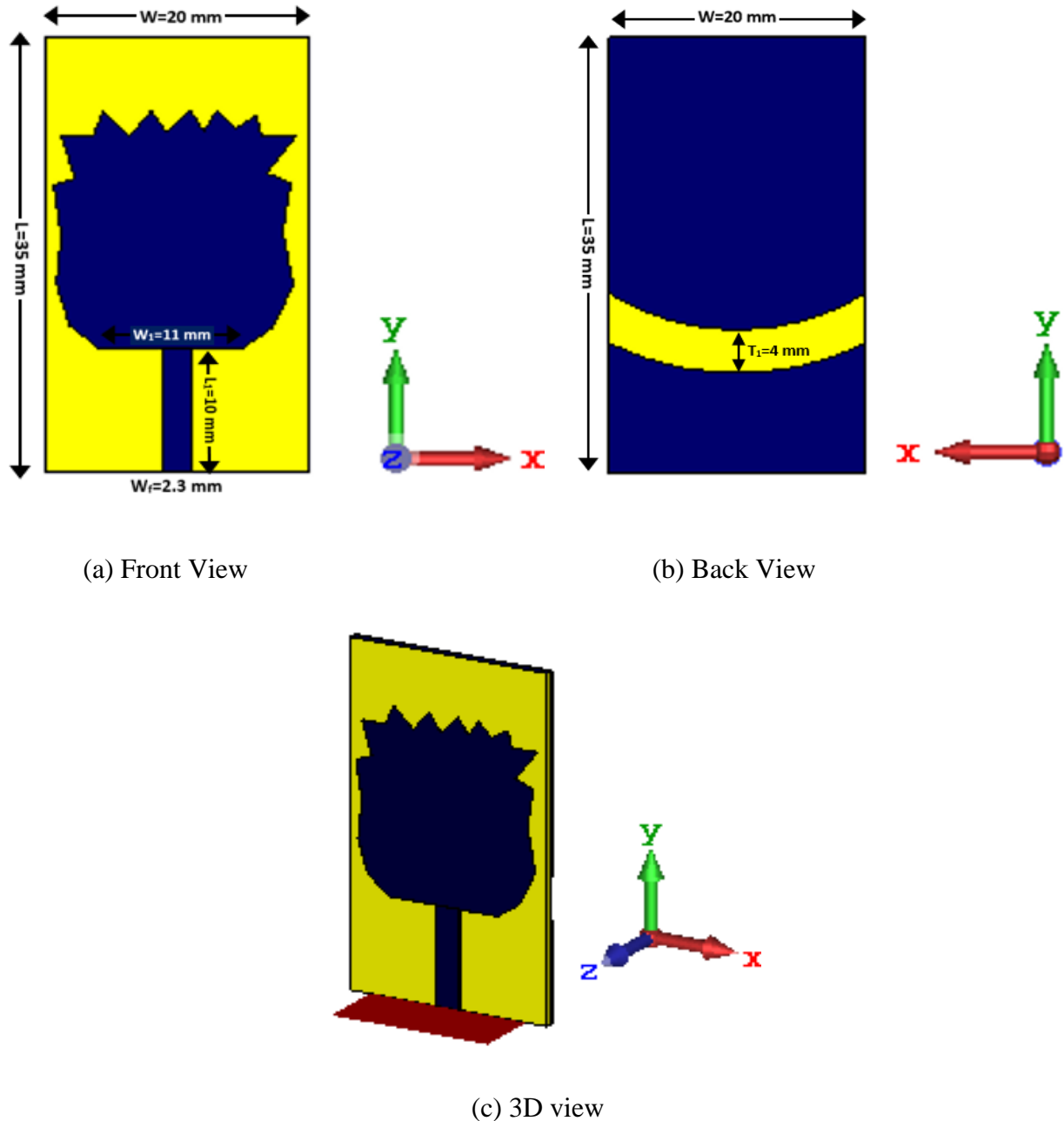


Fig. 6.3.1: Proposed rose-shaped antenna.

The schematic front view of the antenna is displayed in Fig. 6.3.1 (a) where a feeder of 2.3×10 mm² is used to feed the rose-shaped radiating patch. The width of the lower portion of the rose-shaped radiating patch is 11 mm. A semi-circular slot of thickness 4 mm is inserted on the ground plane as drawn in Fig. 6.3.1 (b). The top zig-zag edge of the rose-shaped patch assists to enhance the radiation performance for the intended application. The position of the slot is optimized to get optimum performance for Sub-6 GHz applications. Fig. 6.3.1 (c) shows the 3D view of the designed Sub-6 GHz antenna. The dimensional summary of the RSPA is mentioned in Table 6.3.1.

TABLE 6.3.1: DESIGN SUMMARY OF PROPOSED RSPA.

Antenna Parameters	Length in mm
W	20
L	35
W ₁	11
W _f	2.3
L ₁	10
T ₁	4

6.4 Results and Analysis of Rose-shaped Antenna

The simulation performance of the rose-shaped patch antenna is well suited for Sub-6 GHz applications. The return loss curve of the rose-shaped patch antenna is drawn in Fig.6.4.1. The RSPA resonates at 3.19 GHz with a very good reflection coefficient of -57.27 dB. The RSPA operates over a wide bandwidth of 3.04 GHz ranging from 2.7 GHz to 5.74 GHz. The wide operating bandwidth is facilitated by the rose-shaped radiating element. In Fig. 6.4.2, the VSWR curve is presented. The VSWR value in the entire bandwidth satisfies $1 < \text{VSWR} < 2$. At centre

frequency 3.19 GHz, the VSWR value is 1.002 which is very close to unity and that ensures very good impedance matching of the designed RSPA.

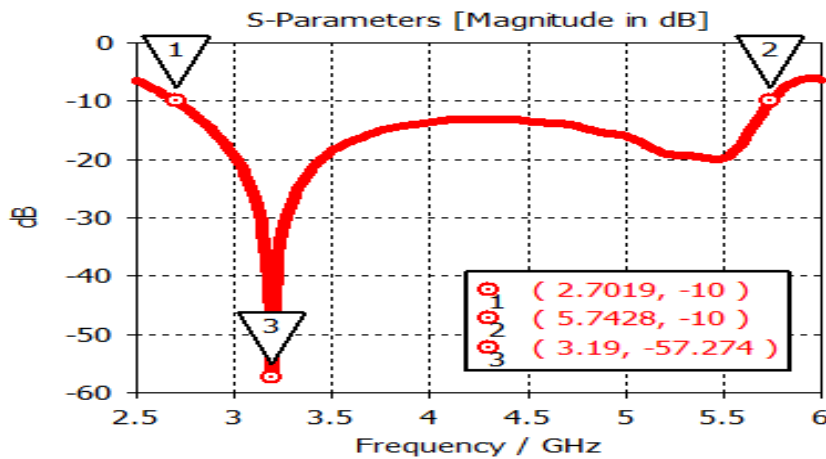


Fig. 6.4.1: S11 Curve of the rose-shaped antenna.

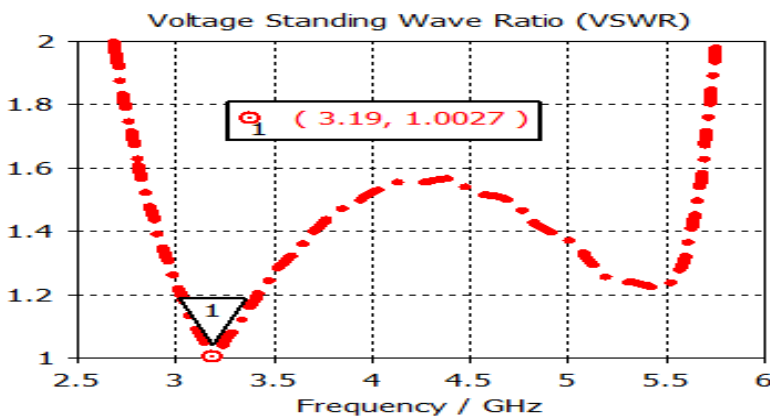
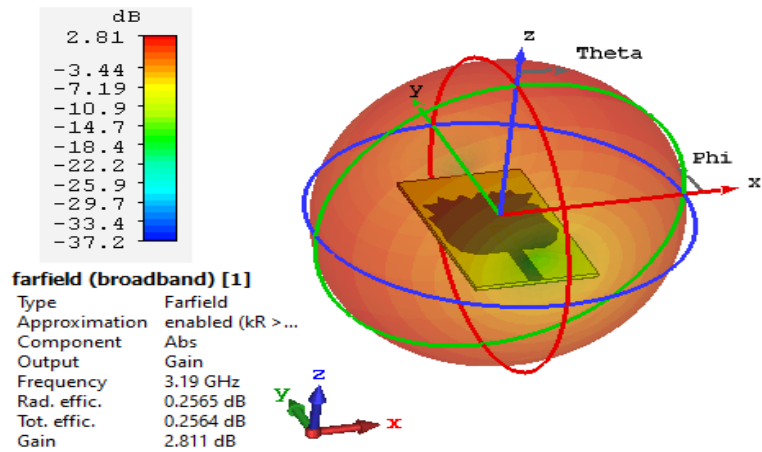
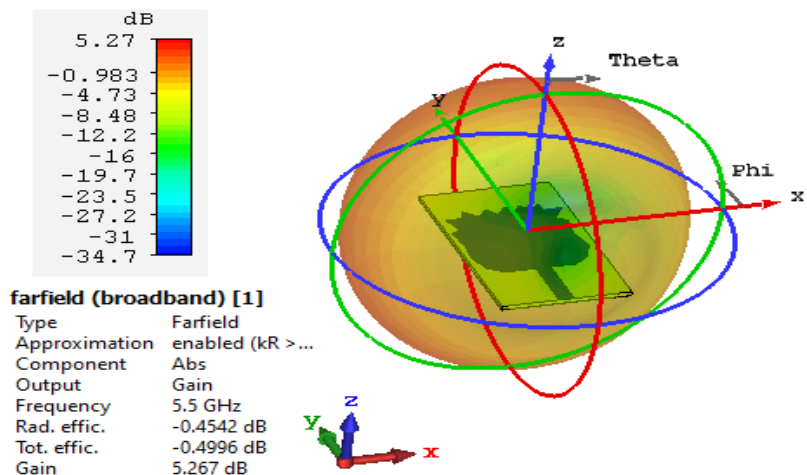


Fig. 6.4.2: VSWR of the rose-shaped antenna.

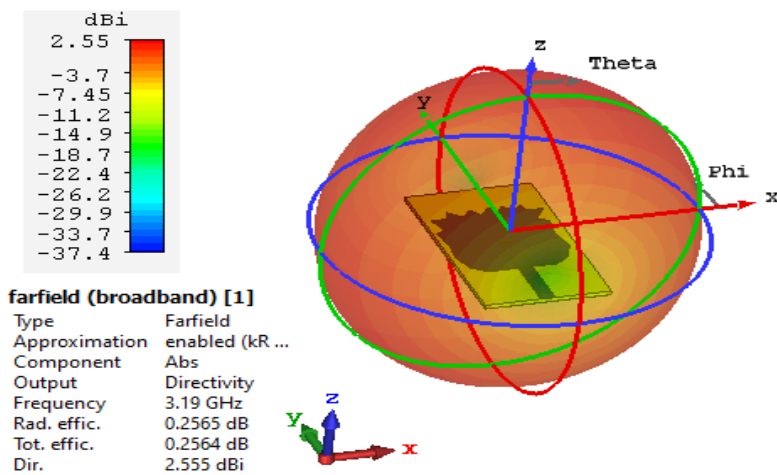
The 3D gain and 3D directivity at centre frequency 3.19 GHz and another higher frequency of 5.5 GHz with gain and directivity vs. frequency graph of the RSPA are presented in Fig. 6.4.3. At a resonant frequency of 3.19 GHz and another frequency of 5.5 GHz, the gains are 2.81 dB and 5.26 dB. The gain of the proposed RSPA over the entire bandwidth varies from 2.13 dB to 5.44 dB which makes it feasible for the intended Sub-6 GHz applications. The directivity of the designed RSPA at 3.19 GHz and another frequency 5.5 GHz are 2.55 dBi and 5.72 dBi respectively which varies from 2.26 dBi to 6 dBi over the entire operating bandwidth as drawn in Fig. 6.4.3 (e).



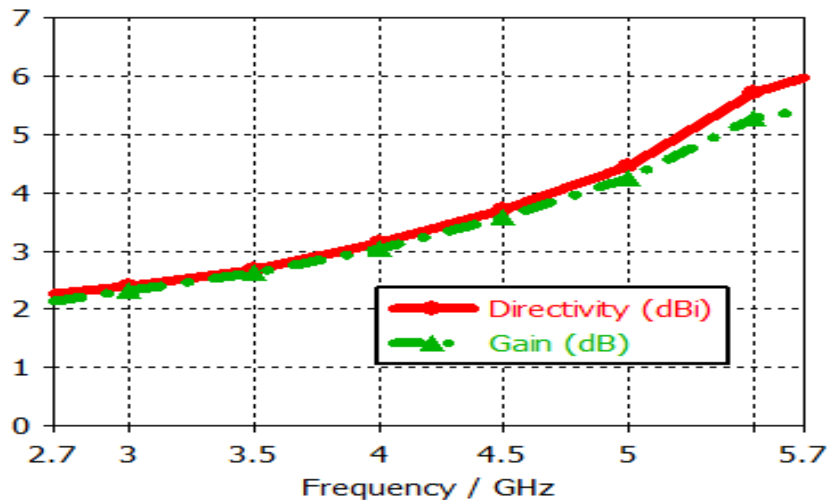
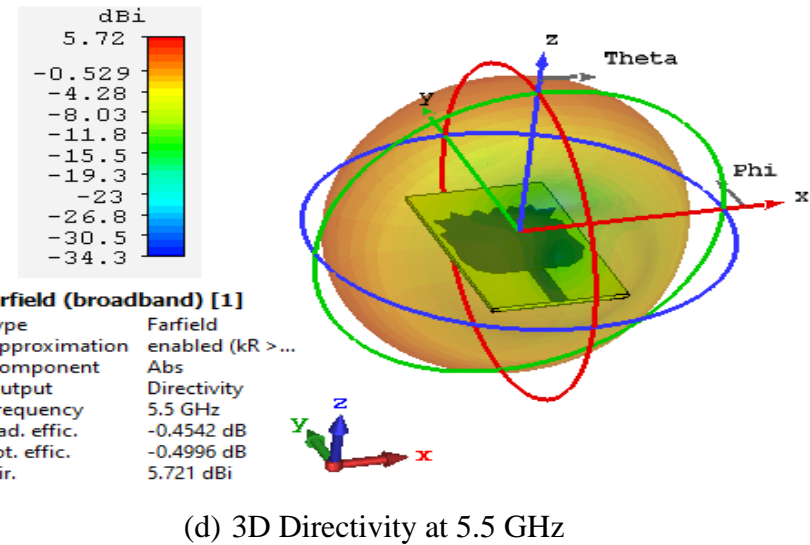
(a) 3D Gain at 3.19 GHz



(b) 3D Gain at 5.5 GHz



(c) 3D Directivity at 3.19 GHz



(e) Gain and directivity vs frequency

Fig. 6.4.3: Gain and directivity curve of the rose-shaped antenna.

At 3.19 GHz and another frequency 5.5 GHz, the polar plot of the radiation pattern of E-field and H-field are presented in Fig. 6.4.4 for azimuth angle $\phi=0^0$ and $\phi=90^0$. The main lobe direction is 2^0 for $\phi=0^0$ and 11^0 for $\phi=90^0$ at 3.19 GHz, while the value of main lobe direction is 179^0 for $\phi=0^0$ and 157^0 for $\phi=90^0$ at 5.5 GHz. From the plotted electric field pattern, it is clear that the main lobe magnitudes at 3.19 GHz and 5.5 GHz are 17.3 dBV/m, 18.5 dBV/m for azimuth angle 0^0 and 17.6 dBV/m, 20 dBV/m for azimuth angle 90^0 . While in terms of H field, the main lobe magnitudes are -34.2 dBA/m, -33 dBA/m for azimuth angle 0^0 and -33.9 dBA/m, -31.5 dBA/m

for azimuth angle 90^0 at 3.19 GHz and 5.5 GHz respectively. The maximum half power beam width (HPBW) known as 3 dB angular width is 117.2^0 at $\phi=0^0$.

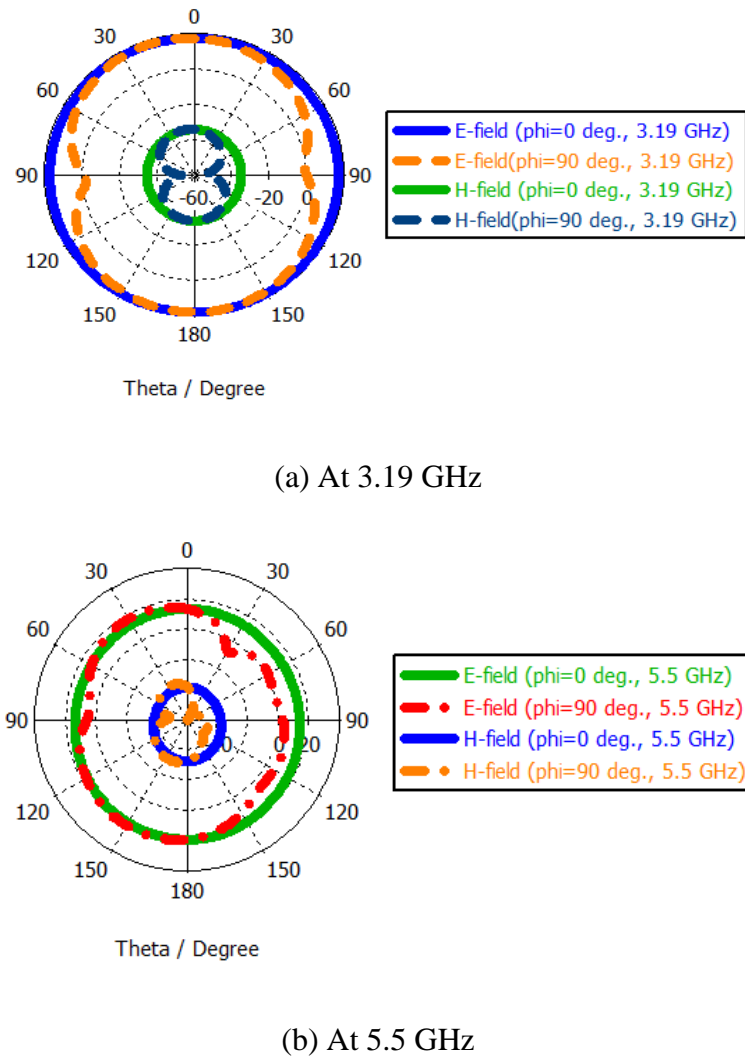
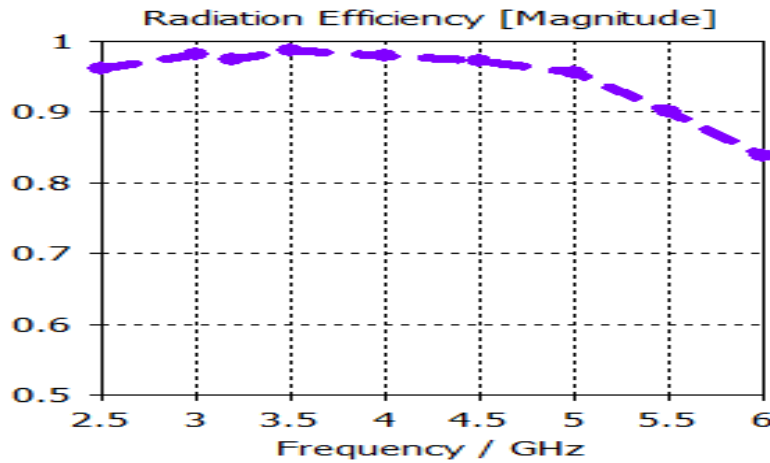
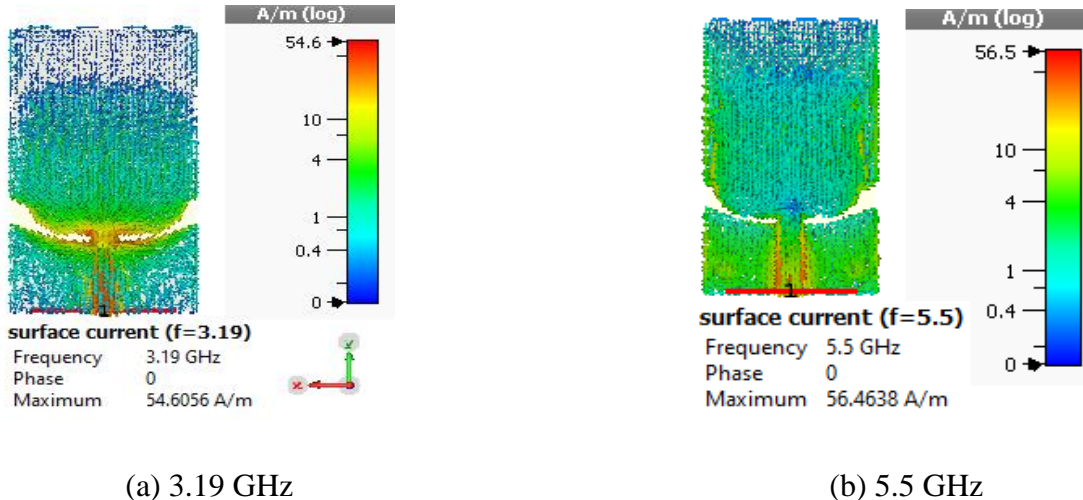


Fig. 6.4.4: Fields (E and H) of the Rose-shaped antenna.

Fig.6.4.5 represents the radiation efficiency of the proposed rose-shaped antenna. The radiation efficiency is the ratio of gain to directivity (G/D). The average radiation efficiency of the RSPA is about 95% and it varies from 87% to 98% over the whole operating band. It represents a good level of impedance matching of the proposed RSPA. The very high radiation efficiency of the antenna ensures that it radiates almost the same amount of input power i.e. approximately loss free radiation.

**Fig. 6.4.5:** Radiation Efficiency.

The combination of a simple planner rose-shaped patch and the semi-circular slot at the ground plane provides a very good current distribution of the antenna which is depicted in Fig. 6.4.6 for 3.19 GHz and 5.5 GHz.



(a) 3.19 GHz

(b) 5.5 GHz

Fig. 6.4.6: Surface current: (a) at 3.19 GHz and (b) at 5.5 GHz

From all the values of radiation patterns, the designed rose-shaped antenna has optimum radiation characteristics. The performance metrics of the proposed rose-shaped patch antenna has been mentioned in the Table 6.4.1.

TABLE 6.4.1: PERFORMANCE METRICS OF THE ROSE-SHAPED PATCH ANTENNA.

Name of the parameter	Value
Return loss (dB)	-57.27
Resonant frequency (GHz)	3.19
Gain (dB)	2.81
Directivity (dBi)	2.55
-10 dB Bandwidth (GHz)	3.04
Lower Cut-off (GHz)	2.7
Higher Cut-off (GHz)	5.74
VSWR	1.002
Maximum Radiation Efficiency (%)	98%

TABLE 6.4.2: COMPARISON WITH RELEVANT WORKS.

Parameter	Reference No.				This work
	[9]	[10]	[11]	[12]	
Size (L×W) mm ²	20×28	58×78	28×40	24×30	20×35
Substrate material	FR4	PET	FR4	FR4	Rogers RT 5880
Centre frequency (GHz)	4.8	5.2	3.83	4.8	3.19
Return loss (dB)	≈ -28	≈ -23.5	-31.15	≈ -41	-57.27
Gain (dB)	2.45	3	2.5	2.36	2.81
BW (GHz)	2.77	2.08	0.7	2.46	3.04
Efficiency (%)	65.35	80	----	67.22	95

6.5 Conclusion

A Rose-shaped patch antenna with a semi-circular slotted ground plane has been designed and presented in this paper for Sub-6 GHz applications. The RSPA is etched on commercially available Rogers RT 5880 (lossy) substrate to achieve a wide bandwidth of 3.04 GHz (2.7-5.74 GHz) with a very good reflection coefficient of -57.27 dB. A good level of impedance matching of the RSPA is ensured by the very high maximum efficiency of 98% and VSWR value of 1.002 at centre frequency. The semi-circular slot at the ground plane enhances the current distribution and radiation performance of the RSPA. The good gain and directivity with Omni-directional property of the rose-shaped patch antenna makes it a potential candidate for Sub-6 GHz applications.

REFERENCES

- [1] Cisco Systems. Mobile Visual Networking Index (VNI) Forecast Project7-Fold Increase in Global Mobile Data Traffic from 2016–2021. Available at: <https://newsroom.cisco.com/press-release-content?ArticleId=1819296> [last accessed on 24 Oct. 2021]
- [2] B. Y. Zikria, S. W. Kim, M. K. Afzal, H. Wang, and M. H. Rehmani, "5G Mobile Services and Scenarios: Challenges and Solutions" *Sustainability*, vol 10, no. 3626, pp 1-9, 2018.
- [3] Y. Kabalci, "5G Mobile Communication Systems: Fundamentals, Challenges, and Key Technologies". In: Kabalci E., Kabalci Y. (eds) *Smart Grids and Their Communication Systems*. Energy Systems in Electrical Engineering, Springer, Singapore, 2019.
- [4] M. Agiwal, A. Roy and N. Saxena, "Next Generation 5G Wireless Networks: A Comprehensive Survey," *IEEE Communications Surveys & Tutorials*, vol. 18, no. 3, pp. 1617-1655, 2016.
- [5] <https://www.qualcomm.com/media/documents/files/5g-spectrum-update-for-mipi-alliance.pdf> [last accessed on 24 Oct. 2021]
- [6] M. K. Islam, M. M. Rana and R. Inum, "A comparative performance analysis of inverted F antenna using different substrates," *Int. Conf. on Electrical Engineering and Information Communication Technology*, 2015, pp. 1-4.
- [7] L. C. Paul et al.,, "Wideband Inset Fed Slotted Patch Microstrip Antenna for ISM Band Applications," *8th Int. Conf. on Informatics, Electronics & Vision*, 2019, pp. 79-84.
- [8] L. C. Paul, A. K. Sarkar, M. A. Haque, P. Miah, P. M. Ghosh and M. R. Islam, "Investigation of the Dependency of an Inset Feed Rectangular Patch Antenna Parameters

- With the Variation of Notch Width for WiMax Applications," Int. Conf. on Electronics, Communication and Aerospace Technology, 2018, pp. 151-154.
- [9] R. Azim, R. Akter, A.K.M.M.H. Siddique, L. C. Paul, M.T. Islam, "Circular patch planar ultra-wideband antenna for 5G sub-6 GHz wireless communication applications," Journal of Optoelectronics and Advanced Materials, Vol. 23, no. 3-4, pp. 127-133, 2021.
 - [10] A. Desai, T. Upadhyaya, J. Patel, R. Patel, M. Palandoken, "Flexible CPW fed transparent antenna for WLAN and sub-6 GHz 5G applications," Microwave and Optical Technology Letters, vol 62, no. 12, pp. 1-14, 2020.
 - [11] A. Kapoor, R. Mishra and P. Kumar, "Compact wideband-printed antenna for sub-6 GHz fifth-generation applications", Int. Journal on Smart Sensing and Intelligent Systems, vol 13, no 1, pp. 1-10, 2020.
 - [12] R. Azim, T. Alam, L. C. Paul, R. Aktar, A. K. M. Moinul Hoque Meaze and M. T. Islam, "Low Profile Multi-slotted Patch Antenna for Lower 5G Application," IEEE Region 10 Symposium, 2020, pp. 366-369.
 - [13] I. Ishteyaq, I. S. Masoodi and K. Muzaffar, "A compact double-band planar printed slot antenna for sub-6 GHz 5G wireless applications," Int. Journal of Microwave and Wireless Technologies, vol 13, no 5, pp. 469 - 477, 2020.
 - [14] X. Tang et al., "Ultra-Wideband Patch Antenna for Sub-6 GHz 5G Communications," Int. Workshop on Electromagnetics: Applications and Student Innovation Competition, 2019, pp. 1-3.
 - [15] R. Azim et al., "A multislotted antenna for LTE/5G Sub-6 GHz wireless communication applications," International Journal of Microwave and Wireless Technologies, vol 13, pp. 486–496, 2020.
 - [16] W. An, Y. Li, H. Fu, J. Ma, W. Chen and B. Feng, "Low-Profile and Wideband Microstrip Antenna With Stable Gain for 5G Wireless Applications," IEEE Antennas and Wireless Propagation Letters, vol. 17, no. 4, pp. 621-624, 2018.
 - [17] Y. Li, Z. Zhao, Z. Tang, Y. Yin, "A low-profile, dual-band filtering antenna with high selectivity for 5G sub-6 GHz applications," Microw Opt Technol Lett., vol. 61, pp. 2282–2287, 2019.
 - [18] A. Zhirong and H. Mang, "A Simple Planar Antenna for Sub-6 GHz Applications in 5G Mobile Terminals," ACES Journal, Vol. 35, No. 1, pp. 10-15, 2020.

Chapter - 7

A SLOTTED PLUS SHAPED PATCH ANTENNA WITH DGS FOR SUB-6 GHz/WiMAX APPLICATIONS

7.1 Abstract

A slotted plus shaped patch antenna (PSPA) is designed and proposed for Sub-6 GHz and WiMAX wireless applications using CST MWS suite. The PSPA incorporated with a plus shaped radiating patch and a defected ground structure. The antenna is designed on Rogers RT5880 (lossy) substrate with a compact dimension of $20 \times 35 \times 0.79$ mm³. It resonates at 3.12 GHz with a very good reflection coefficient of -52.06 dB and operates over a wider bandwidth of 2.56 GHz (2.67-5.23 GHz) to accommodate suitable sub-6 GHz bands. It shows gain of 2.44 dB, directivity of 2.53 dBi and VSWR of 1.005 at centre frequency 3.12 GHz respectively with omnidirectional radiation characteristics. The maximum efficiency of the proposed PSPA is about 98% for almost loss free power radiation. The maximum gain and directivity are 4.65 dB and 4.95 dBi respectively. The DGS at the ground plane improves current distribution and proper impedance matching which makes the PSPA a suitable candidate for sub-6 GHZ wireless applications of multiple purposes.

7.2 Introduction

The world is facing the technological revolution in 21st century which introduced a redefined civilization of global connectivity. Wireless communication is one of the key features of this technological revolution, which has a great impact on our daily life. To fulfill the key performance factors of wireless communication such as higher data traffic, huge connectivity, low latency of various wireless devices, the sub-6 GHz wireless technology is a suitable candidate. Sub-6 GHz wireless bands are assigned for multiple wireless technologies such as WiMAX, Wi-Fi, WLAN, 3G, 4G(LTE) and most promising sub-6 GHz lower 5G applications.

Sub-6 GHz 5G has opened the door of a new era of innovation and connectivity which enables cloud computing, smart traffic system, AI services, automated industrial infrastructure, robotics, HD live streaming, virtual reality, augmented reality, space and astronomy, smart-home, smart transportation, IoT, remote education and health services specially during a period of global pandemic like Covid-19 [1-2]. To provide these numerous services sub-6 GHz 5G has some key features such as higher data rate, massive connectivity, ultra-low latency, higher reliability, wider coverage area and higher mobility [3-4]. Similarly due to very high peak data rate, higher mobility, multi-device connectivity Worldwide Interoperability for Microwave Access or WiMAX technology is used widely. The most popular WiMAX band used is the sub-6 GHz band of 3.5 GHz (3.3 – 3.6 GHz) [5]. WiMAX technology is widely used for cellular backhaul, broadband internet, VoIP, interactive gaming, IP multimedia subsystem (IMS) etc.

Though mm-wave 5G provides very fast data rate with high spectrum, the sub-6 GHz 5G technology is more practical ready-to-go technology with its wider coverage and implementation capability. The most popular sub-6 GHz 5G band is the 3.5 GHz band of (3.3 – 4.2 GHz). Various countries have deployed or licensed sub-6 GHz 5G with different spectrum shown in Table 7.2.1 [6].

TABLE 7.2.1: SUB-6 GHZ 5G FREQUENCY BANDS FOR DIFFERENT COUNTRIES AND REGIONS.

Country / Region	Frequency Band (GHz)
USA	3.7 - 4.2
Europe	3.4 - 3.8
China	3.3 - 3.6 and 4.8 - 5
Japan	3.6 – 4.1 and 4.5 – 4.9
Korea	3.4 - 3.7 and 3.7 – 4
India	3.3 – 3.6
Australia	3.4 - 3.7

In wireless technology, antennas are the key element to set up a communication link. Numerous researchers are developing various types of antennas all over the world. Microstrip patch antennas are the most popular types of antennas for its important features. Microstrip patch

antennas has some desirable features like simplicity, robust, compatibility of integration, cost effective, energy efficient, light weight and ease of fabrication. These salient features of microstrip patch antennas (MSPA), makes them hot cake of sub-6 GHz wireless communication. They are evolving with independent shapes of numerous designs by the modern-day researchers with respect to their usability and requirement. Different methods are used to design a MSPA among which DGS (Defected ground structure) is one of the popular strategies to improve the radiation performance of an antenna [7]. DGS is a very popular technique for its versatility and independence of structure [8]. Through the years, different types of antennas have been developed to follow the increasing demand in numerous applications of wireless technologies. Some notable works for sub-6 GHz and WiMAX applications are introduced in [9-18]. In [9], a circular patch planner antenna is introduced for Sub-6 GHz wireless applications. The antenna covers a wider bandwidth of (3.05 - 5.82 GHz) with its simplest structure without any lumped element. The rectangular slot on the ground plane improves the impedance matching. Despite of its simplicity and omnidirectional radiation, it shows comparatively lower average gain and efficiency. A compact F-shaped slotted antenna is proposed in [10] for WLAN/WiMAX applications. The antenna is designed on FR4 substrate with a compact dimension of $19 \times 25 \text{ mm}^2$. The rectangular patch with two F-shaped slots and a circular patch at ground plane facilitate the triple band operation with proper impedance matching. For WLAN, WiMAX and Bluetooth applications, a fork-shaped antenna is proposed and fabricated in [11] with a dimension of $24 \times 35 \text{ mm}^2$. It is incorporated with a T-shaped ground plane, a I-shaped monopole and two branch lines which act as cavity resonator for dual band operation where the gain and directivity are unspecified. In [12], a stepped patch antenna is introduced with multiple slots which improves capacitive effect and facilitated wider coverage of 2.4 GHz. Though it is designed and fabricated with compact dimension of $20 \times 30 \text{ mm}^2$, it shows comparatively lower average gain of 2.35 dBi and efficiency of 74.7%. A line stripe ultra-wideband antenna with dielectric resonators is demonstrated in [13] for 5G applications. The rectangular resonators enhance the efficiency of the antenna despite of its miniaturized structure. In [14], a compact dual-band antenna with rectangular slot and inverted U-shaped stub is presented for sub-6 GHz 5G wireless applications. It provides high peak gain of 7.17 dBi in spite of its smaller dimension ($36 \times 31 \text{ mm}^2$) but the bandwidth is very narrow. It shows optimum SAR value but using dielectric back cover has huge impact on its performance parameters. A circularly polarized ring slot antenna is proposed in

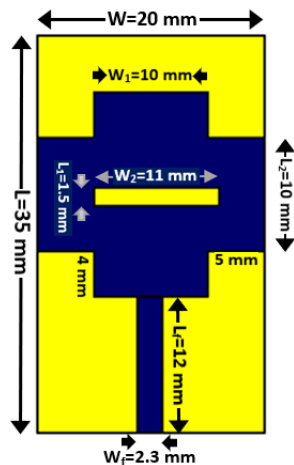
[15]. It is designed on FR4 substrate with a L-shaped feedline and circular ring slot as radiator. The coupling between feedline and circular ring slot is done by radial slot and narrow slot. The circular polarization is ensured by slits on the ground plane for very narrow bandwidth operation. A planner antenna with circular-shaped patch and long fed-line is introduced in [16] for 5G wireless applications. Though it has a simplest structure with a partial ground plane, it covers a wider bandwidth of 2.9 GHz. It shows moderate gain and at the ground plane two rectangular parasitic element is used to enhance the impedance matching as well as frequency shifting. In [17], a Circular Ring microstrip patch antenna is proposed with a dimension of $30 \times 30 \text{ mm}^2$. To improve the gain and return loss performance of the multiband antenna 4 circular ring used with a partial ground plane. The multiband antenna has peak gain of 4 dB for WiMAX applications. For 3.5 GHz 5G applications, 3 distinct elliptical patch antennas are studied in [18] where all of them resonates at 3.5 GHz with different radiation performances. The overall dimension and slots at ground plane differentiated their performance parameters.

In this chapter, a slotted plus shaped patch antenna (PSPA) is demonstrated for sub-6 GHz and WiMAX applications. The proposed PSPA is designed on Rogers RT5880 substrate with a compact dimension of $20 \times 35 \times 0.79 \text{ mm}^3$. It covers a wider bandwidth of 2.56 GHz (2.67 - 5.23 GHz) with high peak gain, directivity and efficiency for sub-6 GHz operation. The chapter is further structured as follows: in section 7.3: design and structure of PSPA, in section 7.4: simulation, result and discussion of the antenna and finally in section 7.5: conclusion.

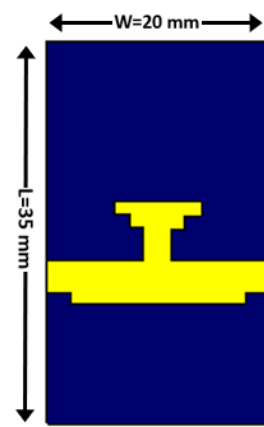
7.3 Design and Structure of the PSPA

The slotted plus shaped patch antenna (PSPA) with DGS is optimized and simulated using CST-MWS suite 2018. The proposed PSPA is designed on Rogers RT5880 (lossy) substrate (2.2, 0.0009) with thickness of 0.79 mm. To design the radiating plus shaped patch, feed line along with DGS, copper (annealed) material is used with thickness of 0.035 mm. The proposed antenna has a compact dimension of $20 \times 35 \times 0.79 \text{ mm}^3$. The schematic front view and back view of geometrical structure of the designed plus shaped patch antenna (PSPA) with defected ground structure (DGS) is presented in Fig. 7.3.1(a) and 7.3.1(b). The PSPA is fed by a feeder of size ($12 \times 2.3 \text{ mm}^2$). The width of 4 outer portion of the plus shaped radiating patch is about 10 mm.

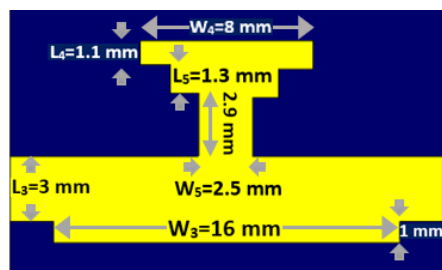
The distance of vertical portion from the edge of the horizontal outer portion is about 5 mm where the distance of horizontal portion from the edge of vertical outer portion is about 4 mm. The size of the slot of radiating patch is $(11 \times 1.5 \text{ mm}^2)$. At the ground plane a defected ground structure is introduced to enhance impedance matching as well as for required radiation performance. The amplified slot is shown at Fig. 7.3.1(c) where a stepped T-shaped slot is designed with an arm of width 8 mm which improves the current distribution of the antenna. At the lower portion of the DGS a $(16 \times 1 \text{ mm}^2)$ sized slot is etched. The schematic 3D view of the proposed PSPA for sub-6 GHz/WiMAX application is shown in Fig. 7.3.1(d). All the design parameters of the PSPA are listed in the Table 7.3.1.



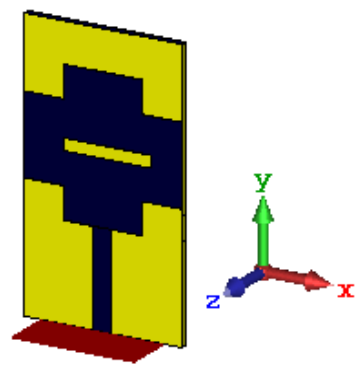
(a) Front View



(b) Back View



(c) Amplified Slot



(d) 3D View

Fig. 7.3.1: Proposed PSPA with DGS.

TABLE 7.3.1: PARAMETERS' LIST OF THE DESIGNED PSPA

Description and symbol	Value (mm)
Substrate's length (L)	35
Substrate's width (W)	20
Substrate's thickness (h)	0.79
Metal's thickness (t)	0.035
Feeder length (L_f)	12
Feeder width (W_f)	2.3
Horizontal edge length of patch (L_2)	10
Vertical edge width of patch (W_1)	10
Width of Slot at patch (W_2)	11
Length of Slot at patch (L_1)	1.5
Lower ground slot width (W_3)	16
Upper ground slot length (L_3)	3
Stepped T upper arm width (W_4)	8
Stepped T lower arm width (W_5)	2.5

7.4 Simulation, Results and Discussion

The simulated results of all the performance parameters makes the PSPA a well-suited candidate for sub-6 GHz and WiMAX applications. The scattering parameter (S11-curve) or reflection coefficient curve of the proposed PSPA is depicted in Fig.7.4.1. The PSPA covers a wider bandwidth of 2.56 GHz ranging from 2.67 GHz to 5.23 GHz with a superior reflection coefficient value of -52.06 dB. The slot at the radiating patch improves the reflection coefficient values. The DGS structure at ground plane increases the bandwidth of operation.

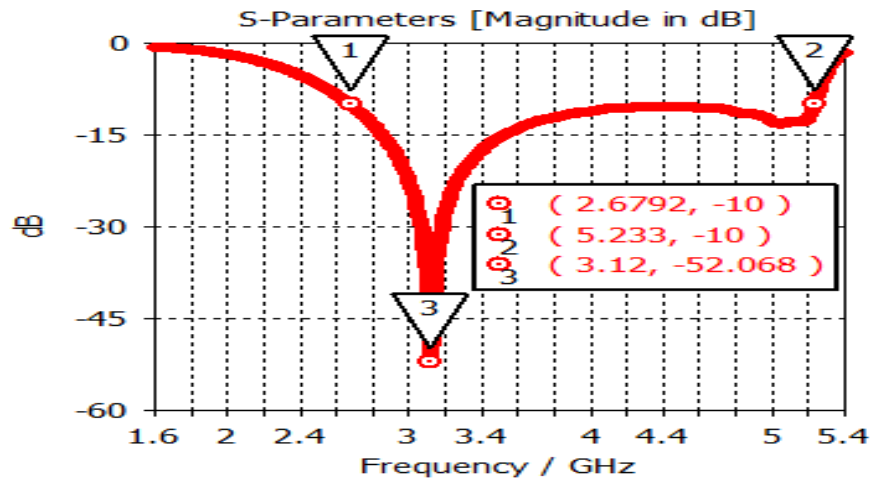
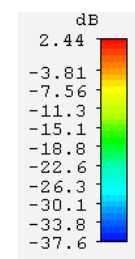
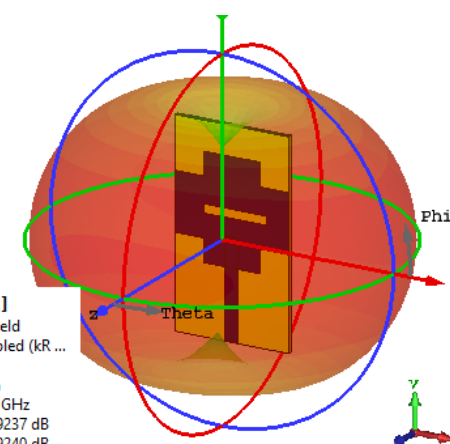


Fig. 7.4.1: Reflection coefficient of the designed PSPA.

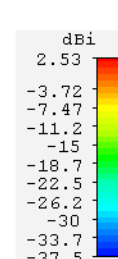
In Fig.7.4.2, the 3D gain and 3D directivity at centre frequency 3.12 GHz with another gain and directivity vs frequency curve are presented to demonstrate gain and directivity performance of the proposed PSPA. The 3D gain of PSPA at centre frequency 3.12 GHz is 2.44 dB. Over the whole operating bandwidth, the gain of PSPA varies from 2.17 dB to 4.65 dB. The antenna provides a higher peak gain of 4.65 dB for its optimized ground structure. The 3D directivity of the proposed PSPA is about 2.53 dBi at centre frequency 3.12 GHz. The directivity of the antenna over the whole operating bandwidth varies from 2.27 dBi to a higher peak directivity of 4.95 dBi which ensures well directive radiation performance of the proposed PSPA. The gain and directivity of the proposed PSPA can be improved in the future work by further optimization.



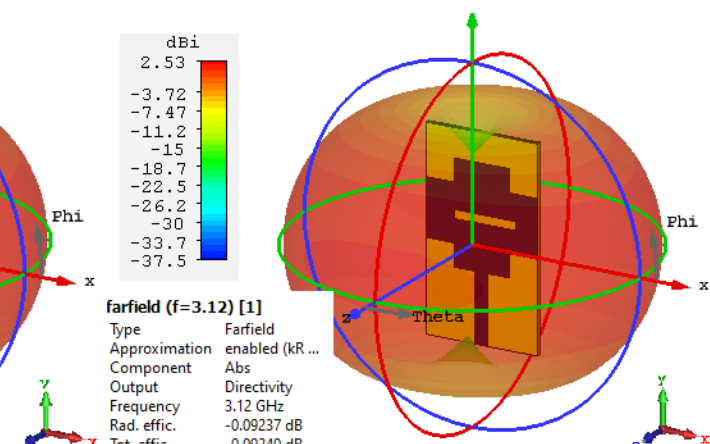
farfield (f=3.12) [1]
 Type Farfield
 Approximation enabled (kR ...)
 Component Abs
 Output Gain
 Frequency 3.12 GHz
 Rad. effic. -0.09237 dB
 Tot. effic. -0.09240 dB
 Gain 2.440 dB



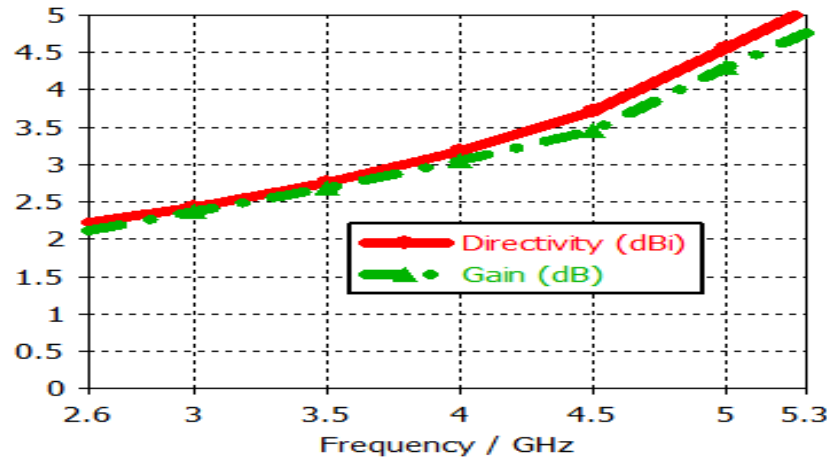
(a) Gain (3D) at 3.12 GHz.



farfield (f=3.12) [1]
 Type Farfield
 Approximation enabled (kR ...)
 Component Abs
 Output Directivity
 Frequency 3.12 GHz
 Rad. effic. -0.09237 dB
 Tot. effic. -0.09240 dB
 Dir. 2.533 dBi



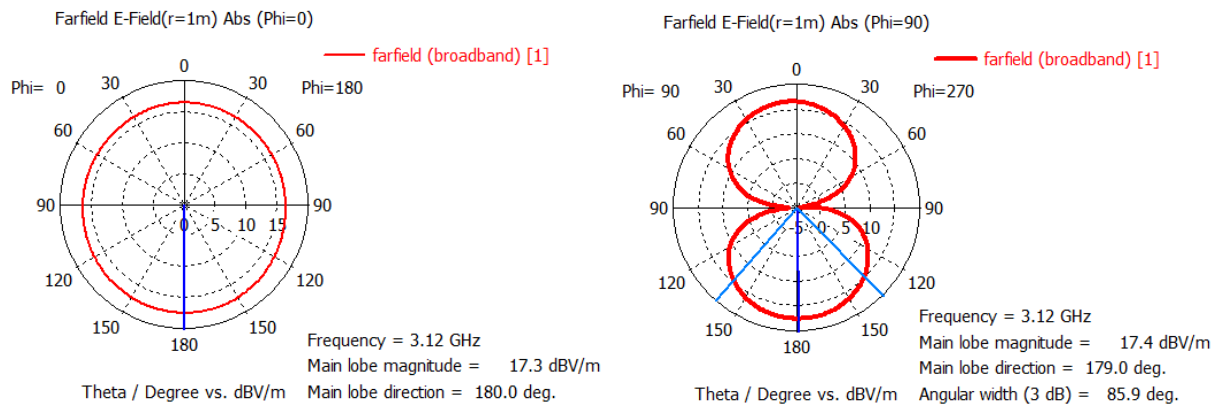
(b) Directivity (3D) at 3.12 GHz.



(c) Gain and directivity Vs frequency curve

Fig. 7.4.2: Gain and directivity curve of the designed PSPA.

The radiation pattern of both E-field and H-field of the proposed PSPA in terms of polar plot are presented in Fig.7.4.3. The field patterns are expressed for azimuth angle $\phi = 0^\circ$ and 90° at the centre operating frequency of 3.12 GHz. The main lobe direction at $\phi = 0^\circ$ and 90° are about 180° and 179° for both electric and magnetic field pattern. In terms of electric field pattern (E-Field) the main lobe magnitude for both azimuth angle $\phi = 0^\circ$ and 90° are 17.3 dBV/m and 17.4 dBV/m respectively. In terms of magnetic field pattern (H-Field) the main lobe magnitudes for azimuth angle $\phi = 0^\circ$ and 90° are both -34.2 dBA/m. The 3 dB angular width or half power beam width (HPBW) at $\phi = 90^\circ$ for both E-Field an H-Field is 85.9° . These radiation pattern performances of the proposed slotted PSPA makes it an intended contender of required sub-6 GHz applications.



(a) E-Field at phi =0°

(b) E-Field at phi =90°

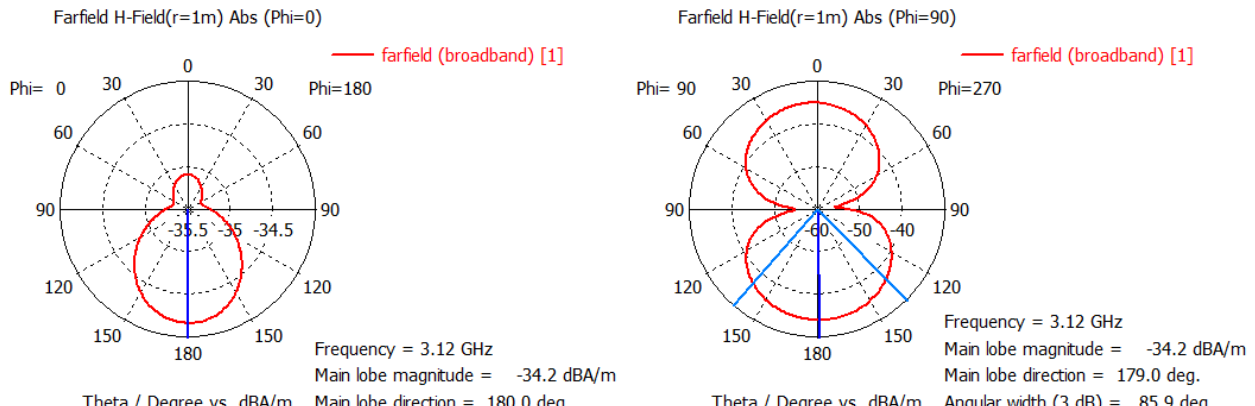


Fig. 7.4.3: E-field and H-field curve of the PSPA.

In Fig.7.4.4, the voltage standing wave ratio or VSWR curve is depicted. The VSWR value at the centre frequency 3.12 GHz is 1.005 which is about to unity and indicates minimal mismatch between antenna and the connecting feeder. Over the entire operating bandwidth, the VSWR value assures the condition $1 < \text{VSWR} < 2$ which ensures very well optimized impedance matching of the proposed PSPA.

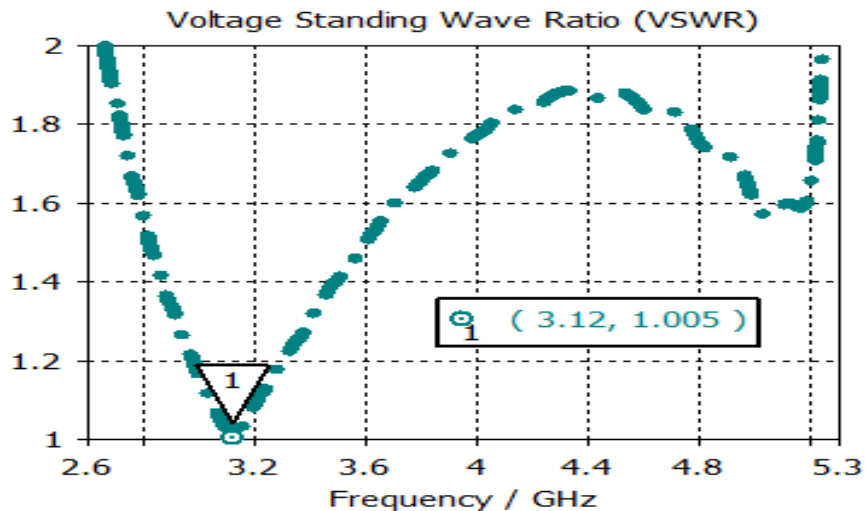


Fig. 7.4.4: VSWR of the PSPA.

The radiation efficiency of an antenna ensures how efficiently the antenna radiates the power fed to it and it is one of the key performance factors for microstrip patch antennas. The radiation efficiency curve of the proposed PSPA is presented in Fig.7.4.5 where the average radiation efficiency is approximately 95% which varies from 93% to a higher peak value of 98% over the entire bandwidth. This very high radiation efficiency of 98% increases its power radiation capability for required wireless applications as it radiates approximately all the power fed to it.

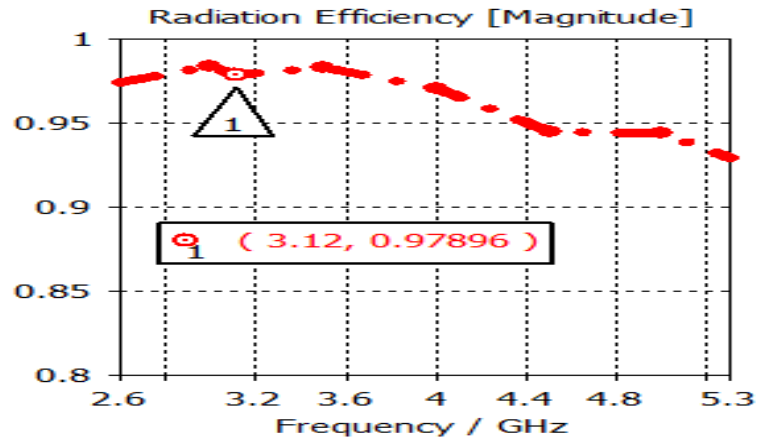


Fig. 7.4.5: Radiation Efficiency.

The surface current distribution of the proposed slotted antenna is displayed in Fig.7.4.6. The proper distribution of surface current over the whole antenna is aided by the DGS at ground plane along with slot at the radiating patch. The maximum value of surface current is about 66.43 A/m.

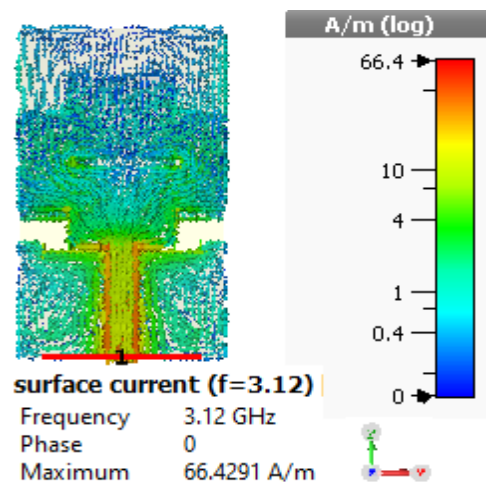


Fig. 7.4.6: Current distribution of the PSPA at 3.12 GHz.

In Fig.7.4.7, the Z-parameters curve of the proposed antenna for both real and imaginary part are presented. At the centre frequency the real part value is 50.33 ohm which is very close to standard 50 ohm for conventional patch antennas. On the other hand, the imaginary part value at centre frequency 3.12 GHz is 0.14 ohm which is near the standard 0 ohm value. These values of Z-parameters ensure the proper impedance matching of the proposed PSPA with standard impedance of the port.

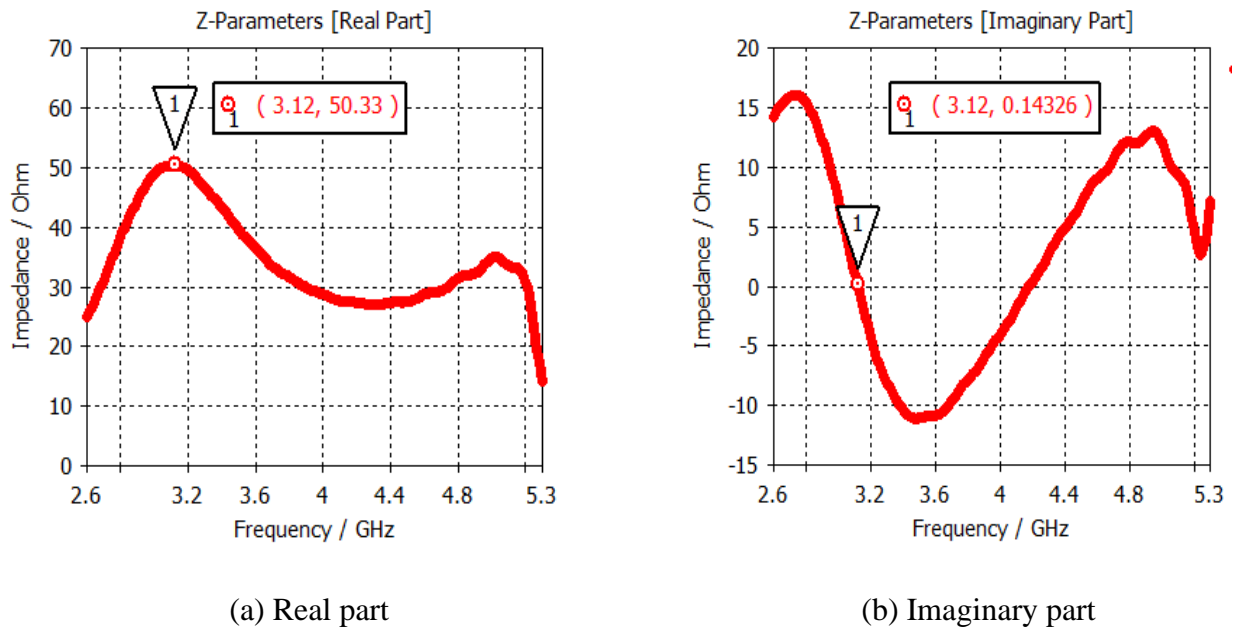


Fig. 7.4.7: Z – Parameters (a) Real part and (b) Imaginary part.

All the parametric results of the designed PSPA are listed in Table 7.4.1 and comparison of this work some recent relevant works are shown in Table 7.4.2.

TABLE 7.4.1: RESULTS OF THE DESIGNED PSPA

Description	Value
Lower cut off (GHz)	2.67
Upper cut off (GHz)	5.23
-10 dB Bandwidth (GHz)	2.56

Resonant frequency (GHz)	3.12
Return loss (dB)	-52.06
VSWR	1.005
Maximum gain (dB)	4.65
Maximum directivity (dBi)	4.95
Maximum radiation efficiency (%)	98
Impedance (Real Part) (ohm)	50.33
Impedance (Imaginary Part) (ohm)	0.14

TABLE 7.4.2: COMPARISON TABLE.

Parameter	Reference No.				This work
	[9]	[12]	[14]	[18]	
Size (L×W) mm ²	20 × 28	20× 30	36×31	46×26	20×35
Substrate material	FR4	FR4	FR4	FR4	Rogers RT 5880
Centre frequency (GHz)	4.8	4.71	3.3 and 4.5	3.5	3.12
Return loss (dB)	≈ -28	-32.6	≈ -22 and -23	-20.44	-52.06
Maximum Gain (dB)	2.45	2.69	7.17	4.42	4.65
BW (GHz)	2.77	2.4	0.34 and 0.81	2.15	2.56
Maximum Efficiency (%)	87.13	79.6	≈ 80	-----	98

7.5 Conclusion

A Plus shaped patch antenna with DGS is demonstrated in this paper for Sub-6 GHz and WiMAX applications. The slot at the radiating patch and DGS at the ground plane enhances its radiation performances for required operation. The proposed PSPA resonates at 3.12 GHz with a very good return loss of -52.06 dB. It operates over a wider bandwidth of 2.56 GHz. The VSWR value of the proposed antenna fulfill $1 < \text{VSWR} < 2$ over the entire bandwidth which ensures proper impedance matching of the proposed PSPA. In spite of simplest structure and compact size ($20 \times 20 \text{ mm}^2$), it shows higher maximum gain, directivity and efficiency with omnidirectional radiation characteristics for Sub-6 GHz wireless communication. The performance the proposed work can be further improved by optimization in future work

REFERENCES

- [1] <https://www.qualcomm.com/news/onq/2021/10/06/qualcomm-smart-cities-accelerate-2021-leaders-discuss-digital-transformation>
- [2] Heejung Yu, Howon Lee and Hongbeom Jeon, "What is 5G? Emerging 5G Mobile Services and Network Requirements", Sustainability, 2017 - mdpi.com
- [3] M. Agiwal, A. Roy and N. Saxena, "Next Generation 5G Wireless Networks: A Comprehensive Survey," in IEEE Communications Surveys & Tutorials, vol. 18, no. 3, pp. 1617-1655, thirdquarter 2016, doi: 10.1109/COMST.2016.2532458.
- [4] M. Shafi et al., "5G: A Tutorial Overview of Standards, Trials, Challenges, Deployment, and Practice," in IEEE Journal on Selected Areas in Communications, vol. 35, no. 6, pp. 1201-1221, June 2017, doi: 10.1109/JSAC.2017.2692307.
- [5] M. Rezvani; L Asadpor; R. Vahedpour, "A Compact Dual-Band Microstrip Monopole Antenna for WiMAX and WLAN Applications", ICEEM January 2017
- [6] <https://www.qualcomm.com/media/documents/files/5g-spectrum-update-for-mipi-alliance.pdf>
- [7] Mishra B, Verma RK, Yashwanth N, Singh RK (2021). A review on microstrip patch antenna parameters of different geometry and bandwidth enhancement techniques. International Journal of Microwave and Wireless Technologies 1–22. <https://doi.org/10.1017/S1759078721001148>
- [8] Rohit Kumar Nirala, “An Overview on Defected Ground Structure in Aspect of Microstrip Patch Antenna” International Journal on Recent and Innovation Trends in Computing and Communication ISSN: 2321-8169 Volume: 6 Issue: 1

- [9] R.Azim, R. Aktar, A. K. M.M.H. Siddique, L. C. Paul and M.T. Islam, "Circular patch planar ultra-wideband antenna for 5G sub-6 GHz wireless communication applications," Journal of Optoelectronics and Advanced Materials, vol. 23, no. 3-4, pp. 127-133, 2021.
- [10] A. K. Gautam, L. Kumar, B. K. Kanaujia and K. Rambabu, "Design of Compact F-Shaped Slot Triple-Band Antenna for WLAN/WiMAX Applications," in IEEE Transactions on Antennas and Propagation, vol. 64, no. 3, pp. 1101-1105, March 2016, doi: 10.1109/TAP.2015.2513099.
- [11] Kunwar, A., & Gautam, A. (2017). Fork-shaped planar antenna for Bluetooth, WLAN, and WiMAX applications. International Journal of Microwave and Wireless Technologies, 9(4), 859-864. doi:10.1017/S1759078716000647
- [12] R. Azim et al., "A multislotted antenna for LTE/5G Sub-6 GHz wireless communication applications," International Journal of Microwave and Wireless Technologies, vol 13, pp. 486–496, 2020.
- [13] Md Zulfiker Mahmud, Md Samsuzzaman, Liton Chandra Paul, Md Rashedul Islam, Ayman A. Althuwayb, Mohammad Tariqul Islam, A dielectric resonator based line stripe miniaturized ultra-wideband antenna for fifth-generation applications, International Journal of Communication Systems, 10.1002/dac.5013, 34, 18, (2021).
- [14] I. Ishteyaq, I. S. Masoodi and K. Muzaffar, "A compact double-band planar printed slot antenna for sub-6 GHz 5G wireless applications," Int. Journal of Microwave and Wireless Technologies, vol 13, no 5, pp. 469 - 477, 2020.
- [15] Mohamed Nasrun Osman et al "Wideband Circularly Polarized Printed Ring Slot Antenna for 5 GHz – 6 GHz"2018 IOP Conf. Ser.: Mater. Sci. Eng. 318 012040
- [16] R. Azim, A. K. M. M. Haque Meaze, M. Shuhrawardy and L. C. Paul, "A Low Profile Wideband Planar Antenna for 5G Wireless Communication Applications," National Conf. on Communications, 2020, pp. 1-4.
- [17] R Bhakkiyalakshmi and M S Vasanthi " A Simple Multiband Microstrip Circular Ring Antenna for Wimax, Wlan, X, and Ku Band Applications " 2021 J. Phys.: Conf. Ser. 1964 062045
- [18] M. M. Hasan, Z. Rahman, R. Shaikh, I. Alam, M. A. Islam and M. S. Alam, "Design and Analysis of Elliptical Microstrip Patch Antenna at 3.5 GHz for 5G Applications," 2020 IEEE Region 10 Symposium (TENSYMP), 2020, pp. 981-984, doi: 10.1109/TENSYMP50017.2020.9230897.

Chapter - 8

CONCLUSION

8.1 Conclusion

Parametric study of different shaped planar antennas is performed in this thesis work for handheld wireless communications. Different shapes and defected ground structure (DGS) are introduced in these antennas to optimize the radiation parameters. CST Microwave Studio Suite is used to design and simulate these antennas. A wideband antenna is introduced in chapter 3 with slotted ground plane for fifth generation wireless application. The antenna operates at 27.47 GHz with a wider bandwidth of 4.846 GHz. It shows higher peak gain and directivity of 6.1 dB and 7.8 dBi respectively. Another mm-wave operated low profile patch antenna is analyzed in chapter 4 for 5G application. The DGS helps the antenna to show very good parametric performances with a similar compact dimension of $20 \times 20 \times 0.79$ mm³ like the previous one. It shows a large bandwidth of 5.85 GHz with higher gain and directivity of 5.11 dB and 7.1 dBi respectively at resonant frequency 27.26 GHz. Now the spiral-shaped patch antenna is demonstrated in chapter 5 for Sub-6 GHz wireless application where the spiral shape of the radiator helps the antenna to get proper current distribution and omnidirectional radiation pattern. It's a dual band antenna which resonates at 3.61 GHz and 5.56 GHz with very good return loss of -41.29 dB and -37.85 dB respectively. The VSWR values are 1.017 and 1.025 at resonant frequencies which indicates very good impedance matching of the antenna. A rose-shaped patch antenna with a semi-circular slot is designed and simulated in chapter 6 followed by the spiral shaped one. It resonates at 3.19 GHz with a very good reflection coefficient of -57.27 dB and a large bandwidth of 3.04 GHz (2.7-5.74 GHz) despite of its compact size which makes it a suitable candidate of Sub-6 GHz handheld applications. It is more efficient than the previous one. Finally, another slotted plus-shaped antenna is analyzed in chapter 7 which incorporated with a defected ground structure. The antenna resonates at 3.12 GHz with a very good reflection coefficient of -52.06 dB and operates over a wider bandwidth of 2.56 GHz (2.67-5.23 GHz). It shows higher peak gain and directivity of 4.65 dB and 4.95 dBi respectively with very high

efficiency of 98% which makes it suitable for Sub-6 GHz handheld applications with multiple purposes. This research aimed to study the parametric performances along with design and simulation of different planar antennas for handheld wireless applications.

TABLE 8.1.1: SUMMARIZATION OF THE RESEARCH.

PARAMETER	CHAPTER NUMBER				
	3 (Slotted)	4 (DGS)	5 (Spiral)	6 (Rose)	7 (Plus)
Size (L×W) mm²	20×20	20×20	20×20	20×35	20×35
Substrate material	Rogers RT5880	Rogers RT5880	Rogers RT5880	Rogers RT5880	Rogers RT5880
Centre frequency (GHz)	27.47	27.26	3.61 and 5.56	3.19	3.12
Return loss (dB)	-35.03	-35.353	-41.29 and -37.85	-57.27	-52.06
Gain (dB)	6.1	6	3.95	5.44	4.65
Directivity (dBi)	7.8	7.9	5	6	4.95
BW (GHz)	4.846	5.85	0.166 and 2.53	3.04	2.56
Efficiency (%)	77	66	83	98	98
Applications	5G (mm-wave)	5G (mm-wave)	5G (Sub-6 GHz), WiFi-5/6	Sub-6 GHz, 5G	Sub-6 GHz, WiMAX
Comments	Wideband, 28 GHz 5G, Patch antenna	Low Profile, Microstrip Patch	Dual Band, Miniaturized, RT5880	Ground Slot, Wideband, Omni-directional	Slotted, DGS, High efficiency, PSPA

8.2 Recommendation for Future Work

As better performance from a compact size planar antenna is the most desirable in handheld applications, the size of these antennas can be reduced more by further optimization of many design factors such as introducing split-ring resonators, parasitic elements and different types of

Chapter 8

slots in the patches. The gain and directivity of these antennas can be improved further by proper positioning of parasitic elements of different shapes. We did the design and simulation of these antennas by using CST Microwave Studio Suite and planned to fabricate all the designs step by step to compare the simulated results with the measured values.

As this research work is based on single patch, single feed antennas, we will use same methodology in MIMO antennas, which are more efficient to apply in AI, Bio-medical and space applications. We will incorporate machine learning with these antennas to use in different innovative purposes. By minimizing these antennas to a threshold level, we can use these antennas in wearable devices. Then we will focus on Vivaldi antennas for different UWB (ultra-wideband) applications.

APPENDIX

List of Publications:

1. **Title:** A Wideband Microstrip Patch Antenna with Slotted Ground Plane for 5G Application, **Name of conference:** International Conference on Science & Contemporary Technologies (ICSCT), 2021, pp. 1-5, doi: 10.1109/ICSCT53883.2021.9642597, **Publisher:** IEEE
2. **Title:** A Low Profile Microstrip Patch Antenna with DGS for 5G Application, **Name of conference:** International Conference on Science & Contemporary Technologies (ICSCT), 2021, pp. 1-5, doi: 10.1109/ICSCT53883.2021.9642644., **Publisher:** IEEE
3. **Title:** A Dual Band Miniaturized Spiral-shaped Patch Antenna for 5G and WiFi-5/6 Applications, **Name of conference:** International Conference on Signal Processing, Information, Communication and Systems (SPICSCON), **Publisher:** IEEE
4. **Title:** A Wideband Rose-shaped Patch Antenna with a Ground Slot for Sub-6 GHz Applications, **Name of conference:** Indian Conference on Antennas and Propagation (InCAP), 2021, pp. 901-904, doi: 10.1109/InCAP52216.2021.9726293, **Publisher:** IEEE